

A Portable Monitor for Automated, On-line Cardiorespiratory State Classification

Semienchuk, Sasha

Department of Biomedical Engineering,
McGill University, Montreal

January, 2006

A thesis submitted to McGill University in partial fulfillment of the
requirements of the degree of Master in Biomedical Engineering

Copyright © S Semienchuk, 2006



Library and
Archives Canada

Bibliothèque et
Archives Canada

Published Heritage
Branch

Direction du
Patrimoine de l'édition

395 Wellington Street
Ottawa ON K1A 0N4
Canada

395, rue Wellington
Ottawa ON K1A 0N4
Canada

Your file Votre référence

ISBN: 978-0-494-25012-9

Our file Notre référence

ISBN: 978-0-494-25012-9

NOTICE:

The author has granted a non-exclusive license allowing Library and Archives Canada to reproduce, publish, archive, preserve, conserve, communicate to the public by telecommunication or on the Internet, loan, distribute and sell theses worldwide, for commercial or non-commercial purposes, in microform, paper, electronic and/or any other formats.

The author retains copyright ownership and moral rights in this thesis. Neither the thesis nor substantial extracts from it may be printed or otherwise reproduced without the author's permission.

AVIS:

L'auteur a accordé une licence non exclusive permettant à la Bibliothèque et Archives Canada de reproduire, publier, archiver, sauvegarder, conserver, transmettre au public par télécommunication ou par l'Internet, prêter, distribuer et vendre des thèses partout dans le monde, à des fins commerciales ou autres, sur support microforme, papier, électronique et/ou autres formats.

L'auteur conserve la propriété du droit d'auteur et des droits moraux qui protègent cette thèse. Ni la thèse ni des extraits substantiels de celle-ci ne doivent être imprimés ou autrement reproduits sans son autorisation.

In compliance with the Canadian Privacy Act some supporting forms may have been removed from this thesis.

Conformément à la loi canadienne sur la protection de la vie privée, quelques formulaires secondaires ont été enlevés de cette thèse.

While these forms may be included in the document page count, their removal does not represent any loss of content from the thesis.

Bien que ces formulaires aient inclus dans la pagination, il n'y aura aucun contenu manquant.


Canada

Acknowledgements

I would like to thank my supervisors Dr. Robert E. Kearney and Dr. Henrietta L. Galiana for their guidance; Dr. Karen A. Brown for familiarizing me with the operating and post-anesthesia recovery rooms at the Montreal Children's Hospital; and Dr. Alexis L. Motto with whom I worked intimately on all aspects of the project. I would also like to thank Dr. Ross Wagner for his help and advice with realizing the electronics and machining of the clinical monitoring system. Finally, I would like to thank the staff at the Montreal Children's Hospital for accommodating my intrusion into their workplace, as well as all the families who have volunteered themselves for the study of apnea. This work was supported by a grant from the Natural Sciences and Engineering Research Council of Canada.

Abstract

Apnea is a condition characterized by the spontaneous cessation of respiratory airflow during sleep. The current gold standard for the diagnosis of apnea is the manual analysis of cardiorespiratory data records by trained personnel; this restricts the study of apnea to the clinical setting, and is costly, time-intensive, subjective, and prone to human error. We have developed a monitor that non-invasively acquires, classifies, annotates and displays patient cardiorespiratory data in an on-line and fully-automated manner. The monitor is robust, portable and battery-operated and has a graphical user interface for patient monitoring by a clinician. The unit has received approval for use in the post-operative recovery room at the Montreal Children's Hospital as a point-of-care diagnostic tool to monitor infants for post-operative apnea.

Résumé

L'apnée est une condition caractérisée par la cessation spontanée du flux d'air respiratoire pendant le sommeil. La référence méthodologique encore en vigueur en matière de diagnostic de l'apnée est l'analyse manuelle des enregistrements cardiorespiratoires effectuée par un personnel qualifié; cela confine l'étude de l'apnée au cadre clinique, ce qui est onéreux, à forte consommation en temps, subjectif et sous le joug de l'erreur humaine. Aussi avons-nous développé un moniteur, peu ou non inconfortable pour le patient, qui acquiert, classe, annote et affiche les données cardiorespiratoires de celui-ci de façon automatique et en ligne. Ce moniteur est robuste, portable, utilise des batteries rechargeables et est doté d'une interface graphique pour la surveillance de la qualité respiratoire du patient par un clinicien. L'unité a reçu l'approbation pour être utilisée dans la salle postopératoire de l'Hôpital de Montréal pour Enfants comme outil d'aide au diagnostic de l'apnée postopératoire.

Table of Contents

Acknowledgements	ii
Abstract	iii
Résumé	iv
Table of Contents	- 5 -
Table of Figures	- 7 -
Table of Symbols and Acronyms	- 9 -
1 Introduction	- 11 -
2 Background.....	- 14 -
2.1 Physiology of Respiration.....	- 14 -
2.2 Central Sleep Apnea	- 16 -
2.3 Obstructive Sleep Apnea.....	- 17 -
2.4 Post-Operative Apnea	- 19 -
2.5 Cardiorespiratory Monitoring	- 20 -
2.5.1 Respiratory Inductance Plethysmography.....	- 21 -
2.5.2 Pulse Oximetry and Finger Plethysmography.....	- 25 -
2.6 Current Methods for Cardiorespiratory Data Analysis	- 27 -
2.7 New Methods for Cardiorespiratory Data Analysis.....	- 29 -
2.7.1 Asynchronous Breathing Test Statistic	- 30 -
2.7.2 Respiratory Pause Test Statistics.....	- 31 -
2.7.3 Gross Body Movement Test Statistics	- 32 -
2.7.4 Finite Impulse Response Filters	- 33 -
2.7.5 Event Detection	- 34 -
2.7.6 Statistical Thresholds	- 35 -
2.8 Current Apnea Monitors	- 38 -
2.9 Thesis Objective.....	- 38 -
3 The Cardiorespiratory Monitor.....	- 40 -
3.1 Clinical Monitoring System.....	- 41 -
3.1.1 The Overall Hardware Structure	- 42 -
3.1.2 System Electronics	- 44 -
3.1.3 Respiratory Inductance Plethysmograph.....	- 47 -
3.1.4 Pulse Oximeter	- 49 -
3.1.5 Anti-Aliasing Filtering	- 50 -
3.1.6 Battery	- 53 -
3.1.7 Output of Clinical Monitoring System.....	- 54 -
3.2 Cardiorespiratory Workstation.....	- 55 -
3.2.1 Notepad Computer	- 56 -
3.2.2 Data Acquisition.....	- 56 -
3.2.3 Overall Software Structure.....	- 57 -
3.2.4 Interactive Graphical User Interface	- 58 -
3.2.5 On-Line Analysis	- 59 -
3.2.6 Off-Line Analysis.....	- 71 -
3.2.7 File Management.....	- 73 -
4 Analyses of Cardiorespiratory Data Sets	- 76 -
4.1 Statistical Analyses	- 77 -
4.1.1 Methodology for Computing Statistics	- 78 -
4.1.2 Methodology for Setting Statistical Thresholds.....	- 79 -
4.1.3 Statistical Analysis: <i>MUR</i>	- 80 -
4.1.4 Statistical Analysis: <i>MOSS</i>	- 87 -

4.2	Performance Evaluations	- 93 -
4.2.1	Methodology for Performance Evaluations	- 94 -
4.2.2	Performance Evaluation Results	- 95 -
4.2.3	Patient Data Record: <i>MUR</i>	- 96 -
4.2.4	Patient Data Record: <i>MOSS</i>	- 97 -
4.2.5	Discussion of Statistical Analyses	- 99 -
4.2.6	Discussion of Performance Evaluations	- 100 -
4.3	Representative Visual Examples	- 102 -
4.3.1	Gross Body Movement	- 103 -
4.3.2	Respiratory Pause	- 106 -
4.3.3	Asynchrony	- 108 -
5	Summary and Future Work	- 110 -
5.1	Future Work	- 111 -
5.1.1	Statistical Thresholds and Test-Statistics	- 111 -
5.1.2	Evaluating the Performance of the Monitor	- 112 -
6	Appendices	- 114 -
6.1	User Operating Manuals	- 114 -
7	References	- 142 -

Table of Figures

Figure 2-1: Location of Medulla oblongata.....	- 15 -
Figure 2-2: Segment of infant breathing marked as CSA.	- 16 -
Figure 2-3: Obstructed human upper airway.....	- 17 -
Figure 2-4: Synchronous breathing and asynchronous breathing.	- 19 -
Figure 2-5: Respiratory inductance plethysmography bands.	- 22 -
Figure 2-6: Obtaining amplitude and phase from RIP signals.	- 24 -
Figure 2-7: Pulse Oximetry SpO ₂ sensor	- 25 -
Figure 2-8: Block diagram of asynchronous breathing test statistic	- 30 -
Figure 2-9: Sample distributions of the test statistic $T_2[n;N]$	- 37 -
Figure 3-1: The cardiorespiratory monitor.	- 40 -
Figure 3-2: Clinical monitoring system.....	- 41 -
Figure 3-3: Overall hardware structure of clinical monitoring system.	- 42 -
Figure 3-4: Interior of clinical monitoring system.	- 43 -
Figure 3-5: Standard power pin jacks.....	- 44 -
Figure 3-6: Circuit diagram of clinical monitoring system electronics.	- 45 -
Figure 3-7: Panels of clinical monitoring system.....	- 46 -
Figure 3-8: Power cable fashioned for portable RIP unit.....	- 48 -
Figure 3-9: Bessel anti-aliasing filter response characteristics	- 51 -
Figure 3-10: Bessel anti-aliasing filter group delay	- 52 -
Figure 3-11: Overall data flow schematic	- 55 -
Figure 3-12: Overall software structure	- 57 -
Figure 3-13: Representative samples of displays of graphical user interface	- 58 -
Figure 3-14: Block diagram of test statistic for gross body movement.....	- 60 -
Figure 3-15: Block diagram for computing decision for gross body movement.....	- 61 -
Figure 3-16: Movement Simulink block diagram	- 62 -
Figure 3-17: Block diagram of test statistic for respiratory pause	- 63 -
Figure 3-18: Block diagram for computing decision for respiratory pause	- 63 -
Figure 3-19: Pause Simulink block diagram	- 65 -
Figure 3-20: Asynchrony Simulink block diagram	- 67 -
Figure 3-21: Interface for on-line execution	- 69 -
Figure 3-22: On-line analysis of data captured by clinical monitoring system.....	- 70 -
Figure 3-23: Graphical display of CHIME group cardiorespiratory data record	- 72 -
Figure 3-24: Interface for exporting cardiorespiratory data record for EDF format	- 74 -
Figure 4-1: Sample distributions of the test statistic $T_3 [n;N]$ for <i>MUR</i> data set.....	- 82 -
Figure 4-2: Sample distributions of the test statistic $T_4 [n;N]$ for <i>MUR</i> data set.....	- 82 -
Figure 4-3: Sample distributions of the test statistic $T_5 [n;N]$ for <i>MUR</i> data set.....	- 83 -
Figure 4-4: Sample distributions of the test statistic $T_6 [n;N]$ for <i>MUR</i> data set.....	- 83 -
Figure 4-5: Sample distributions of the test statistic $T_1 [n;N]$ for <i>MUR</i> data set.....	- 85 -
Figure 4-6: Sample distributions of the test statistic $T_2 [n;N]$ for <i>MUR</i> data set.....	- 86 -
Figure 4-7: Sample distributions of the test statistic $T_A [n;N]$ for <i>MUR</i> data set.....	- 87 -
Figure 4-8: Sample distributions of the test statistic $T_3 [n;N]$ for <i>MOSS</i> data set	- 88 -
Figure 4-9: Sample distributions of the test statistic $T_4 [n;N]$ for <i>MOSS</i> data set	- 89 -
Figure 4-10: Sample distributions of the test statistic $T_5 [n;N]$ for <i>MOSS</i> data set.....	- 89 -
Figure 4-11: Sample distributions of the test statistic $T_6 [n;N]$ for <i>MOSS</i> data set.....	- 90 -
Figure 4-12: Sample distributions of the test statistic $T_1 [n;N]$ for <i>MOSS</i> data set.....	- 91 -
Figure 4-13: Sample distributions of the test statistic $T_2 [n;N]$ for <i>MOSS</i> data set.....	- 91 -
Figure 4-14: Sample distributions of the test statistic $T_A [n;N]$ for <i>MOSS</i> data set.	- 92 -
Figure 4-15: Automated analysis of data containing segment marked as central apnea	- 105 -

Figure 4-16: Automated analysis of data containing segment marked as obstructive apnea ... - 107 -
Figure 4-17: On-line automated analysis of data from Department of BME..... -109 -

Tables of Symbols and Acronyms

Acronyms

CSA	Central sleep apnea.
HBIR	Hering-Breuer Inspiratory Reflex.
OSA	Obstructive sleep apnea.
PDF	Probability density function.
POA	Post-operative apnea.
PSG	Polysomnography
RIP	Respiratory Inductance Plethysmography.
TAS	Thoracoabdominal asynchrony.

Symbols

N_A	Length of window over which phase estimate is computed.
N_{RMS}	Length of window over which pause and movement test statistics are computed.
$T_1[n; N_{RMS}]$	Abdomen respiratory pause test statistic.
$T_2[n; N_{RMS}]$	Ribcage respiratory pause test statistic.
$T_3[n; N_{RMS}]$	First abdomen gross body movement test statistic.
$T_4[n; N_{RMS}]$	First ribcage gross body movement test statistic.
$T_5[n; N_{RMS}]$	Second abdomen gross body movement test statistic.
$T_6[n; N_{RMS}]$	Second ribcage gross body movement test statistic.
$\phi[n; N_A]$	Normalized estimate of phase between the two RIP signals by phase estimator.
γ_A	Decision threshold for asynchronous breathing detector.
γ_M	Threshold on averaging filter on gross body movement detector.
γ_P	Threshold on averaging filter on respiratory pause detector.

γ^{AB}_{M1}	Decision threshold on T_3 for gross body movement detector.
γ^{AB}_{M2}	Decision threshold on T_5 for gross body movement detector.
γ^{AB}_P	Decision threshold on T_1 for respiratory pause detector.
γ^{RC}_{M1}	Decision threshold on T_4 for gross body movement detector.
γ^{RC}_{M2}	Decision threshold on T_6 for gross body movement detector.
γ^{RC}_P	Decision threshold on T_2 for respiratory pause detector.

1 Introduction

Apnea is a Greek word meaning ‘without breathing’; it is also the clinical term for the spontaneous cessation of respiratory airflow during sleep. First described in 1965 [1], apnea is classified into two categories: central apnea, resulting from disorders in respiratory control; and obstructive apnea, resulting from physical obstruction of the upper airways by the adenoids, enlarged soft tissue, or lax throat muscles [2]. Apnea affects both infants and adults.

Polysomnography (PSG), which involves recording and assessing a patient’s sleep and cardiorespiratory states, is the gold standard for the diagnosis of apnea-related disorders [3]. During PSG a variety of measures of physiological state are recorded and evaluated, including the electroencephalogram, the electrooculogram, the electrocardiogram, nasal airflow, abdominal and/or thoracic movements, and blood oxygen saturation. These measurements are taken simultaneously in a sleep laboratory under the continuous observation of trained personnel.

For the home or recovery room, cardiorespiratory monitoring, which involves recording a subset of the PSG signals (abdominal and thoracic movements, pulse oximetry, and finger plethysmography), is used [3]. Assessing the cardiorespiratory state of a patient involves determining the condition of the patient’s cardiovascular and respiratory systems by manual analysis of the data [4, 5]. Episodes of apnea are identified as part of this manual scoring.

However, manual analysis restricts the study of breathing disorders to the domain of sleep labs staffed by trained personnel. As a result, analyzing data records for a large number of patients requires significant personnel time and is costly; moreover, the results of the analysis are subjective, and the likelihood of human error is high [6].

There is a need for a system that automates the analysis of cardiorespiratory data records; this would eliminate the need for human scorers, allowing the analysis of

cardiorespiratory data to be performed inexpensively and quickly, permitting a systematic investigation of the etiology of breathing disorders such as apnea.

Algorithms have been developed and validated at the Department of Biomedical Engineering at McGill University for performing objective, standardized off-line detection of respiratory pauses, movement artifacts and asynchronous breathing movements from cardiorespiratory data [7-9].

The aim of this thesis was to acquire and configure hardware and software into a single device, capable of measuring and logging patient cardiorespiratory data non-invasively, and providing a digital signal processing architecture to physically realize the detection methods that were developed to analyze this cardiorespiratory data. The detection methods were modified for real-time use to permit the monitor to analyze cardiorespiratory data on-line as it is acquired. The monitor was constructed and configured to be robust, portable and battery-operated to make it suitable for use in the post-operative recovery room at the Montreal Children's hospital (Montreal, QC, CA) as a point-of-care diagnostic tool.

A Matlab toolbox was developed to perform file-storage and indexing of the annotated data and to provide the clinician a user-friendly interactive graphical interface for on-line patient monitoring and for off-line inspection and analysis of cardiorespiratory data sets. Full documentation of the development and theory of operation of the monitoring system, as well as hardware and software operating manuals, are provided in this thesis and in its Appendix.

As opposed to most existing cardiorespiratory monitors, which are large and cumbersome, require expert operators, and perform only apnea detection, the monitor developed here is portable, can be left unattended, and analyzes patient cardiorespiratory data continuously. The monitor permits the on-line analysis of patient cardiorespiratory data directly in the post-operative recovery room.

This thesis is structured as follows: Chapter 2 presents a review of the physiology of apnea, as well as the current standards for cardiorespiratory monitoring (instrumentation, signal processing, and analysis); Chapter 3 is a description of the hardware and software of the cardiorespiratory monitor; Chapter 4 illustrates the functionality of the monitor on clinical data, including performance evaluations; Chapter 5 concludes the thesis and provides direction for future development. Hardware and software operating manuals are provided in the Appendix.

2 Background

Apnea is defined by the American Sleep Apnea Association as a cessation of breathing during sleep that lasts at least ten seconds [10]. Occasional brief pauses in airflow are generally harmless; however, if apnea episodes are long enough in duration and/or occur with a high enough frequency, they may result in health complications.

Sleep apnea is most often associated with Sleep Apnea Syndrome, a chronic disorder that affects as many as 5% of middle-aged adults and 1-3% of children [11]. During an apnea episode, blood oxygen levels may become low, placing strain on the heart [12, 13]. Apnea has been linked to hypertension, stroke, coronary artery disease, congestive heart failure, fatigue, and depression [14]. Infants are at a particularly high risk post-operatively [15, 16], and apnea has been linked to Sudden Infant Death Syndrome (SIDS) [17].

2.1 Physiology of Respiration

A normal adult has a respiratory rate of 14–18 breaths per minute at rest, inspiring and expiring 6-8 liters of air per minute; infants have a respiratory rate that can range between 20 and 40 breaths per minute [18]. During respiration, oxygen (O₂) is absorbed into the blood, and carbon dioxide (CO₂) is excreted via the alveolar capillary interface [19].

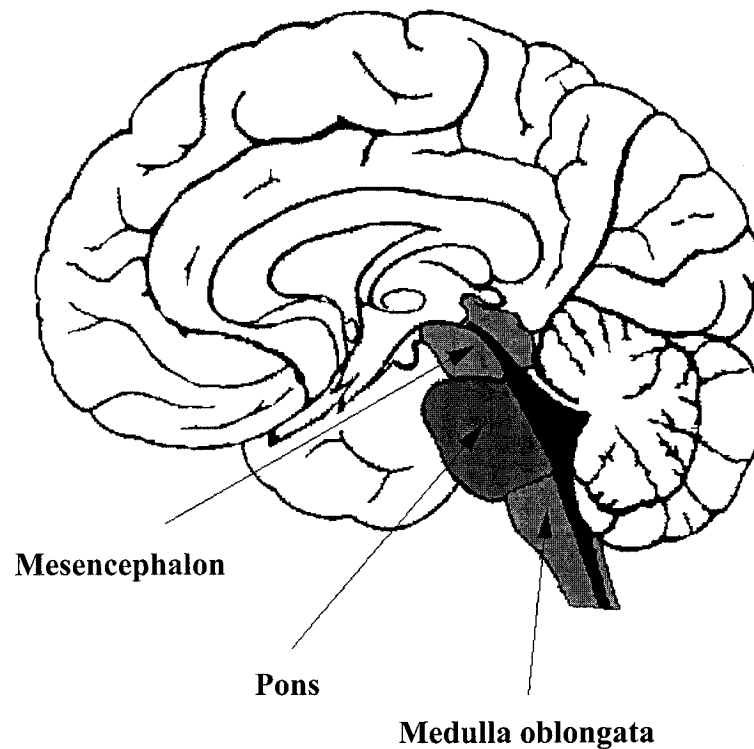


Figure 2-1: Location of Medulla oblongata [20].

Spontaneous respiration is dependent upon rhythmic discharges of the respiratory centre in the medulla oblongata (Fig. 2-1) [19]. Increases in ventilation are achieved by increases in the rate and intensity of these discharges. If an individual experiences a rise in CO_2 concentration of arterial blood, chemoreceptors alert the respiratory center in the brain, and the level of respiratory centre activity is increased; this increase in ventilation serves to restore blood oxygenation to normal levels [19].

In the case of infants, the breathing pattern is highly irregular, which is thought to be a result of the immaturity of their ventilatory control system. An infant will experience spontaneous variations in breathing frequency and amplitude throughout sleep [21]. Anesthesia will further disturb the pattern [19].

2.2 Central Sleep Apnea

Central sleep apnea (CSA) is a condition that occurs when the brain fails to signal the breathing muscles to perform respirations [2]. This is believed to be the result of disorders ranging from lesions in the ganglion to changes in the excitability of the motoneurons as a result of anesthesia [19]. Infants have been shown to have a particularly high incidence of central sleep apnea [22]; perhaps due to the immaturity of their ventilatory control system.

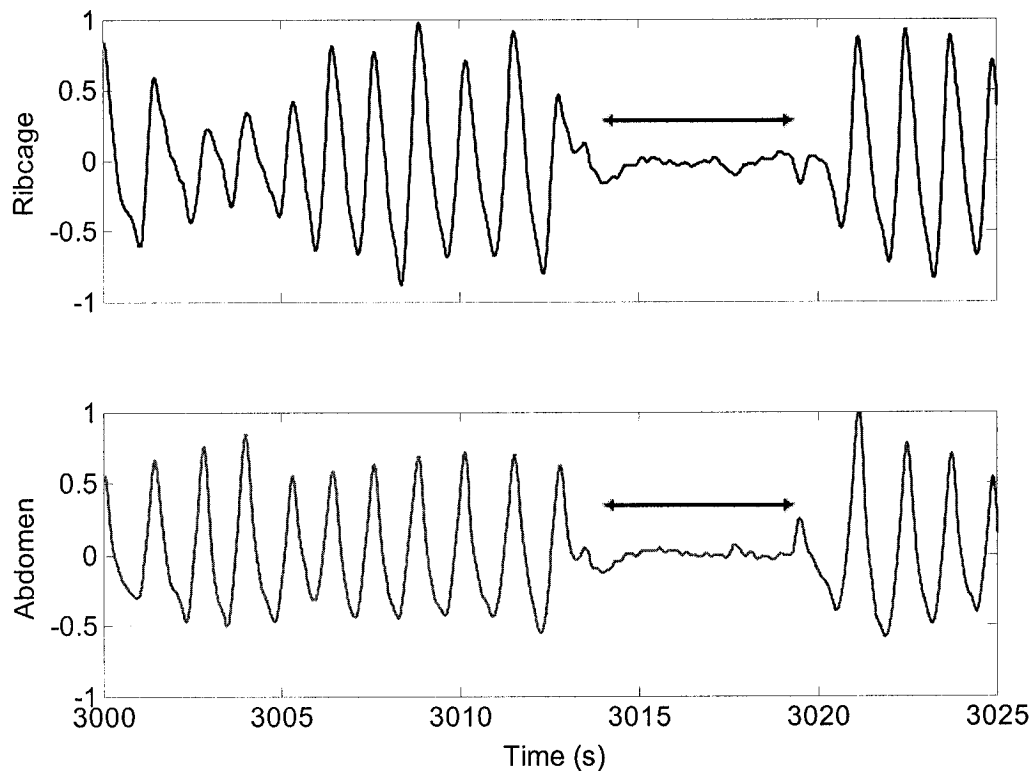


Figure 2-2: Segment of infant breathing visually annotated as CSA (Montreal Children's Hospital Study ID: *MUR*): (top) ribcage respiratory inductance plethysmography signal, (bottom) abdomen respiratory inductance plethysmography signal; the annotated segment is indicated by arrows; raw data was filtered using the bandpass filter reported in [7], so that the respiratory event would be more evident for illustrative purposes.

CSA can be identified by analyzing the magnitudes of the respiratory movements at the thorax and abdomen. The lack of proper central respiratory input leads to the absence of breathing movements or to breathing movements that are very low in amplitude

compared to normal breathing; this can be observed from Figure 2-2, which shows a segment of infant breathing, acquired at the Montreal Children's Hospital (unless stated otherwise, all Montreal Children's Hospital data presented are from a study performed with appropriate ethics approval and informed parental consent, as previously reported by Brown et al. [23]). The segment from 3012s to 3019s was marked as a central apnea by a clinician. This segment exhibited respiratory movements that were low amplitude compared to regular breathing, resulting in a flat period on the breathing movement signals.

2.3 Obstructive Sleep Apnea

Obstructive Sleep Apnea (OSA) is the condition most often investigated by sleep clinics [24]. During OSA, a partial or complete obstruction of the upper airway during sleep results in a reduction or complete cessation of airflow; the location of the obstruction is usually the soft palate at the base of the tongue (Fig. 2-3) [2].

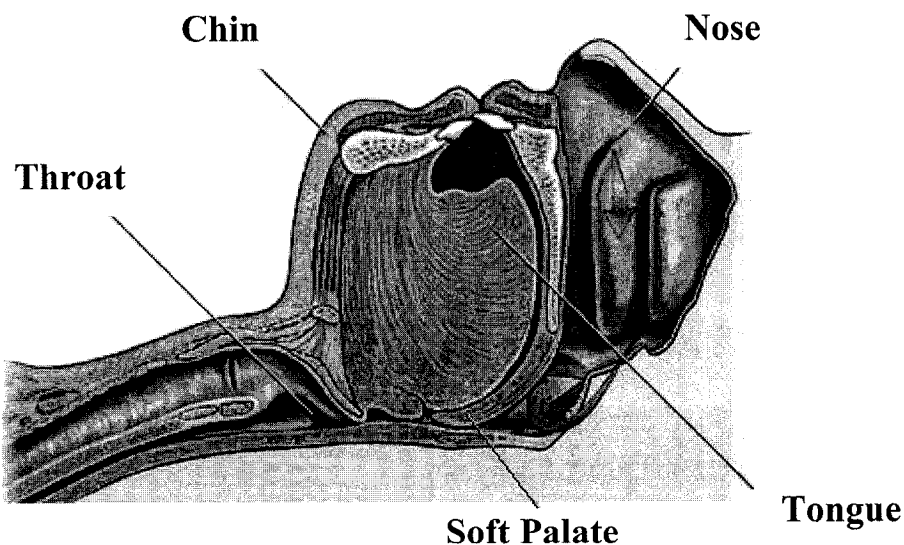


Figure 2-3: Major structures of obstructed human upper airway [25].

When an individual is awake, the upper airway muscles keep the passageway open. However, with the onset of sleep there is a gradual narrowing of the upper airway as the muscles relax [26]. During OSA, these muscles relax so much that the airway collapses. Because there are no rigid structures such as cartilage or bone to hold the airway open, the result is an obstruction that completely or partially impedes air from flowing through the nose or mouth. The origin of the apnea is sometimes due to enlarged tonsils or neuromuscular degeneration, but often cannot be identified [24].

During normal breathing the abdominal and thoracic movements occur approximately simultaneously and are in phase. However, when an individual's airway is obstructed, respiratory effort is increased in an attempt to overcome the obstruction. This increase in breathing effort, coupled with the increased airway resistance and negative pleural pressure, results in inward movements of the rib cage and a phase difference between the thoracic and abdominal excursions. This is called thoracoabdominal asynchrony (TAS). At complete obstruction, these two signals are in counter-phase. As a result, the detection of OSA and its severity is commonly based on the assessment of the degree of phase asynchrony between the respiratory movements at the thorax and at the abdomen [23, 27, 28].

Figure 2-4 shows a patient breathing record exhibiting both synchronous and asynchronous breathing movements. In the top segment of Figure 2-4, the ribcage and abdominal breathing movement signals are approximately synchronous; conversely, the ribcage and abdominal breathing movement signals in the bottom segment of Figure 2-4 exhibit a significant phase difference.

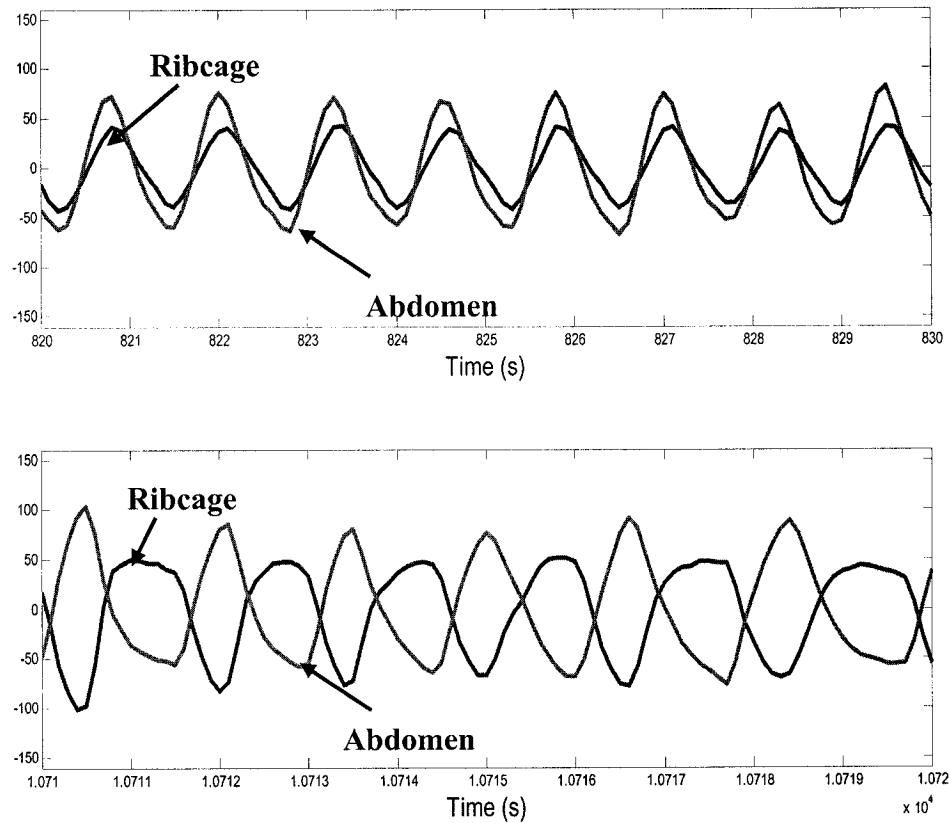


Figure 2-4: Ribcage and abdomen respiratory inductance plethysmography signals shown concurrently for both (top) synchronous breathing, and (bottom) asynchronous breathing (data from top and lower panels were obtained from Study ID 12064 and Study ID 12050 of the CHIME Alice 3 database) [29]; raw data was filtered using a bandpass filter similar to that which was reported in [7] but of order 40, so that the respiratory event would be more evident for illustrative purposes.

2.4 Post-Operative Apnea

Infants are at an increased risk for apnea post-operatively; post-operative apnea (POA) incidence is between 11% and 13% for infants under 2 months of age [15, 16]. However, the underlying pathophysiology of POA is still unknown.

Anesthesia can change the excitability of the neurons involved in respiratory control [30], affecting the pattern of central integration of stretch receptor activity. This disturbance

may be exacerbated in infants, because of their immature ventilatory control system. It has been shown that anesthesia affects both the respiratory centre and the respiratory muscles, and that this can result in inadequate respiratory rate and/or tidal volume and decreased oxygen saturation [31]. The effects on the respiratory control mechanisms can persist for several days following an operation [32].

Furthermore, anesthesia may also disrupt the Hering-Breuer Inspiratory Reflex (HBIR). The HBIR is a negative feedback system whereby increasing lung volume inhibits the respiratory centre; this reflex is believed to prevent over-inflation of the lungs and to help coordinate the transition between inspiration and expiration [19]. Anesthesia, which decreases lung volume [19], may stimulate the pulmonary receptors to increase sigh frequency in order to restore this volume. Because sighs lead to an increase in lung volume, they may illicit the HBIR and result in apnea. The HBIR reflex is particularly strong in infants: it has been shown that lung inflation even within the normal tidal volume can produce apnea in infants [33, 34].

Only a minority of infants are at a health risk due to POA; however, there is no way to identify these infants. Since POA can be life threatening, all infants under 2 months of age are monitored for apnea in the hospital post-operatively. A systematic investigation of the cardiorespiratory patterns of POA patients could help identify the etiology of the disorder and potentially predict which children should be given increased attention.

2.5 Cardiorespiratory Monitoring

Polysomnography is the current standard for the diagnosis of apnea-related disorders in sleep laboratories [24]. For the recovery room or home, cardiorespiratory monitoring is used, which involves recording a subset of the PSG signals. Generally this consists of the abdominal and thoracic movements, pulse oximetry, and finger plethysmography. Apnea results in both abnormal breathing movements and a drop in blood oxygen level; consequently, the clinical standard is that episodes of apnea are detected from the respiratory movements and blood oxygen saturation data [35, 36].

For young children, good quality PSG recordings require meticulous set-up and frequent adjustment of the equipment by a trained technologist [3]. Furthermore, the presence of experienced pediatric staff, and a parent throughout the study are required; as a result, PSG monitoring for children necessitates a staff-to-patient ratio that can be as high as one-to-one [3]. Moreover, PSG monitoring is invasive, since it requires masks and sensors over the face that pose the risk of entanglement and strangulation during unobserved sleep, which is unacceptable for an infant study. Furthermore, many of the PSG devices require subject cooperation, which is impossible with infants.

Conversely, cardiorespiratory monitoring is non-invasive and robust, can be applied in the home or recovery room without continuous monitoring by a clinician, and does not require subject cooperation, all of which makes it ideal for infant monitoring. Cardiorespiratory monitoring permits the study of sleep-disordered breathing outside the clinical environment: it can be performed in the patient's home, with the sensors being applied and removed by the patient or by family members, limiting disruption to the patient's sleep and to their family. It is also inexpensive, making it suitable for widespread application.

2.5.1 Respiratory Inductance Plethysmography

Respiratory Inductance Plethysmography (RIP) provides a measure of patient breathing movements. RIP is noninvasive, minimizing discomfort, and making it more appropriate for both long term and infant monitoring. Furthermore, RIP does not affect the breathing pattern or respiratory rate, which invasive forms of respiratory measurement such as spirometer and pneumotachometer have been shown to do [37]. RIP is the clinical standard for non-invasive, quantitative and qualitative respiratory measurements in infants and adults.

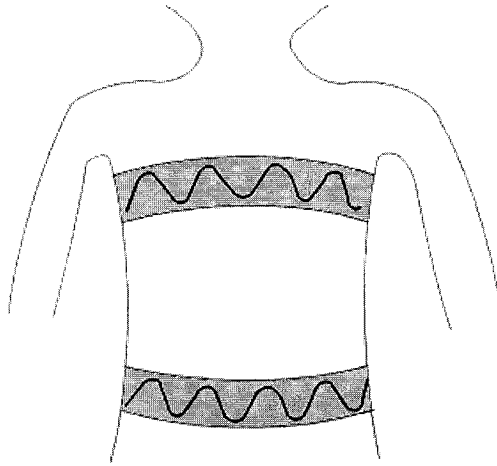


Figure 2-5: Respiratory inductance plethysmography bands [38].

RIP uses two elasticized cloth bands which are placed around the patient's ribcage (just under the axillae) and abdomen (at umbilical level) (Fig. 2-5). Each band has a coiled wire sewn into it in a sinusoidal pattern, constituting electrical coils whose inductance is proportional to the encircled cross-sectional areas.

The inductance of a conductor is given by [39]:

$$L = \frac{V}{\frac{\partial I(t)}{\partial t}} \quad (2.1)$$

where,

V is the voltage induced on the conductor and I is the current passing through it.

The voltage induced is determined using Faraday's Law of Induction:

$$V(t) = -\frac{\partial \phi}{\partial t} = -\int \vec{B}(t) \cdot d\vec{A} \quad (2.2)$$

If a symmetric, circular coil is assumed, the magnetic field B due to current I in the coil can be found using the Biot-Savart Law:

$$d\vec{B} = \frac{\mu_o I}{4\pi} \frac{\partial \vec{l} \times \vec{R}}{R^3} \quad (2.3)$$

where,

$\mu_o = 4\pi \times 10^{-7}$ (permeability of vacuum),

I is the current on the wire segment ∂l ,

R is the distance between the source point and the field point.

Using numerical techniques, (2.3) can be integrated along the coil to obtain $B(t)$, which along with (2.2), can be used to obtain the inductance of the wire coil. This inductance increases linearly with the radius.

For RIP, an oscillator excites each wire with a low-level current (~ 20 mv, ~ 300 kHz sine wave), creating a magnetic field. As the subject breathes, the cross-sectional area of each band changes. This results in a proportional change in the inductance of each wire. Each wire is part of an oscillator circuit whose resonant frequency varies with the self-inductance of the wire; consequently, the frequency of the oscillator output varies with the cross-sectional area.

This frequency is demodulated to produce analog waveforms of ribcage and abdomen movement. Ribcage movement primarily reflects the activity of the intercostal muscles and, to a lesser extent, the accessory muscles of breathing; while abdomen movement primarily reflects the activity of the diaphragm. As a result, the amplitudes of the RIP waveforms represent the magnitudes of these movements, while the phase difference between the waveforms represents phase between the thoracic and abdominal movements. It has been shown that RIP provides an accurate and linear measure of the changes in cross-sectional area of physiological shapes and has negligible baseline drifts

in AC coupled mode [40]. However, its calibration is sensitive to posture, so it can be problematic for quantitative measurements.

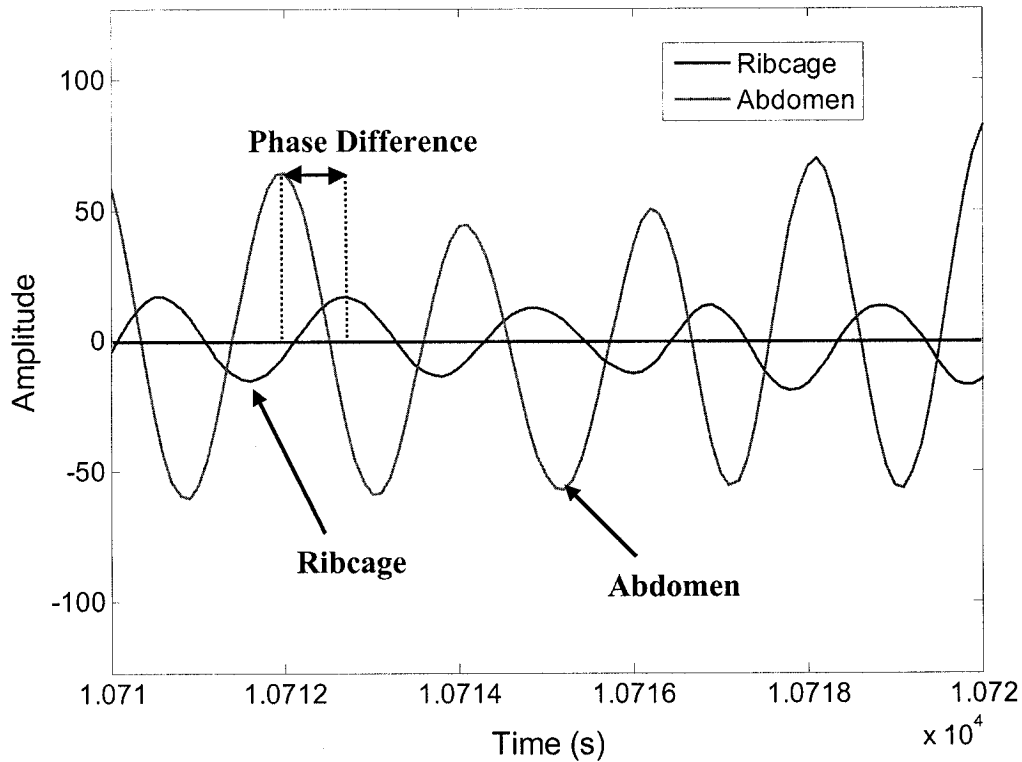


Figure 2-6: Obtaining the amplitude and phase of respiratory movements from RIP signals (data obtained from Study ID 12064 of the CHIME Alice 3 database [29]); ribcage and abdomen RIP signals shown concurrently; raw data was filtered using a bandpass filter similar to that which was reported in [7], so that the respiratory event would be more evident for illustrative purposes.

Consequently, both the magnitude and phase relationship of breathing movements can be computed. For example, Figure 2-6 shows the RIP signals for a patient breathing record: the ribcage movement signal and the abdomen breathing movement signal are shown on the same plot. From this figure, the magnitudes of the breathing excursions can be obtained from the amplitudes of the RIP signals, while the phase between the breathing movements can be obtained from the phase between the RIP signals. The amplitudes of the RIP signals can be used to identify central apneas and other respiratory pauses, while the phase relationship of the RIP signals can be used to identify TAS and obstructive apneas.

2.5.2 Pulse Oximetry and Finger Plethysmography

Pulse oximetry provides a measure of the level of oxygen saturated in the blood; this is expressed as the percentage of hemoglobin molecules in arterial blood saturated with oxygen; normal readings in a healthy adult range between 94% and 100% [41].

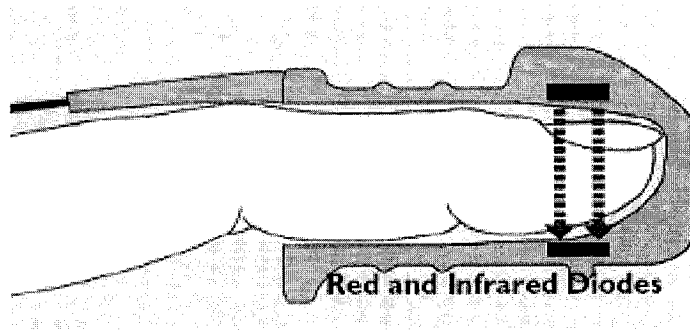


Figure 2-7: Pulse oximetry SpO₂ sensor [41].

Light emitting diodes shine red (660 nm) and infrared (940 nm) light through an extremity, such as a finger, toe or ear [42]. The light that passes unabsorbed through the extremity is received by a light-sensitive detector opposite the emitter (Fig. 2-7) and the amount of red and infrared light absorbed is calculated. Oxygenated hemoglobin (HbO₂) absorbs more infrared light than red light, while deoxygenated hemoglobin (Hb) absorbs more red light than infrared light. Consequently, from the levels of red and infrared light received, the amount of oxygen bound to hemoglobin in the blood can be calculated.

Although venous blood, tissue and bone absorb most of the light, over a short window of time this component remains relatively constant, while the amount absorbed by arterial blood changes due to pulsation. Consequently, the arterial blood component can be isolated. Mathematically, this is performed by calculating the ratio of absorbed red and infrared light:

$$SpO_2 = \frac{[HbO_2]}{[HbO_2] + [Hb]} \quad (2.4)$$

where,

$[HbO_2]$ is the concentration of oxyhaemoglobin,

$[HbO_2 + Hb]$ is the concentration of total haemoglobin.

It can be shown [i.e. 43]:

$$SpO_2 = f \left[\frac{\log_{10} \left(\frac{I_{r_{absorbed}}}{I_{r_{transmitted}}} \right)}{\log_{10} \left(\frac{I_{i_{absorbed}}}{I_{i_{transmitted}}} \right)} \right] \quad (2.5)$$

where,

$I_{r_{absorbed}}$ is the intensity of red light detected at the receiver,

$I_{r_{transmitted}}$ is the intensity of red light transmitted by the emitter,

$I_{i_{absorbed}}$ is the intensity of infrared light detected at the receiver,

$I_{i_{transmitted}}$ is the intensity of infrared light transmitted by the emitter,

f depends on the colors of the light emitting diodes (LED's) producing the light,

which are fixed by the manufacturing processes and material .

The measurement obtained from a pulse oximeter is termed SpO_2 , because it is only an estimate of the arterial blood oxygen saturation SaO_2 . Pulse oximetry measures the oxygen saturation of only functional hemoglobin (Hemoglobin capable of carrying oxygen), which includes oxygenated hemoglobin (HbO_2) and deoxygenated hemoglobin (Hb); while SaO_2 measures the saturation of both functional and nonfunctional Hemoglobin (Hemoglobin which is not capable of carrying oxygen). Non-functioning hemoglobin includes carboxyhemoglobin ($HbCO$) and methemoglobin ($METHb$) hemoglobin. The fluctuations in the signals due to arterial blood pressure pulses are also used to generate a finger plethysmographic pulse waveform, which is more suitable for infant monitoring than ECG which requires the application of additional electrodes.

Pulse oximetry is the standard for continuous monitoring of blood oxygen saturation in the intensive care unit and operating room [44]; it is non-invasive, compact, portable, robust and simple to use; furthermore, it does not require calibration, which is essential for infant monitoring, and monitoring in the home or surgery and post-anesthetic care units. It has been shown that when blood oxygen saturation is above 90%, pulse oximetry has a mean difference of less than 1% and a standard deviation of less than 2% as compared to the measurement standard, which is the multiwavelength CO oximeter [45].

Blood oxygen level may become low during an apnea, and heart rate exhibits a small decrease after the onset of apnea and a brief increase prior to the offset of apnea [46]. Consequently, heart rate and blood oxygen saturation are important to apnea detection [35]. The current standard is that a 4% drop from baseline is required for a cessation in respiration to be considered a clinically relevant apnea [47]. Because these changes in blood oxygen saturation and heart rate occur quickly, continuous monitoring is a necessity.

2.6 Current Methods for Cardiorespiratory Data Analysis

The current standard for analyzing cardiorespiratory data records is manual scoring; this entails the visual analysis of large volumes of data. Usually this analysis is performed by segmenting the data record into 10-30s epochs. Each epoch is visually inspected and categorized by a trained scorer as regular breathing, a respiratory event (sigh, central apnea, obstructive apnea, etc.), a movement artifact, or technically poor data.

Manual scoring is extremely cumbersome and time-consuming: a four hour study can involve more than 1000 segments to analyze, and demand hours for a clinician to complete. Additionally, manual analysis is subjective and the likelihood of human error is high [6]. As a result, analysis is restricted to sleep labs by dedicated, trained personnel and the analysis of cardiorespiratory data records for large numbers of patients is costly and unrealistic.

Methods have been developed to automate the process of cardiorespiratory data analysis. These include time domain algorithms that detect central apnea and hypopnea from the amplitude of RIP signals [48]; these time-domain methods exhibit reasonable performance but cannot identify obstructive apneas. Detection of obstructive apnea is usually performed by computing the phase relation between the abdominal and thoracic movements. Of the time domain methods, it has been shown [49] that the most successful at estimating this phase relation are maximum linear correlation and cross-correlation [23, 50]; however, these methods assume an underlying waveform which is quasi-stationary. As a result, they perform poorly on clinical data sets, which are non-stationary in general. Additionally, they exhibit a large number of false positives when applied to clinical data sets containing movement artifacts.

Methods have been realized to detect both central apneas and obstructive apneas employing artificial neural network (ANN) analysis of respiration signals (nasal airflow and/or RIP) [28, 51]. These methods develop networks based on breathing pattern training sets from PSG records annotated by clinicians. These algorithms then classify patient breathing into apneas or normal breathing by pattern recognition. However, these methods perform poorly when applied to clinical data sets, whose variability presents a more dispersed set of breathing patterns.

Methods using fuzzy logic systems have also been attempted. These involve characterizing the current state of the patient from the current cardiorespiratory data and the previous cardiorespiratory states [52]. However, these methods also perform poorly when analyzing clinical data sets, which exhibit a large degree of variability. In particular, these methods must be trained on and applied to data sets with no movement artifacts.

Overall all of these methods behave well when applied to clean data sets from adults. However, most encounter difficulty, and exhibit extremely high rates of false detection when applied to clinical data sets where movement artifacts are more prominent, and where there is a greater variability in breathing rate and amplitude. Consequently, these

methods are particularly unreliable for infants, who move frequently and whose respiratory patterns are particularly variable.

An automated system would eliminate the need for manual scoring, making the study of sleep disorders inexpensive and open to widespread, standardized, systematic analysis; furthermore, automated systems could permit on-line apnea detection and apnea prediction in the home or recovery room. Consequently, the development of automated methods for cardiorespiratory data analysis remains an active area of research.

2.7 New Methods for Cardiorespiratory Data Analysis

Validated, objective algorithms have been developed in the Department of Biomedical Engineering at McGill University for the off-line analysis of cardiorespiratory data [7, 8]. These algorithms can be applied to detect asynchronous breathing, respiratory pauses, and movement artifacts from breathing movements measured by un-calibrated respiratory inductance plethysmography.

These methods present several advantages over previous attempts at automating cardiorespiratory data analysis. Foremost, they do not assume quasi-constant breathing frequency and amplitude, which makes them more suitable for actual breathing; this is particularly important for infant breathing, which exhibits time-varying breathing amplitude and breathing rate. Additionally, they do not require that the underlying frequency of breathing be estimated, they are computationally simple, and they analyze un-calibrated RIP signals, which is important because RIP calibration has been shown to be inaccurate and not feasible for infants [53]. The new methods developed are less restrictive, less biased, and easier to implement than other methods. The three algorithms and their application to the analysis of cardiorespiratory data are described below.

2.7.1 Asynchronous Breathing Test Statistic

An algorithm was developed for estimating the phase relation between the thoracic and abdominal breathing movements [7]; it effectively maps the RIP signals into a quantitative estimate in the range from 0° to 180° , using finite-impulse response (FIR) filters. This phase estimate is then used as a test statistic for detecting obstructive sleep apnea. The algorithm is shown in block diagram form in Figure 2-8; it is outlined in detail below.

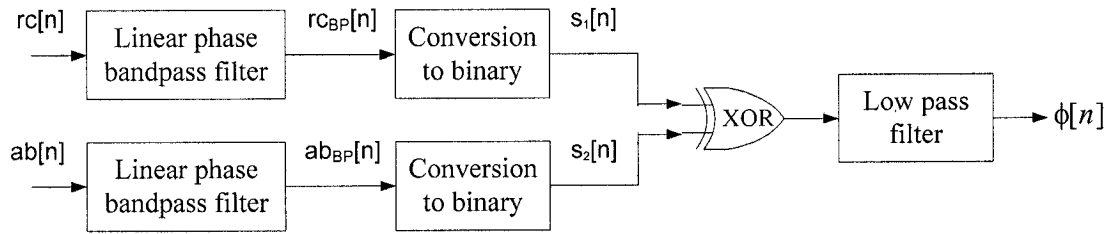


Figure 2-8: Block diagram of algorithm for estimating the phase relation between the thoracic ($rc[n]$) and abdominal ($ab[n]$) breathing movements.

RIP quiet breathing segments from 22 infants, obtained at the Montreal Children's Hospital, exhibited a power-spectral density that was negligibly small outside the bandwidth $[0.4\text{Hz}, 4\text{Hz}]$. Consequently, the RIP signals are first band pass filtered in this range to increase their signal-to-noise ratio (SNR).

After the signals are filtered, they are each converted to binary according to the following relation:

$$s[n] = \begin{cases} 0 & \text{if } u[n] < 0 \\ 1 & \text{if } u[n] \geq 0 \end{cases} \quad (2.6)$$

where,

$u[n]$ is the band pass filtered signal from $rc[n]$ or $ab[n]$ measurements.

Their phase relationship is then estimated using an Exclusive-OR (XOR) logic gate. The XOR gate outputs 1 when $s_1[n] \neq s_2[n]$ and 0 when $s_1[n] = s_2[n]$. The proportion of time that $s_1[n] \neq s_2[n]$ is computed using a low pass filter to provide a normalized estimate of the absolute value of the phase between $rc[n]$ and $ab[n]$.

The test statistic for asynchrony is defined as:

$$T_A[n; N_A] = \phi[n; N_A] \quad (2.7)$$

where,

$\phi[n; N_A]$ is the normalized estimate of the phase between the two RIP signals over a window of N_A sample points.

2.7.2 Respiratory Pause Test Statistics

Assuming that RIP technology accurately reflects the cross-sectional area changes of the ribcage and abdomen, a respiratory pause (central apnea or post-sigh apnea) will be associated with a RIP signal segment that has low-energy relative to normal breathing. As a result, respiratory pauses can be detected by identifying periods where both the ribcage and abdominal RIP signals have low energy concurrently. This can be determined by estimating the root-mean square (RMS) energy of the signals.

To do this, the RIP signals are first band pass filtered [0.4Hz, 4Hz] to increase their signal-to-noise ratio (SNR). The RMS energy of the filtered abdominal RIP signal over a window of length N_{RMS} sample points is then computed from:

$$E_{ab}[n; N_{RMS}] = \sqrt{\frac{\sum_{k=n-N_{RMS}+1}^n ab_{BP}^2[k]}{N_{RMS}}} \quad (2.8)$$

where,

$ab_{BP}[n]$ is the band pass filtered abdominal RIP signal.

The RMS energy of the filtered ribcage RIP signal over the same window, denoted as $E_{rc}[n; N_{RMS}]$, can be similarly defined. Consequently, estimates of the RMS energy of the RIP signals can be computed using linear filters, and simple operators. We can define the following test statistics:

$$T_1[n; N_{RMS}] = E_{ab}[n; N_{RMS}] \quad (2.9)$$

$$T_2[n; N_{RMS}] = E_{rc}[n; N_{RMS}] \quad (2.10)$$

2.7.3 Gross Body Movement Test Statistics

Making the same assumptions on the accuracy of RIP, it can be assumed that gross body movement will generate RIP signals that are high-energy relative to normal breathing. Consequently, we can define the following two test statistics, which investigate the entire bandwidth of RIP data:

$$T_3[n; N_{RMS}] = \hat{E}_{ab}[n; N_{RMS}] = \sqrt{\frac{\sum_{k=n-N_{RMS}+1}^n ab^2[k]}{N_{RMS}}} \quad (2.11)$$

$$T_4[n; N_{RMS}] = \hat{E}_{rc}[n; N_{RMS}] = \sqrt{\frac{\sum_{k=n-N_{RMS}+1}^n rc^2[k]}{N_{RMS}}} \quad (2.12)$$

These test statistics are identical to the test statistics presented earlier for respiratory pause, except the RIP signals are not band pass filtered prior to their computation.

We also hypothesize that gross body movement exists mostly outside the bandwidth of respiration. Consequently, test statistics that investigate the energy of the RIP signal, while attenuating the contribution from the respiratory band ([0.4Hz, 4Hz]) are used. The RMS energy contribution from the band pass filtered RIP signal, representing the range of normal breathing, is subtracted from the total RMS energy of the un-filtered RIP signal to isolate the contribution of gross body movement.

We define:

$$T_5[n; N_{RMS}] = \frac{\hat{E}_{ab}[n; N_{RMS}] - E_{ab}[n; N_{RMS}]}{\hat{E}_{ab}[n; N_{RMS}]} \quad (2.13)$$

$$T_6[n; N_{RMS}] = \frac{\hat{E}_{rc}[n; N_{RMS}] - E_{rc}[n; N_{RMS}]}{\hat{E}_{rc}[n; N_{RMS}]} \quad (2.14)$$

2.7.4 Finite Impulse Response Filters

The event detection algorithms presented were developed for off-line use. However, the cardiorespirator monitor that will be presented in the next chapter modifies them for on-line application. During on-line analysis, finite-impulse response filters produce a numerical delay according to [54]:

$$delay = \frac{(N-1)}{2 * F_s} \quad (2.15)$$

where,

N is the length of the filter,

F_s is the sampling rate.

2.7.5 Event Detection

Detection of each type of respiratory event is performed by selecting between two hypotheses:

H_0 : Respiratory event absent

vs.

H_1 : Respiratory event present

Using the appropriate test statistics a decision between these two hypotheses is made using comparators for each case. The three detectors are applied in combination. We assume that the probability of respiratory pauses and obstructive sleep events during periods of gross body movement is zero. We hypothesize that applying the comparators in combination will improve their performance.

Asynchronous Breathing Movement:

The phase comparator decides:

$$H_0 \text{ if } T_A \leq \gamma_A$$

$$H_1 \text{ if } T_A > \gamma_A$$

where

γ_A is a real constant between 0 and 1, corresponding to the range 0° to 180° , set by the statistical analysis of infant respiratory data.

For example, $\gamma_A = 0.5$ would result in phase estimates greater than 90° being detected as asynchrony present, whereas phase estimates less than or equal to 90° would be detected as acceptable asynchrony.

Respiratory Pauses:

The respiratory pause detector decides:

$$H_0 \text{ if } T_1 > \gamma_{\text{P}}^{\text{ab}} \text{ or } T_2 > \gamma_{\text{P}}^{\text{rc}}$$

$$H_1 \text{ if } T_1 \leq \gamma_{\text{P}}^{\text{ab}} \text{ and } T_2 \leq \gamma_{\text{P}}^{\text{rc}}$$

where

$\gamma_{\text{P}}^{\text{ab}}$ and $\gamma_{\text{P}}^{\text{rc}}$ are real constants, greater than or equal to zero, set by the statistical analysis of infant respiratory data.

Movement Artifacts:

The movement artifact detector decides:

$$H_0 \text{ if } (T_3 \leq \gamma_{\text{M1}}^{\text{ab}} \text{ or } T_5 \leq \gamma_{\text{M2}}^{\text{ab}}) \text{ and } (T_4 \leq \gamma_{\text{M1}}^{\text{rc}} \text{ or } T_6 \leq \gamma_{\text{M2}}^{\text{rc}})$$

$$H_1 \text{ if } (T_3 > \gamma_{\text{M1}}^{\text{ab}} \text{ and } T_5 > \gamma_{\text{M2}}^{\text{ab}}) \text{ or } (T_4 > \gamma_{\text{M1}}^{\text{rc}} \text{ and } T_6 > \gamma_{\text{M2}}^{\text{rc}})$$

where

$\gamma_{\text{M1}}^{\text{ab}}$ and $\gamma_{\text{M1}}^{\text{rc}}$ are real constants, greater than or equal to zero and less than or equal to one; $\gamma_{\text{M2}}^{\text{ab}}$, and $\gamma_{\text{M2}}^{\text{rc}}$ are real constants, greater than or equal to zero; all are set by the statistical analysis of infant respiratory data.

2.7.6 Statistical Thresholds

Respiratory event detection is realized using the aforementioned test statistics along with appropriately set statistical thresholds. The thresholds γ_{A} , $\gamma_{\text{P}}^{\text{ab}}$, $\gamma_{\text{P}}^{\text{rc}}$, $\gamma_{\text{M1}}^{\text{ab}}$, $\gamma_{\text{M2}}^{\text{ab}}$, $\gamma_{\text{M1}}^{\text{rc}}$ and $\gamma_{\text{M2}}^{\text{rc}}$ are determined by the statistical analysis of patient data records visually annotated by clinicians. This is performed by computing the test statistics on patient data records, segmented according to respiratory event (respiratory pause, gross body movement, asynchronous breathing, other), as annotated by a clinician. This is performed to obtain

distributions of the test statistics for each of the respiratory events. These distributions can then be used to determine the thresholds in order to estimate whether a respiratory event is present or absent.

For example, the statistical threshold γ^c_p and γ^{ab}_p can be set to tailor the respiratory event detector to a single patient's cardiorespiratory data. This would be done by computing the test statistics T_1 and T_2 for both the abdominal and ribcage RIP signals of the patient data record being investigated, where the record was segmented and grouped according to having a respiratory pause absent (H_0), or present (H_1).

As a representative example, the probability density functions (PDF) of the test statistic T_1 for a single patient data record are given in Figure 2-9. The PDF's for the mutually exclusive hypotheses of absence or presence of respiratory pause on the abdomen RIP signal are denoted as $dF(T_1;H_0)$ and $dF(T_1;H_1)$ respectively. The data set was segmented for analysis using visual annotation performed by Dr. Karen A. Brown.

In this example, the aim is to set the threshold γ^c_p on the test statistic T_1 so as to discriminate between the two PDF's in Figure 2.9 at some desired confidence level, and consequently distinguish between a respiratory pause being present or absent on the abdomen RIP signal.

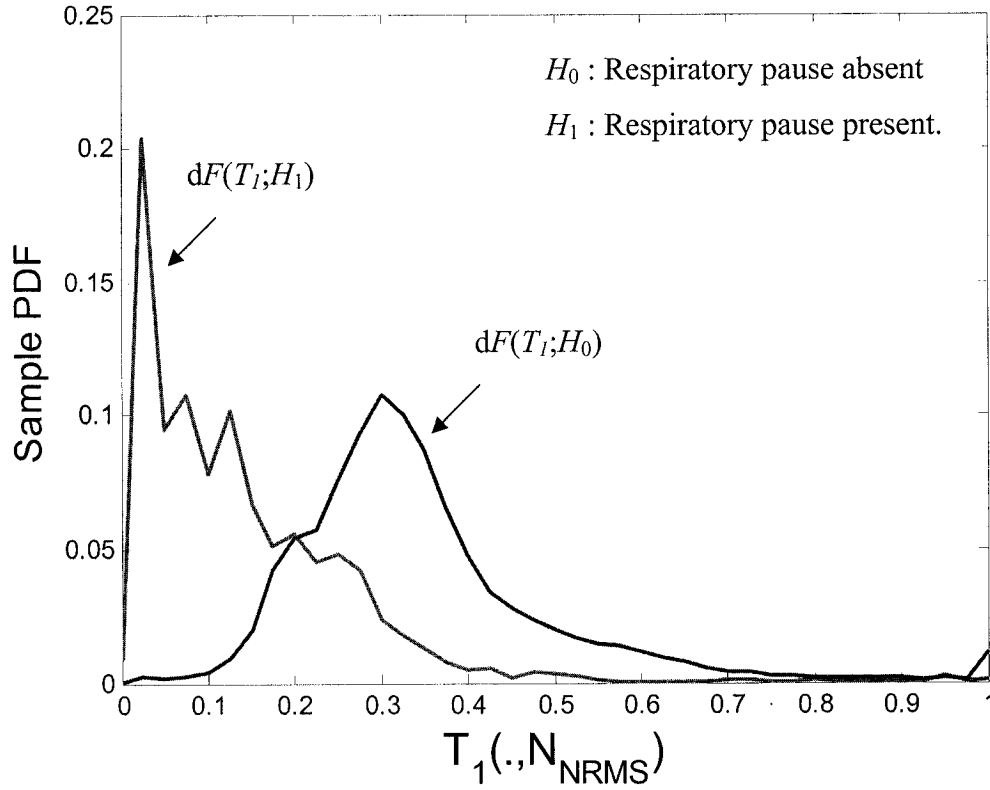


Figure 2-9: Sample distributions of the test statistic $T_1[n; N_{RMS}]$ for $N_{RMS}=251$ (5s at 50Hz), under the hypotheses H_0 (respiratory pause absent) and H_1 (respiratory pause present) for the abdomen RIP signal of a single patient data record (Montreal Children's Hospital Study ID: *MUR*).

The performance of this type of detector depends on the discrimination between the probability density functions. It cannot be assumed that this decision will be made without error unless the PDF's exhibit no overlap, however we can aim to achieve a performance commensurate with human scorers. For example in Figure 9, the threshold γ_P^c on T_1 can be selected to detect respiratory pause at a certain confidence level and rate of false detection. If statistical models for respiratory events were available, the determination of optimal thresholds could be achieved using the Bayesian, the Minimax or the Neyman-Pearson detection frameworks (e.g. see [55]). The construction of statistical models from the entire library of data acquired and visually annotated at the Montreal Children's Hospital and the determination of optimal statistical thresholds is the subject of future work (see Chapter 5).

2.8 Current Apnea Monitors

Current apnea detection systems, which show adequate performance in the literature [i.e. [28, 48, 51, 52], generally perform poorly on clinical data as a result of their underlying automated algorithms. Additionally, these systems do not state the expected percentage of missed apneas and/or false detections, making it difficult to assess their true performance. Most current monitors also require expert operators, making them unsuitable for unattended care, and are large and cumbersome, making them inappropriate for home and recovery room monitoring.

Current monitors are inadequate for the study of apnea; most perform apnea event detection exclusively and do not log or analyze cardiorespiratory data preceding or following the apnea event. As a result, they provide no insight into the relation between apneas and trends in patient cardiorespiratory state, and are not useful for investigating the pathophysiology and etiology of apnea. Furthermore, a monitor that analyzes the entire data record on-line and continuously is necessary if apnea *prediction* is to be realized in the future.

2.9 Thesis Objective

Manual analysis of cardiorespiratory data records is time-consuming, costly, and so is limited to a small number of patients. Furthermore, the results are subjective and prone to human error.

Widespread, systematic study of the pathophysiology and etiology of apnea requires a portable, automated system that is not restricted to sleep labs, and can be applied to analyze data as it is acquired. Current monitors, which perform poorly and are generally restricted to sleep labs, are inadequate for this task.

The objective of this thesis was to acquire and configure hardware and software to construct a monitor capable of measuring and logging patient cardiorespiratory data, and

providing a digital signal processing architecture to physically realize the automated, respiratory event detection algorithms previously developed here at McGill University.

The monitor was designed to be robust, portable and battery-operated to make it suitable for immediate use in the post-operative recovery room at the Montreal Children's hospital as a point-of-care diagnostic tool. The automated detection methods were also modified for real-time use and the monitor applies them on-line as it acquires the cardiorespiratory data.

3 The Cardiorespiratory Monitor

The objective of this thesis was to acquire and configure hardware and software to construct a monitor that measures and analyzes patient cardiorespiratory data. This monitor would provide a digital signal processing architecture to physically realize the automated, respiratory event detection algorithms developed previously at McGill University.

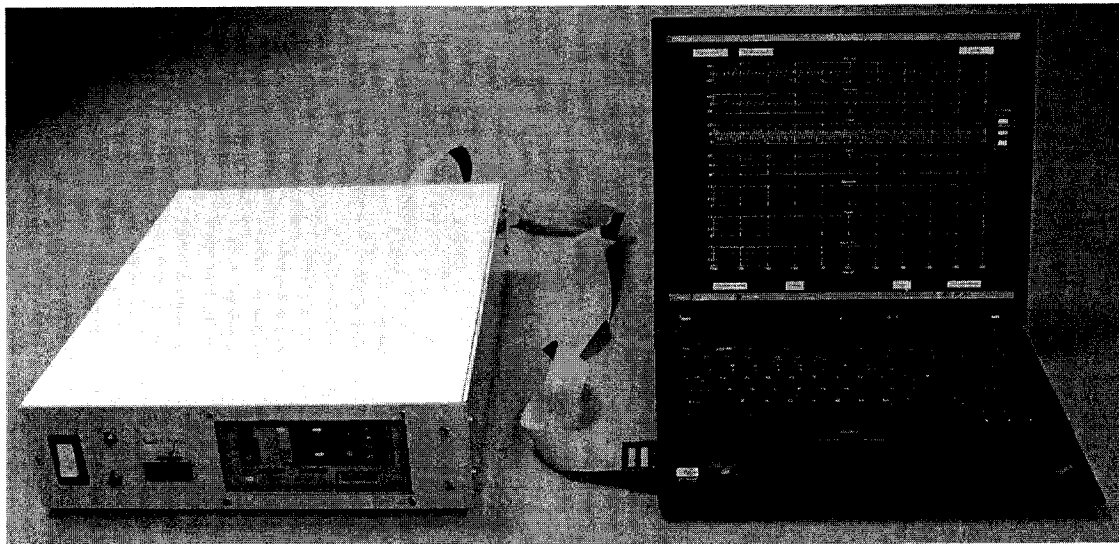


Figure 3-1: The cardiorespiratory monitor: (left) clinical monitoring system, (right) cardiorespiratory workstation.

The monitor constructed consists of a clinical monitoring system and a cardiorespiratory workstation (Fig. 3-1). The clinical monitoring system contains sensors that measure abdominal and thoracic breathing movements, heart rate, and blood oxygen saturation. It was designed to be robust, portable and battery-operated to make it suitable for use in the post-operative recovery room at the Montreal Children's hospital. The cardiorespiratory workstation is a notepad computer, for which a Matlab toolbox was written to perform automated classification, annotation and display of the patient cardiorespiratory data as it is acquired by the clinical monitoring system. The monitor stores and archives both raw and processed data, and provides an interactive graphical user interface for patient monitoring.

3.1 Clinical Monitoring System

The clinical monitoring system measures patient cardiorespiratory data. Hardware was selected for compactness and efficient power consumption. The transducer electronics and analog signal filtering are all contained in a portable and battery-operated unit. Infants will move and be moved as needed and are likely to be picked up by their parents and/or caregiver; as a result, the monitoring system was constructed to be robust.

Ribcage and abdomen expansion are measured by a respiratory inductance plethysmograph; a pulse oximeter measures blood oxygen saturation and finger plethysmographic pulse rate. No changes were made to these devices or their sensors, which are commercially available, robust and approved for clinical use.

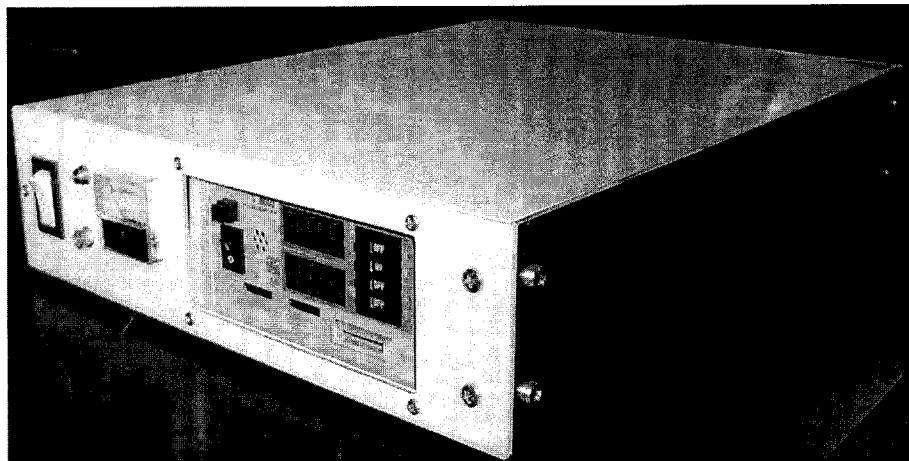


Figure 3-2: Clinical monitoring system.

The clinical monitoring system (Fig. 3-2) has dimensions of 8.89 x 43.18 x 33.02 cm, and a weight of 4.9 kg; it is approximately the size of a briefcase, making it portable and unobtrusive, which is essential for use in the post-operative recovery room. The overall structure of the system as well its individual components are described in detail in the sections that follow.

3.1.1 Overall Hardware Structure

The overall hardware structure is as shown in Figure 3-3. The clinical monitoring system houses the pulse oximeter and the low pass filter. The respiratory inductance plethysmograph is external because it must be near the patient; it is connected to the clinical monitoring system by two cables: a data cable and a power cable.

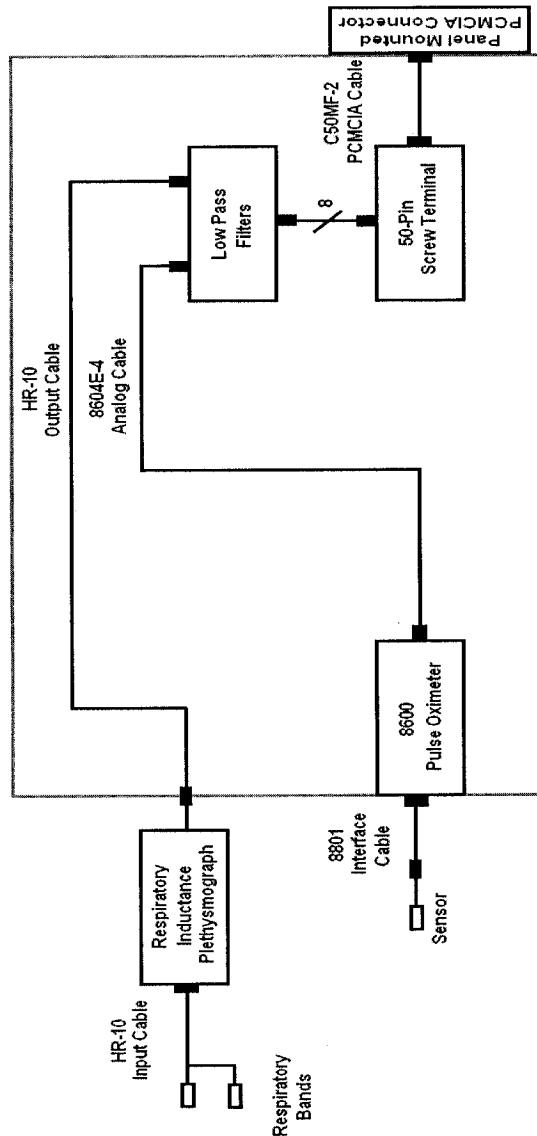


Figure 3-3: Overall hardware structure of the clinical monitoring system.

The hardware components are mounted to the case using adhesive backed cable tie mounts (Panduit, ABMM-A-C, Tinley Park, IL), and cable ties (Panduit, PLT2M-M, Tinley Park, IL). Additionally, pegs were screwed into the case to prevent shifting. The interior of the clinical monitoring system is shown in Figure 3-4. A user guide for operating the clinical monitoring system is provided in the Appendix.

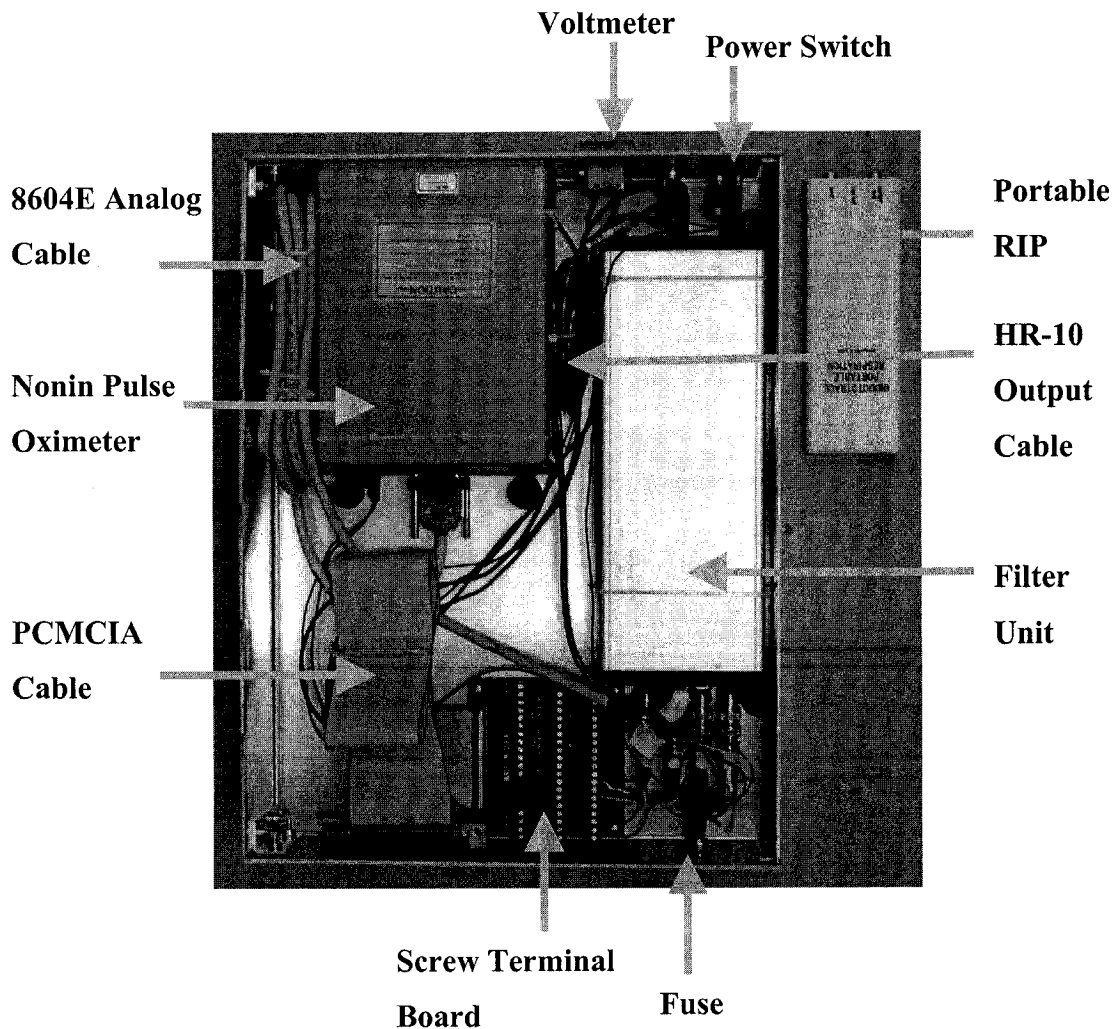


Figure 3-4: Interior of clinical monitoring system.

3.1.2 System Electronics

To connect the components electrically, 22 AWG gage electrical wire was used. Power pin jacks (center positive supply, edge negative supply) were soldered to the wires and used for connecting power cables to hardware components. Power pin jacks were used so that equipment could be easily disconnected and removed for maintenance or replacement. For system power cables that connect externally to the clinical monitoring system (for example, for connecting the system battery to the monitoring system) power pin receptacles were mounted on the enclosure and screw-locking power pin jacks were used; screw-locking jacks decrease the risk of the cables being disconnected during operation (Fig 3-5).

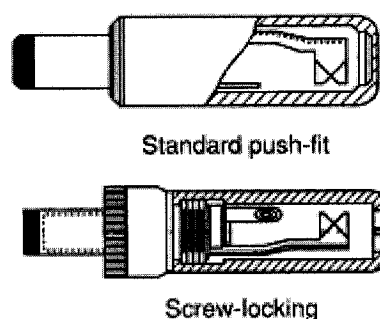


Figure 3-5: Standard power pin-jacks [56].

A 15A system power switch (NKK, WR11BS, Scottsdale, AZ) was used to connect the monitoring system to battery power and the monitoring system was equipped with a fuse to protect the internal monitoring devices from damage due to short-circuits. Inrush currents when the system is immediately turned on were measured using an ammeter and did not significantly exceed the normal operating current, thus a 1A fast-acting fuse (250V, 3AG, axial) (Littelfuse, 312-001, Des Plaines, IL) was used to protect equipment from damage. A fast-acting fuse was used because the electronics of the clinical monitors are sensitive and may be damaged by even brief exposure to incorrect current levels. An external voltage display (DC voltmeter, 0-15V, moving magnet, accuracy: $\pm 5\%$) (Jewell Modutec, OMS-DVV-015-U, Manchester, NH) was mounted to the

enclosure to provide feedback about system operation and to track battery-power level. A simplified circuit diagram is shown in Figure 3-6.

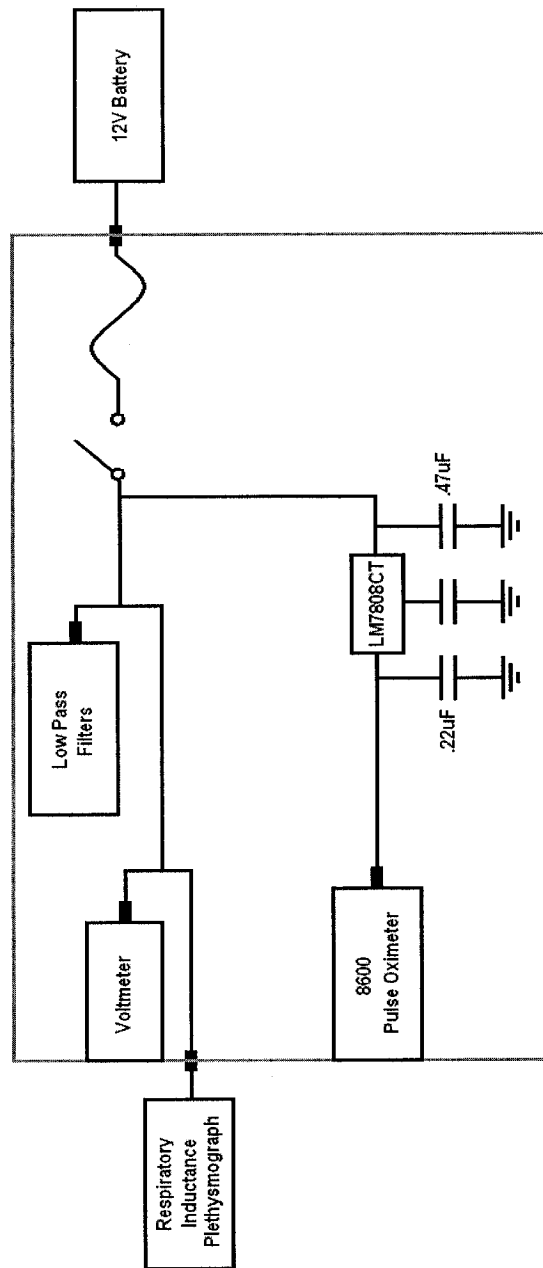


Figure 3-6: Simplified circuit diagram of clinical monitoring system electronics.

The Nonin pulse oximeter operates at 8V, while the other equipment operates at 12V; therefore, an 8V voltage regulator (National Semiconductor, LM7808CT, 8V, 1A, TO-220, Santa Clara, CA) was installed to control the voltage to the pulse oximeter. The current requirements of the pulse oximeter are low (0.15A), and the voltage conversion is only from 12V to 8V, so the heat generated by the regulator is minimal; consequently, the regulator was bolted directly to the aluminum case of the clinical monitoring system, which acts as a heat-sink. Bypass capacitors were connected to the input and output of the regulator for optimum stability and transient response.

The two monitoring devices, as well as the filtering unit were all provided with individual shielding by the manufacturer. All devices were wired to share a common ground with the system electronics. The enclosure of the clinical monitoring system (BUD, Valuline NHC-14155, Willoughby, OH) is made of aluminum, weighs 1.9kg and was attached to this common ground. The enclosure has no ventilation, but the heat produced by the equipment during operation was measured, and was minimal; the temperature of the device did not exceed that of the room. Both the front and back of the enclosure (Fig 3-7) were milled to mount the cable connectors, fuse, power switch, and voltage display; this was performed using a turret milling machine (Millmaster, Model 3VK) retrofitted with a computer controller (Fagor, CNC 8040MC).

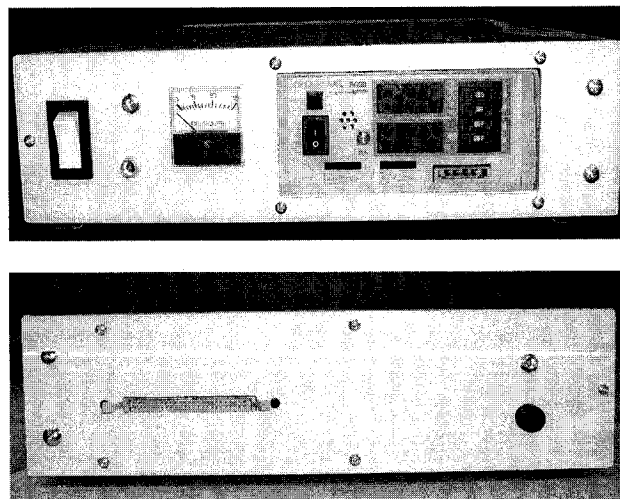


Figure 3-7: Panels of clinical monitoring system: (top) front panel, (bottom) back panel.

3.1.3 Respiratory Inductance Plethysmograph

Respiratory inductance bands (Ambulatory Monitoring Inc., Inductobands, Ardsley, NY) interfaced with a respiratory inductance plethysmograph (Ambulatory Monitoring Inc., Battery Operated Inductotrace, Ardsley, NY) measure ribcage and abdomen movement. Respiratory bands sized for neonates through to adults are available.

The plethysmograph is small (17.7 x 6.2 x 2.2 cm), lightweight (152g), and has low power consumption (3mA at 12V). Also it performs un-calibrated measurements, which is a necessity because of the inaccuracy of RIP calibration for infants.

The ribcage and abdomen outputs are analog voltages in the range [-1.2V, 1.2V], inspiration (increasing volume) causes a positive output. The output signals are internally bandpass filtered by the plethysmograph at 0.007Hz to 4 Hz (-3db). The upper cutoff attenuates noise, while the lower cutoff ensures that disturbances to the respiratory motion signal will eventually decay to baseline, and that baseline drift is eliminated. The unit can monitor respiratory rates in the range of 1 to 110 breaths per minute with a quantitative error of less than 10% introduced by this internal filtering [57].

A six-foot analog data cable (BTX, YV-HR10MCGILLXX, Hawthorne, NY) with a HR10A-7P-6P connector on one end and a HR10A-7P-6S connector on the other end was custom designed to connect the analog output data of the RIP unit to the clinical monitoring system enclosure. All connectors were manufactured by Hirose (Hirose, Simi Valley, CA). The HR10A-7P-6P connector of the RIP output cable mates with a HR10A-7R-6S receptacle connector, panel mounted onto the front of the clinical monitoring system.

Internal to the clinical monitoring system, the pins of the panel mounted connector were soldered to the pins of a HR10-7R-6S connector which was mated with the RIP analog output cable (Ambulatory Monitoring Inc., HR10 Output Cable, Ardsley, NY). Each of the two analog data cable wires was soldered with system ground to a BNC connector.

These two BNC connectors were mated to BNC connectors mounted on the anti-aliasing filter unit.

Though the respiratory inductance plethysmography unit is external to the clinical monitoring system, it is powered from the same system battery. A cable was constructed with a screw-locking power pin jack on one end and a snap-lock battery connector on the other. The screw-locking power pin jack connects to a power pin-jack receptacle on the front panel of the clinical monitoring system, while the snap-lock battery power connector connects to the RIP unit battery power connector (Fig. 3-8). The lid of the RIP unit battery compartment was filed down to close over the cable. Internal to the clinical monitoring system, the connectors of the power-pin receptacle mounted on the front panel were wired directly to the 12V junction of the voltage regulator.

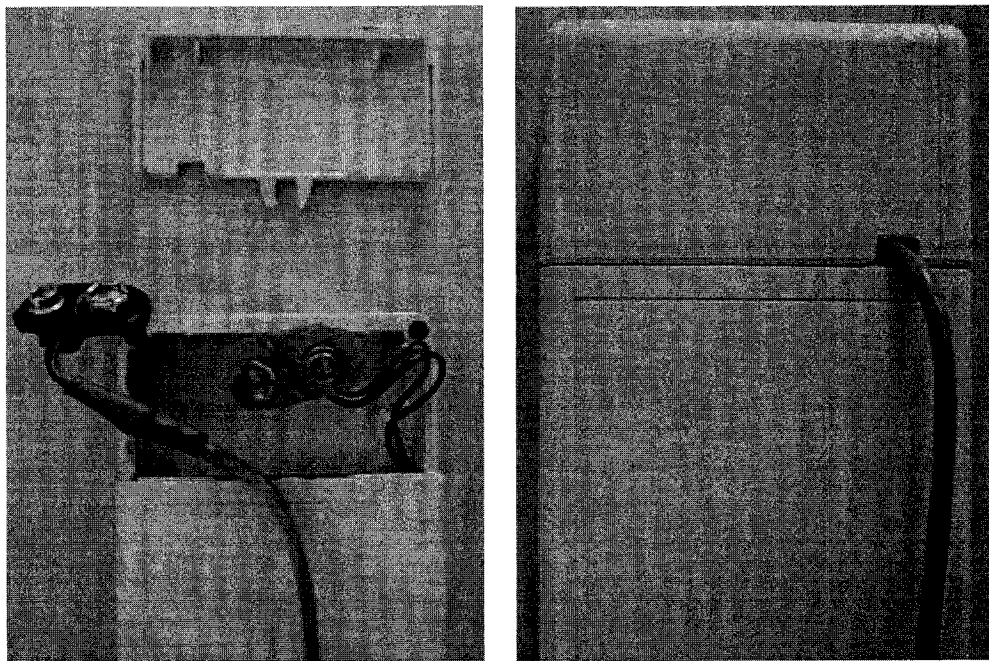


Figure 3-8: Power cable fashioned for portable RIP unit.

3.1.4 Pulse Oximeter

Blood oxygen saturation, and finger plethysmographic heart rate are measured using a pulse oximeter probe sensor interfaced with a pulse oximeter (Nonin, 8600 Tabletop/Portable Digital Pulse Oximeter, Plymouth, MN). The pulse oximeter is small (15 cm x 7 cm x 19 cm), lightweight (624g), and has low power consumption (150mA at 8V). Oximeter probes sized for neonates through to adults are available.

During apneas, oxygenation can change very quickly, so continuous oxygenation monitoring is a necessity to minimize the risk of these changes going undetected. Pulse oximetry performs continuous monitoring, and is non-invasive, operationally simple and does not require routine calibration or maintenance; this permits unattended monitoring and eliminates the requirement of an expert operator, which is important for monitoring in the post-operative recovery room.

The Nonin oximeter is supplied with an internal 5-cell rechargeable Ni-Cad battery pack; this pack was disconnected and removed from the unit. A push-fit power pin jack was fitted to the external power receptacle of the unit; this pin jack was wired directly to the 8V junction of the voltage regulator circuit. The oximeter operates exclusively from the main battery of the clinical monitoring system.

An analog data output cable (Nonin, 8604E-4, Plymouth, MN) was connected to the rear of the pulse oximeter. This cable provides the data output of the pulse oximeter: the blood oxygen saturation is provided as an analog voltage in the range [0V, 1V], corresponding to 0 to 100% SpO₂; while the plethysmographic pulse waveform, representing the pulsatile changes in blood flow, is an analog voltage in the range [0V, 1V]. The system ground of the oximeter is also available via this cable. Each of the two analog data cable wires were soldered differentially with the system ground to BNC connectors. These two BNC connectors were mated with BNC connectors mounted on the anti-aliasing filter unit.

3.1.5 Anti-Aliasing Filtering

The cardiorespiratory signals are coupled differentially to a four-channel, anti-aliasing filter, using BNC connectors. Signals are acquired differentially rather than single-ended to reduce noise. Each of the cardiorespiratory data channels are differenced with system ground; consequently, voltage common to both channels, such as electromagnetic interference, radio-frequency interference and other sources of environmental noise, are rejected. This is imperative in a clinical environment, such as the post-operative recovery room, where there are myriad electrical clinical devices, producing electro-magnetic interference, which could corrupt the data. The two RIP signals are AC coupled to the filters (-3dB at 0.16Hz). The coupling of the input channels (differential, AC) is set by DIP switches on the filter carrier cards internal to the filter unit. A power pin jack was fitted to the power pin receptacle of the filter unit, and wired to the 12V junction of the voltage regulator circuit.

The low-pass, anti-aliasing filter is necessary for two reasons. First the cardiorespiratory data signals are analyzed using digital signal processing techniques, and must be sampled prior to analysis. During sampling, frequency components greater than half the sampling rate "alias" into the frequency band, corrupting the data; consequently these higher frequencies must be filtered out prior to A/D acquisition [54]. Second, low-pass filtering eliminates other sources of noise such as corrupting physiological data signals and environmental noise outside the bandwidth of interest by attenuating higher-frequency components. The low-pass filter serves to minimize corruption in the data channels prior to data-acquisition and digital signal processing by the cardiorespiratory workstation.

Our pilot work showed that respiratory-related information in the ribcage and abdominal RIP signals is at frequencies below 4Hz. Finger plethysmographic pulse waveform and blood oxygen saturation information is at frequencies below 5Hz [58]. Consequently, a cutoff frequency of 10Hz serves to faithfully preserve the amplitude characteristics of the data channels, while attenuating undesired higher-frequency noise components. The cardiorespiratory data is low-pass filtered at a cutoff frequency of 10Hz using an 8-pole Bessel anti-aliasing filter (Kemo, 21.2 rack with 21.2 CardMaster:12/08/03-12/08/07,

Jacksonville, FL) prior to being acquired and sampled by the cardiorespiratory workstation. The performance characteristics of the filter used are given in Figure 3-9.

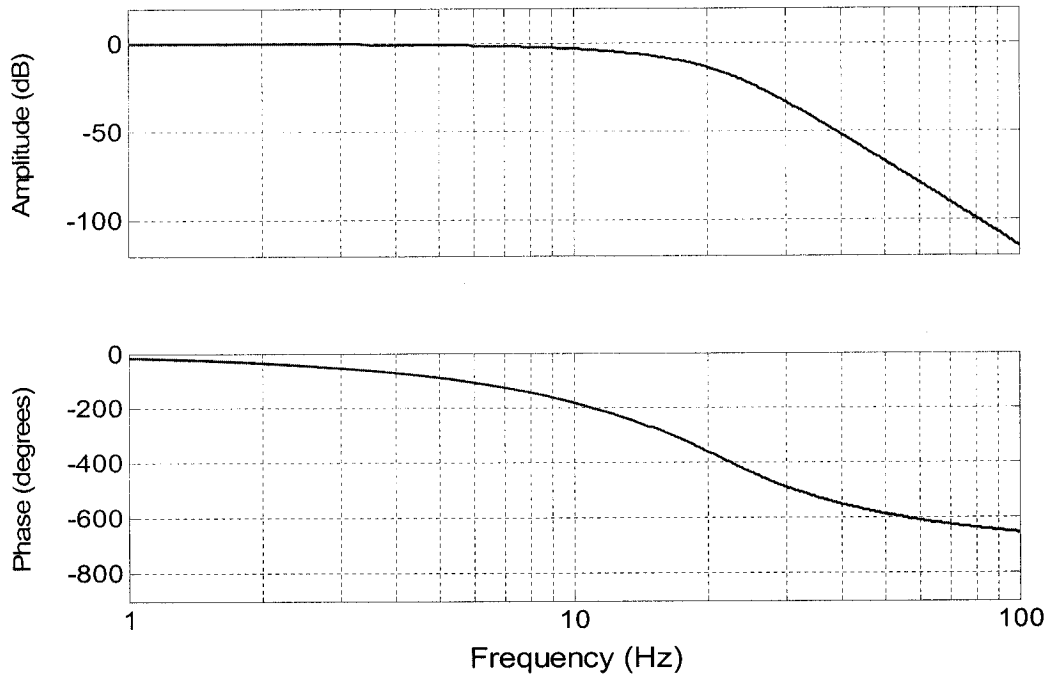


Figure 3-9: Filter response characteristics for Bessel anti-aliasing filter: (top) amplitude response, (bottom) phase response.

Bessel filters were used to preserve the phase information between the thoracic and abdominal excursions. Analog Bessel filters show a linear phase response in the passband, which means that the passband frequencies are delayed an equal amount of time as they pass through the filter; this linearity can be represented by the group delay, which is the derivative of the phase response with respect to frequency [54].

$$D(w) = -\frac{d\Theta(w)}{dw} \quad (3.1)$$

where,

Θ is the phase in radians,

w is the frequency in radians/s.

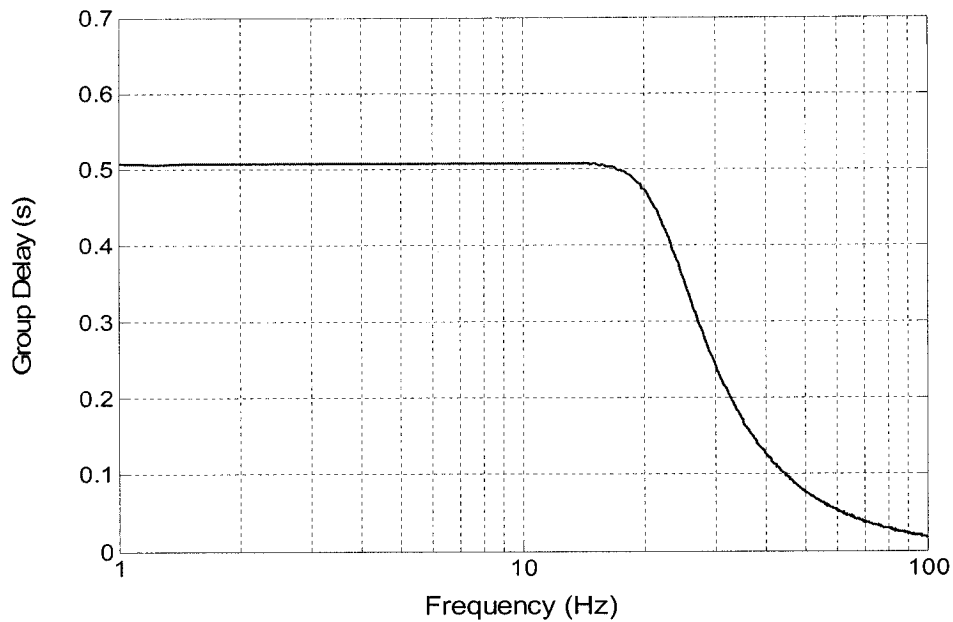


Figure 3-10: Group delay of Bessel anti-aliasing filter.

The group delay for the anti-aliasing filter is shown in Figure 3-10; it can be observed that the filter shows a nearly flat group delay in the pass band. This means that the frequency components are not shifted in phase (or time) with respect to each other. Bessel filters exhibit this near flat group delay in the pass-band at the expense of a less-steep cutoff in the stop-band. This is an acceptable trade-off for the preservation of phase information, which has been shown to be important in the study of obstructive apnea and other breathing disorders [59-61]; in particular, it is the parameter that is used by the respiratory event detection algorithm to detect asynchronous breathing.

The four-channel filter is small (12.7cm x 5cm x 28cm approx.), lightweight (1626g), and has low power consumption (0.47A at 12V). The four filtered output signals are provided from the anti-aliasing unit via BNC connectors, with the shield of the connectors being system ground. BNC connectors were fitted to these outputs and 22 AWG wire was soldered to these connectors to interface them to a PCMCIA analog terminal board.

3.1.6 Battery

A rechargeable battery-pack (Ni-MH, 12V, 4500mAh, Sanyo Cell HR-4/3FAU) powers the clinical monitoring system. Nickel-metal Hydride (Ni-MH) is the battery chemistry with the second-highest energy density after Li-ion. Li-ion, which is the costliest chemistry, was not used because it requires custom-made safety-circuits, and poses the risk of explosion during charging. With NiMh, a long operating time can be obtained with a very compact, lightweight energy source. The NiMh pack is 13.6 x 9.1 x 1.9 cm, weighs 611g and contains 10 Sanyo Cell HR-4/3FAU batteries; it is fitted with a standard power pin jack. The clinical monitoring system is not restricted to this battery-pack—it can operate from any 12V battery if longer operating time is required.

Table 3-1: Electrical current consumption of clinical monitoring system.

Unit	Voltage	Current
Pulse Oximeter	8V	.150A
Inductotrace	12V	.003A
Anti-Aliasing Filter Unit	12V	.470A
Voltage Regulator	-	.008A
Total	-	.631A

The electrical current consumption of the entire monitoring system is 757.2 mA (worst case, multiplied by a factor of 1.2). The Ni-MH battery pack provides a minimum autonomous operating time for the monitoring system of 6h. At the Montreal Children's Hospital, cardiorespiratory data is collected from infants for approximately four hours in the post-operative recovery room, so this battery is adequate for the current studies being performed.

Operating the clinical monitoring system exclusively from battery-power avoids many of the problems associated with being connected to the main power line, such as power supply interruptions, power surges, and in particular electrical shocks to the patient and

patient burns due to leakage current (small amounts of 60Hz power line current that “leak” from patient connections or the metal cases of instruments).

Electrical shock is of particular concern for respiratory inductance plethysmography, which involves placing current-carrying inductance bands around the chest and respiratory muscles of the patient; the proximity of the transducer bands to these important organs can amplify the effects of even small leakage currents. Consequently, there is the risk of shock to the heart, which could result in cardiac arrhythmias; as well as shock to the respiratory muscles, which could result in asphyxia due to respiratory muscle spasms. These risks are particularly pertinent for cardiorespiratory monitoring, because patients may be unconscious or anesthetized and may not respond normally to an electric current.

Additionally, during cardiorespiratory-monitoring, patients may be left unattended. These concerns are of additional importance for infants, as the immaturity of their physiology can make them particularly susceptible to trauma. Operating the system from battery power maximizes patient safety and obviates the need for patient isolation; additionally, it makes the monitoring system portable and eliminates the need for power wires, which are an obstruction in the recovery room and pose the risk of entanglement to the patient.

The NIMH battery-pack is fitted with a power pin jack receptacle. A cable was constructed with a standard power pin jack on one end to connect to the battery-pack and a screw-locking power-pin jack on the other end, which connects with the power-pin jack receptacle on the rear-panel of the clinical monitoring system.

3.1.7 Output of Clinical Monitoring System

As outlined, internal to the monitoring system analog output data cables connect the cardiorespiratory equipment to the lowpass filters differentially. The filtered analog outputs of the anti-aliasing filter are connected to a 50-pin screw terminal board

(Techmatron, CIO-MINI50, QC, CA), bolted to the base of the case of the clinical monitoring system. A 2ft 50-pin PCMCIA cable (Techmatron, C50MF-2, QC, CA) has its female IDC 50-pin connector connected to the terminal panel, and its male IDC 50-pin connector mounted to the chassis of the clinical monitoring system. An aluminum mounting bracket was machined to fix this connector to the case, using the turret milling machine. The filtered analog output signals and system ground are available externally from the rear panel of the clinical monitoring system via this 50-pin PCMCIA male IDC connector. This connector is compatible with any 50 pin PCMCIA cable.

For the cardiorespiratory workstation, a 39-inch 50 pin PCMCIA cable (Techmatron, CPCC-50F-39, QC, CA) connects the clinical monitoring system to the data acquisition card of the notepad PC. The cardiorespiratory workstation is described in the next section.

3.2 *Cardiorespiratory Workstation*

The analog outputs of the clinical monitoring system are interfaced to the cardiorespiratory workstation via a PCMCIA cable, connected to a PCMCIA card (overall data flow schematic shown in Fig. 3-11). A Matlab toolbox was developed to acquire, classify, annotate and display this patient cardiorespiratory data. The toolbox implements the respiratory event detection algorithms developed previously at McGill University. The workstation runs this toolbox to perform these tasks on-line, as the clinical data are acquired, in a fully-automated manner, requiring no expert operator. It is suitable for unattended monitoring in the post-operative recovery room.

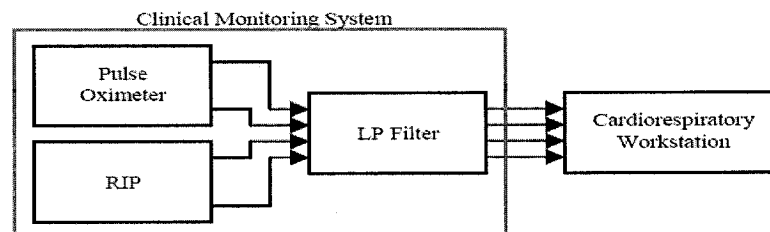


Figure 3-11: Overall data flow schematic of the cardiorespiratory monitor.

The cardiorespiratory workstation consists of a notepad computer, equipped with a PCMCIA data acquisition card. It provides the user with an interactive graphical interface to analyze cardiorespiratory data and perform file management. These components are described individually in the sections that follow.

3.2.1 Notepad Computer

The cardiorespiratory workstation can be any PC-compatible computer that runs Windows NT 4.0, Windows 2000, or Windows XP with a data-acquisition card or board, and having the basic Matlab suite as well as Matlab's Real-Time Workshop and Real-Time Windows Target [62].

At the Montreal Children's Hospital, a notepad computer (IBM, 1.8 GHz, 1024 MB memory, 80 GB hard drive, Markham, ON) is used. The notepad computer is operated from battery power (IBM, T40 Series High Capacity Li-Ion Battery, Ultrabay Slim Li Polymer Battery, Markham, ON). The two laptop batteries permit the workstation to operate, and power the data-acquisition card (150ma at 5V) for six hours. The notepad computer is equipped with Matlab 7.0 (R14), Simulink 6.0 (R14), Real-Time Workshop Toolbox 6.0 (R14), and Real-Time Windows Target 2.5 (R14).

3.2.2 Data Acquisition

A PCMCIA card (PC-CARD-DAS16/16 Measurement Computing PCMCIA, 8 differential inputs, 100 KHz, 16-bit A/D, 8 digital I/O) acquires the four analog outputs of the clinical monitoring system differentially; signals are sampled at 50 Hz with 16 bits of resolution in a range from -1.25V to 1.25V; this provides a resolution of .038mV. The card has a typical noise performance of approximately .068mV RMS, and a slew rate of $\pm 0.7\text{V}/\mu\text{s}$ min [63]. This resolution is compliant with the European Data Format (EDF) for Polygraphic Sleep Recordings, which stores data at 16 bits [64].

A 50Hz sampling rate is appropriate given the signals are lowpass filtered at 10Hz; it also provides adequate resolution for the on-line graphical display, which is used by clinicians for patient monitoring.

3.2.3 Overall Software Structure

The Matlab toolbox provides an interface for both on-line and off-line data analysis. The overall software structure, as presented to the user through the graphical user interface, is shown in Figure 3-12.

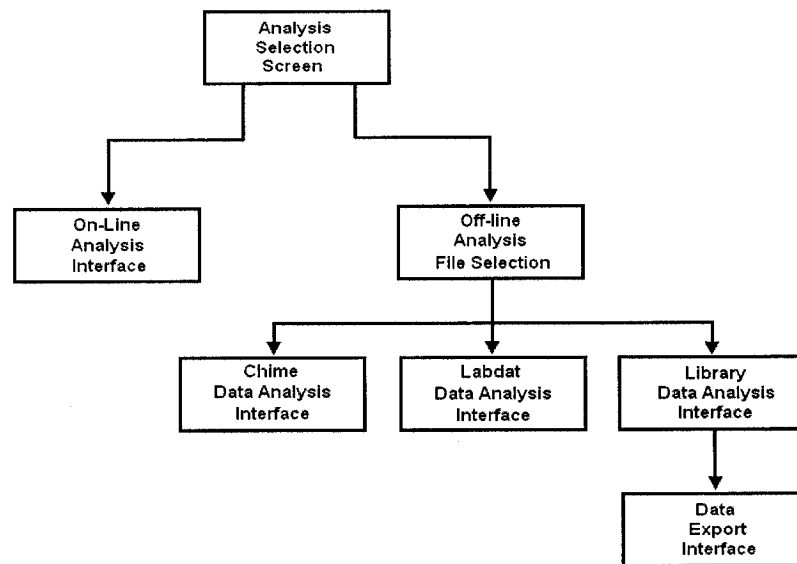


Figure 3-12: Overall structure of software toolbox developed for cardiorespiratory workstation.

The on-line interface allows the user to analyze cardiorespiratory data as they are acquired from the clinical monitoring system and to display the data and its analysis on-line, permitting patient monitoring. The off-line interface permits the user to analyze previously acquired patient data; it supports the off-line analysis of data from the Chime group, which is in the EDF format, as well as data acquired previously at the Montreal Children's Hospital, which is in the Labdat data format.

Cardiorespiratory data can be stored in Matlab and EDF data formats, and as a Microsoft Excel Spreadsheet (see Section 3.2.7). A user operating guide outlining the complete functionality of the user-interface, as well as its installation and operation instructions is provided in the Appendix.

3.2.4 Interactive Graphical User Interface

The interactive graphical user interface was developed using Matlab's GUIDE (Graphical User Interface Development Environment). The interface was designed to be simple and clinician friendly by developing it conjointly with experienced personnel at the Montreal Children's Hospital; this was done to minimize the burden on clinical staff who will use the monitor while they are occupied with the regular requirements of the recovery room. The introductory frames presented to the user on executing the interface are shown in Figure 3-13 as representative samples.

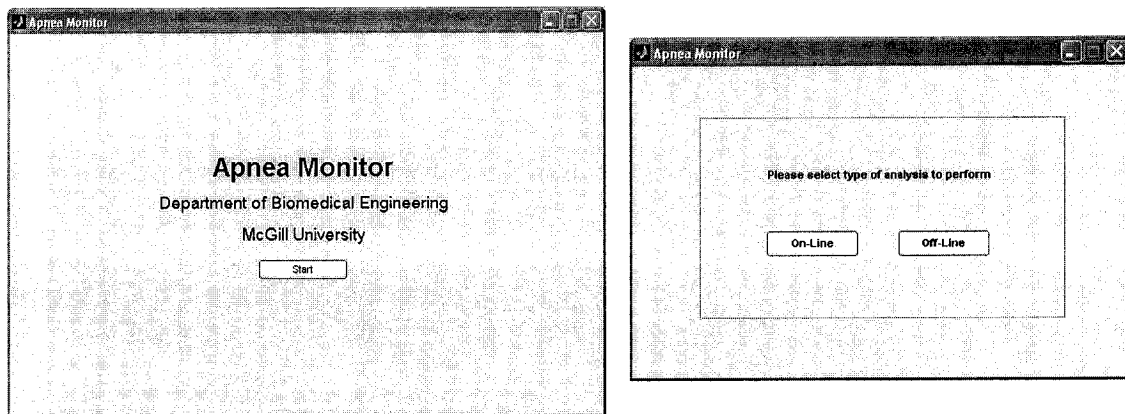


Figure 3-13: Introductory frames of graphical user interface displayed to the user on execution of the software toolbox of the cardiorespiratory workstation.

The interface permits on-line patient monitoring by a clinician. Additionally, the user can tune the settings of the automated algorithms in real-time as the data are acquired; this is important for validation of the algorithms as new data are acquired. The interface also permits viewing and analyzing cardiorespiratory data off-line and provides simple access to the file storage, archiving and management features.

The on-line and off-line functionality, as well as the file management functionality are described individually in the sections that follow. Where appropriate, screen captures of the corresponding graphical user interface displays are provided.

3.2.5 On-Line Analysis

The automated respiratory event detection algorithms were implemented as Matlab Simulink block diagrams (Figs. 3-16, 3-19 and 3-20), which allows them to be applied to analyze data in real-time. This high-level representation is translated by Matlab's Real Time Workshop into real-time code (an executable containing the binary form of the algorithms).

On-line analysis is implemented using Matlab's Real-Time Windows Target 2.5 (R14). The software uses a small real-time kernel, which runs as a kernel-mode driver, and intercepts timer interrupts from the PC clock, ensuring on-line execution of the cardiorespiratory monitoring at CPU ring zero (the highest priority possible) [65]. The real-time code form of the algorithms is applied to the data channels as they are acquired from the clinical monitoring system. All processing for each data sample is completed within the sampling interval (.02s) to ensure real-time performance.

The kernel also maintains clock signals for the Windows operating system, sending timer interrupts at the original rate. As a result, the PC performs all its regular tasks simultaneous with on-line operation of the cardiorespiratory monitoring software. Windows applications continue to run, using the CPU cycles unused by cardiorespiratory data analysis.

The implementation of the three respiratory event detection algorithms previously developed as Simulink diagrams are described individually in the sections below.

Gross Body Movement Detector:

The test statistics for gross body movement outlined in Section 2.7.3 were implemented as a Simulink block diagram using mathematical blocks and FIR filters; additionally, because the algorithms are applied in real-time, delay elements were incorporated to account for FIR filter delays, so that corresponding sample points are aligned during computations. During on-line analysis, the total delay from start of an event to its initial detection is 7.76s. Given that cessation of breathing is only considered apnea if it is at least ten seconds, this is an acceptable delay. This delay is removed during post-processing when the data record's annotation is stored by removing this 7.76s offset from the annotation data.

A simplified block diagram for computing the two gross body movement test statistics for the ribcage signal is shown in Figure 3-14.

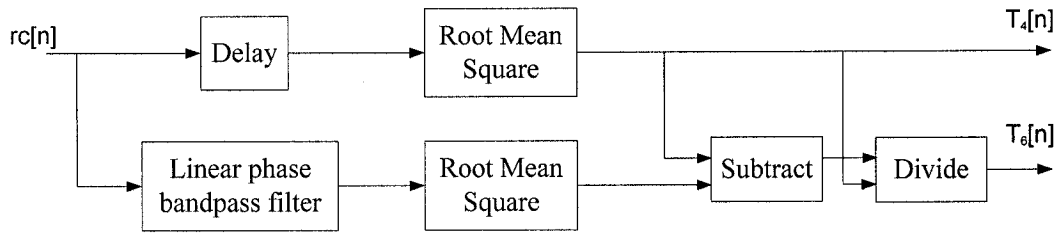


Figure 3-14: Simplified block diagram for computing the two gross body movement test statistics for the ribcage RIP signal.

Comparators were used to compare the test statistics to their statistical thresholds γ_{M1}^{ab} , γ_{M2}^{ab} , γ_{M1}^{rc} and γ_{M2}^{rc} . Logic gates were implemented to generate the decisions H_0 and H_1 (absence or presence of gross body movement) from the binary signals generated by the comparators. A block diagram of the comparators and the subsequent logic implemented to perform the decision on the presence or absence of gross body movement is shown in Figure 3-15.

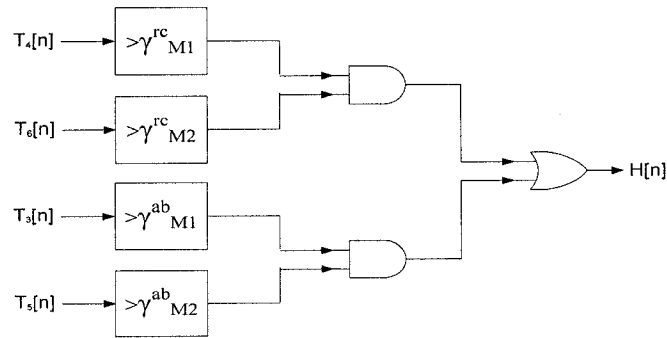


Figure 3-15: Simplified block diagram for computing decision on presence or absence of gross body movement from test statistics computed on the ribcage and abdomen RIP signals.

The binary decision on the presence or absence of gross body movement generated from the logic shown in Figure 3-15 is then low pass filtered to average it over a window of NM previous samples. The averaged decision over this window is then compared to the threshold γ_M to judge whether gross body movement is detected or not.

The FIR filter lengths were established by investigating the statistical properties of cardiorespiratory data sets obtained at the Montreal Children's Hospital. The order of the bandpass filter (NBP) must be high enough to achieve adequate noise reduction, yet low enough to minimize the contribution to the on-line detection delay. Pilot studies based on data from 22 infants, sampled at 50 Hz, gave reasonable results with linear phase digital filters with order 200, corresponding to a 2 second delay. Periods of gross body movement as brief as 2s were identified by clinicians; consequently, the energy filters were set to 4s (NRMS). The low pass averaging filters were set to 3s (NM). The Simulink block diagram for the entire gross body movement detector is shown in Figure 3-16.

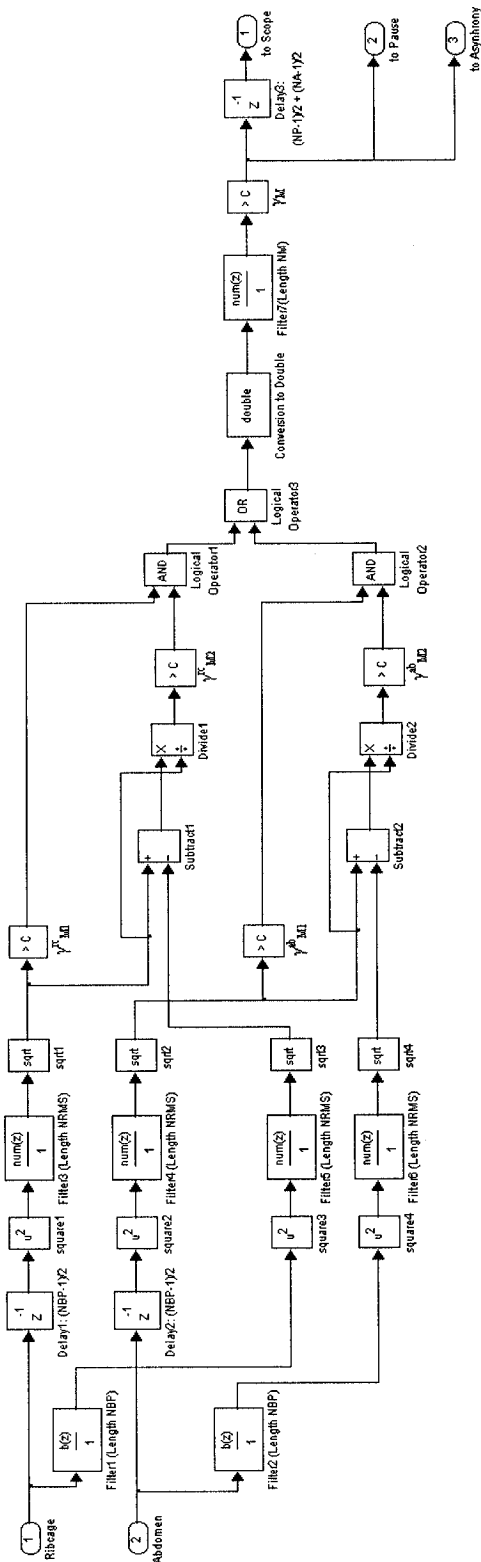


Figure 3-16: Simulink block diagram used by the software toolbox of the cardiorespiratory workstation for the on-line detection of gross body movement from ribcage and abdomen RIP signals.

Respiratory Pauses:

The test statistics for respiratory pauses outlined in Section 2.7.2 were implemented into a Simulink diagram using mathematical blocks, and FIR filters; a simplified block diagram for computing the respiratory pause test statistics is shown in Figure 3-17.

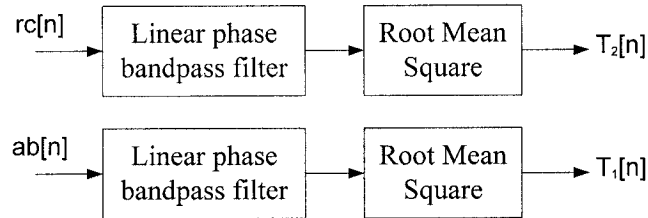


Figure 3-17: Simplified block diagram for computing respiratory pause test statistics.

Comparators were used to compare the test statistics to their statistical thresholds γ_P^{rc} and γ_P^{ab} (Fig. 3-18). A logical *OR* gate was implemented to perform the decision on the absence or presence of respiratory pause from the binary signals generated from these comparators.

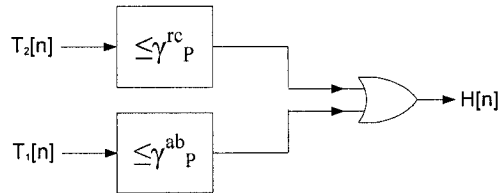


Figure 3-18: Simplified block diagram for computing decision on presence or absence of respiratory pause from test statistics computed on ribcage and abdomen RIP signals.

Additionally, we hypothesize that there are no respiratory pauses during periods of gross body movement. Consequently, the decision from the gross body movement detector was inverted and applied with the decision from the respiratory pause detector to a logical *AND* logic gate. This ensures that a respiratory pause is only detected if there is no gross body movement detected concurrently.

The binary decision on the presence or absence of respiratory pauses is low pass filtered to average it over a window of NP previous samples. The averaged decision over this window is then compared to the threshold γ_p to judge whether a respiratory pause is detected or not.

The FIR filter lengths were established by investigating the statistical properties of cardiorespiratory data sets obtained at the Montreal Children's Hospital. The order of the bandpass filter was of order 200, corresponding to a 2 second delay. The energy filters were set to 4s (NRMS) and the low pass averaging filter was set to 2s (NP). The Simulink block diagram for the entire respiratory pause detector is shown in Figure 3-19.

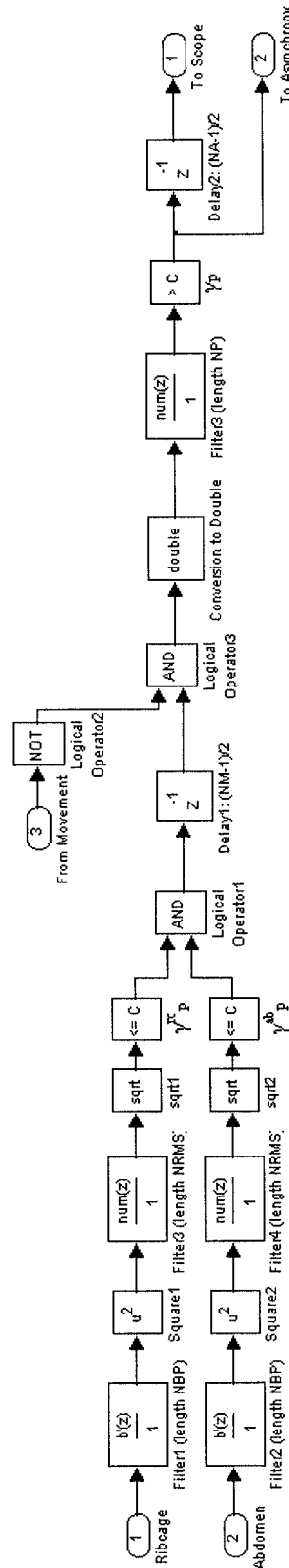


Figure 3-19: Simulink block diagram used by the software toolbox of the cardiorespiratory workstation for the on-line detection of respiratory pause from ribcage and abdomen RIP signals.

Asynchronous Breathing:

The test statistic for asynchronous breathing outlined in Section 2.7.1 was implemented as a Simulink diagram using mathematical blocks and FIR filters, as in Figure 2-8. Additionally, it was hypothesized that there are no obstructive apneas during periods of gross body movement or during periods of respiratory pause. Consequently, the decisions from the gross body movement detector and from the respiratory pause detector are inverted and applied with the decision on asynchronous breathing to a logical *AND* gate. This ensures that obstructive apnea is only detected if there is no gross body movement or respiratory pause detected concurrently. A comparator was implemented to compare the test statistic to the statistical threshold γ_A .

The FIR filter lengths were established by investigating the statistical properties of cardiorespiratory data sets obtained at the Montreal Children's Hospital. The bandpass filter was of order 200. The lower frequency observed for the power spectral density for infant respiration was observed to be 0.4 Hz, consequently the length (NA) of the filter for estimating the phase was chosen to be $1/0.4$ or 2.5 seconds. The Simulink block diagram for the entire asynchronous breathing detector is shown in Figure 3-20.

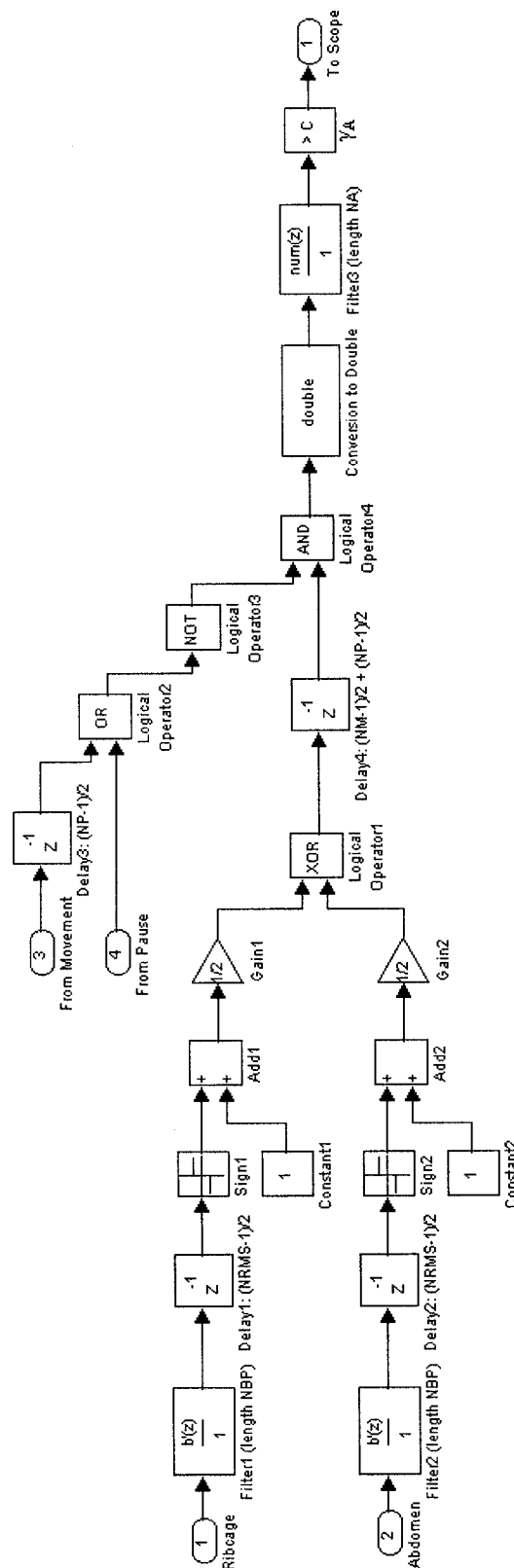


Figure 3-20: Simulink block diagram used by software toolbox of the cardiorespiratory workstation for the on-line detection of asynchronous breathing from ribcage and abdomen RIP signals.

On-Line Statistical Thresholds:

The thresholds for on-line analysis were set as shown in Table 3-2. These were set taking into account both the range of the AMI respiratory inductance plethysmograph (-1.2V, 1.2V), as well as an investigation of the statistics of infant breathing as annotated by Dr. Karen A. Brown.

Table 3-2: Statistical thresholds used by the software toolbox of the cardiorespiratory monitor for on-line analysis.

Parameter	Value
γ_{M1}^{ab}	0.7
γ_{M2}^{ab}	0.05
γ_{M1}^{rc}	0.7
γ_{M2}^{rc}	0.05
γ_P^{ab}	0.001
γ_P^{rc}	0.001
γ_A	0.7
γ_P	0.6
γ_M	0.6

The cardiorespiratory monitor must be applied at the Montreal Children's Hospital to acquire additional cardiorespiratory data sets. The construction of statistical models from data acquired and visually annotated by clinicians at the MCH to optimally determine the statistical thresholds is the subject of future work (see Chapter 5).

The thresholds γ_A , γ_M and γ_P can be manipulated as the data are acquired, using the on-line graphical user interface, which is shown in Figure 3-21; this display permits the user to execute and halt the acquisition and analysis of cardiorespiratory data from the clinical monitoring system, as well as to store the results to file. Its functionality is described at further length in the user manual provided in the Appendix.

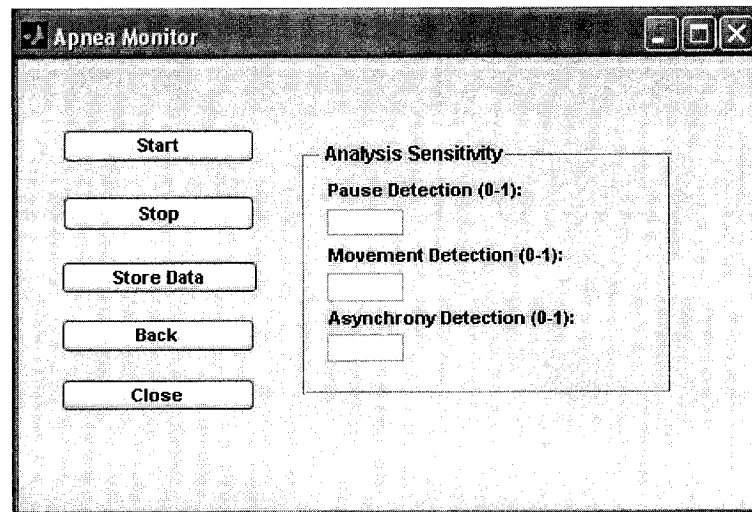


Figure 3-21: On-line graphical user interface for executing and interrupting the acquisition and analysis of cardiorespiratory data from the clinical monitoring system, as well as for manipulating statistical analysis thresholds and performing file storage.

On-Line Data Acquisition:

The raw data and its annotation are logged by the workstation as the data are acquired. At each sample interval, Simulink stores contiguous data points in memory. When a data buffer is filled, Simulink transfers the data to a variable in the Matlab workspace while the real-time application continues to run. After thirty minutes of data has been acquired this Matlab variable is stored to a *.mat* file on the disk drive. The application transfers data from the buffer to the workspace as well as from the workspace to the disk drive, within one sampling interval. Consequently, no data is lost and all data points are contiguous.

The cardiorespiratory data, as well as its analysis, are displayed as the data are acquired. The display (Figure 3-22) provides the four cardiorespiratory data channels, ordered from top to bottom as: ribcage RIP, abdomen RIP, plethysmographic pulse waveform and SaO_2 ; as well as the three cardiorespiratory state channels, which are three binary logical decision signals (a logical one on each of these signals represents the detection of a respiratory event), ordered from top to bottom as gross body movement, respiratory pause, and asynchronous breathing. On-line, one fifty-second epoch of data is displayed at a time, before the frame is refreshed.

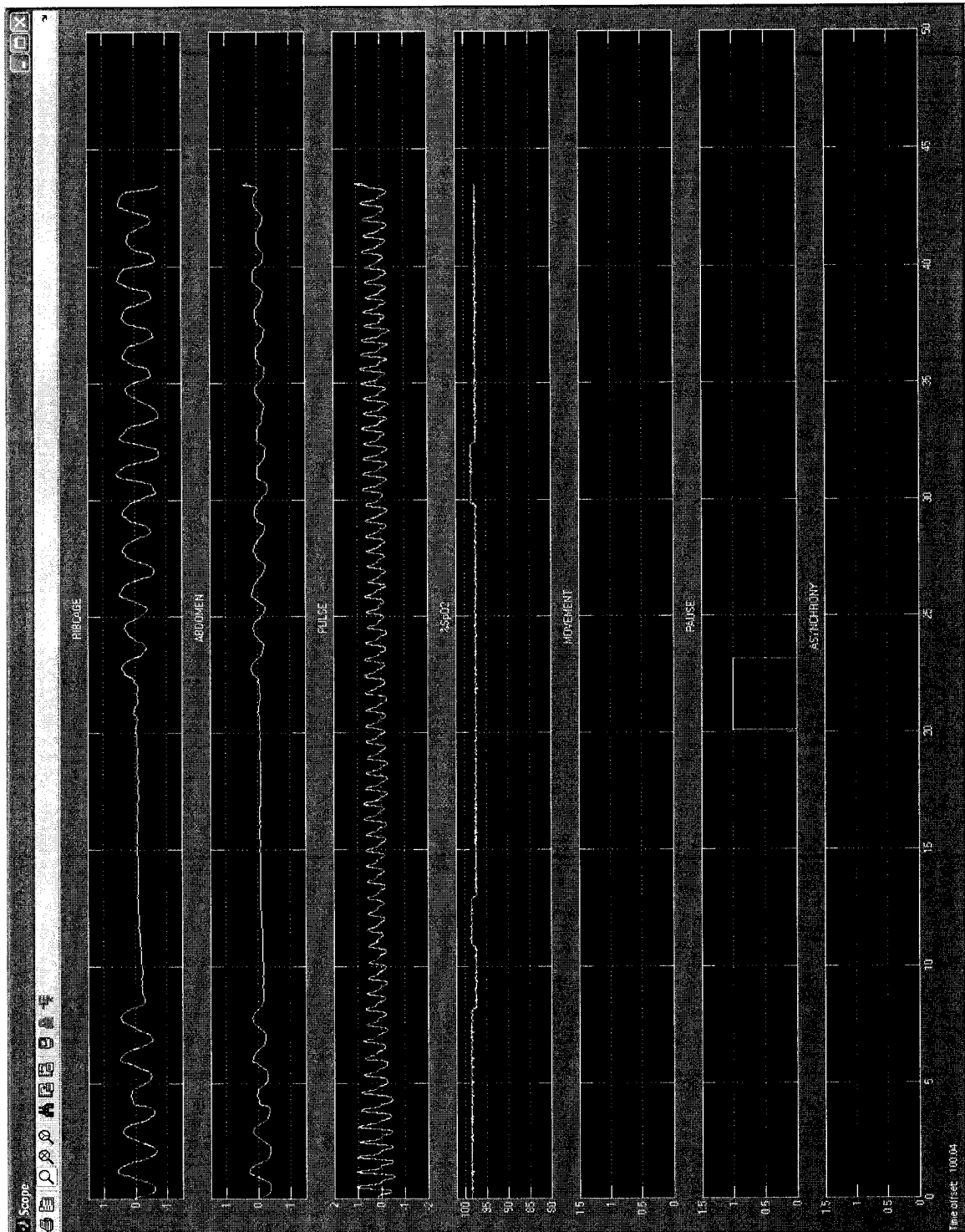


Figure 3-22: On-line graphical display, which provides the four cardiorespiratory data channels, as well as the three respiratory event detection channels as the data are acquired from the clinical monitoring system; a respiratory pause was simulated by the patient and is detected by the monitor (following a 7.6s on-line processing delay), denoted by a logical one on the binary pause classification channel.

3.2.6 Off-Line Analysis

Cardiorespiratory data was acquired previously from infants of various ages at the Montreal Children's hospital. Additionally, the Collaborative Home Infant Monitoring Evaluation (CHIME) Research Group offers a large, public database of cardiorespiratory data records from infants. Both these databases contain data that was annotated by trained clinicians. Consequently, these data sets offer an important resource of data for validating the performance of the cardiorespiratory monitor for detecting apneas against the annotation of clinicians, and assessing the effectiveness of the monitor. As a result, the cardiorespiratory workstation was designed to be capable of analyzing previously acquired data sets.

The workstation supports analysis of data in the LABDAT™ format (RHT-InfoDat, Montreal), which is the format of the data previously acquired at the MCH; it also supports data stored in the European Data Format (EDF) for Polygraphic Sleep Recordings, which is the format of the data acquired by the CHIME group. The CHIME database is the largest longitudinal physiologic dataset of infants publicly available. The workstation can be used to view the analysis of these cardiorespiratory data sets and the annotated data sets can then be archived in a library in the database of the workstation for latter review.

The graphical user interface for viewing CHIME data records, and data annotation performed by the CHIME group, is shown in Figure 3-23. The cardiorespiratory data, as well as its analysis, are displayed concurrently. The four cardiorespiratory data channels are ordered from top to bottom as: ribcage RIP, abdomen RIP, plethysmographic pulse waveform and SaO₂. The next three channels are the binary respiratory event detection signals provided by the clinicians of the CHIME group, ordered on the display from top to bottom as arousal, central apnea and obstructive apnea. One fifty-second epoch of data is displayed at a time. These data records were acquired by the CHIME group with a proprietary monitor called the Alice 3 (Respironics, Inc., Murrysville, PA, USA). The functionality of this interface is described at further length in the user manual provided in the Appendix.

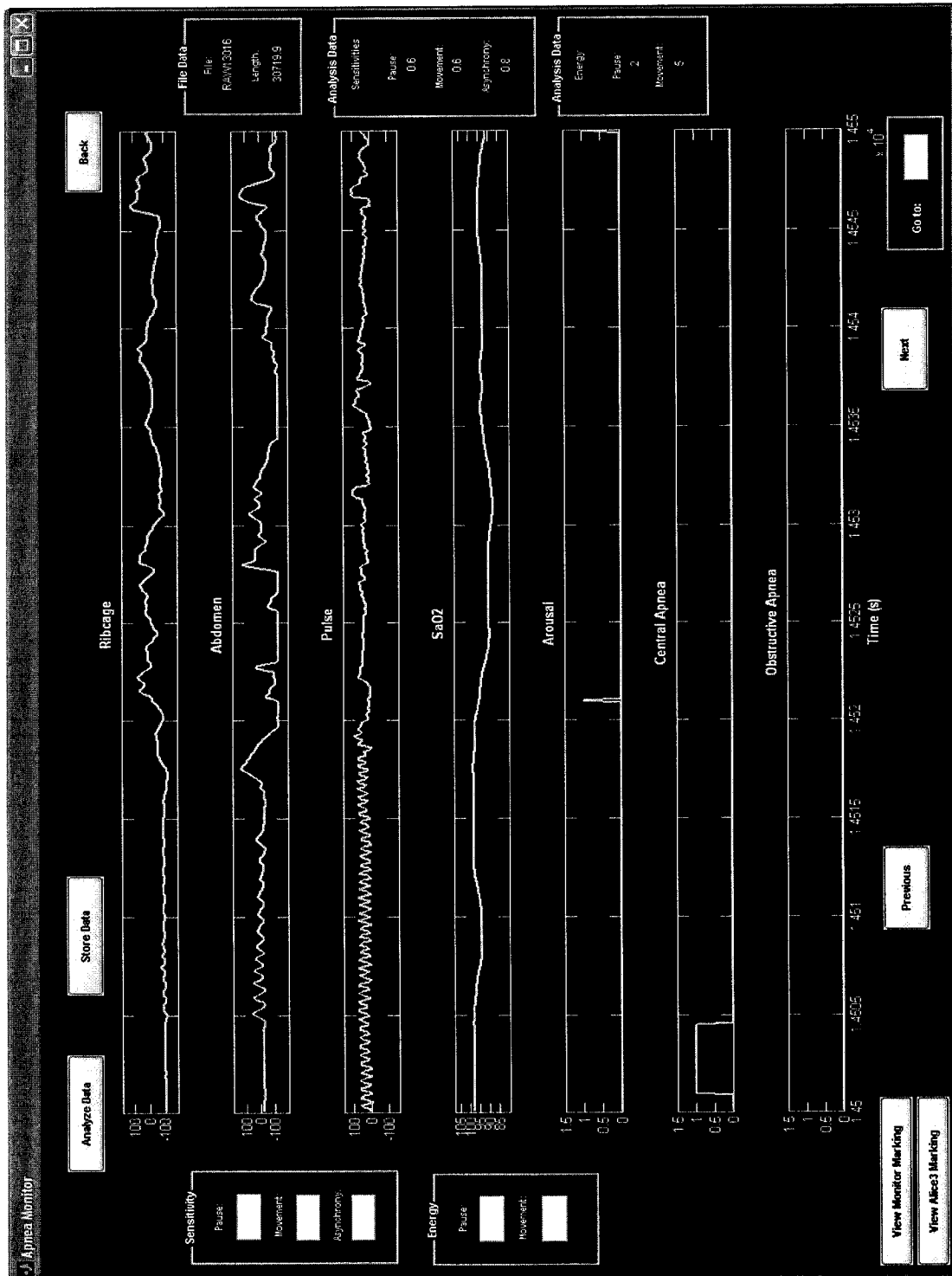


Figure 3-23: Graphical user interface of cardiorespiratory workstation used for viewing CHIME cardiorespiratory data records, which displays the four cardiorespiratory data channels, as well as the three binary CHIME respiratory event detection channels concurrently (CHIME data record Study ID: 13016); in this frame the Alice 3 monitor detected a central apnea followed by an arousal, denoted by logical one's on the corresponding binary classification channels.

3.2.7 File Management

On-line and off-line cardiorespiratory data sets and their annotation by the workstation can be stored and archived in Matlab data format as well as EDF data format. Data can also be exported as a Microsoft Excel spreadsheet, which is preferred by many clinicians for the visual inspection of cardiorespiratory data results. Data files are stored to a library folder, and can be reviewed using the graphical interface (for more detail see the software operating guide found in the Appendix).

Data stored in the Matlab format, as well as data provided as an Excel spreadsheet is stored in columns, ordered as shown in Table 3-3. Data stored in the Matlab format is provided as a *.mat* file, containing an eight column array of doubles; data stored as an Excel spreadsheet is similarly provided as eight-columns of numerical data.

Table 3-3: Column ordering of cardiorespiratory data and its analysis when stored to file by the clinical monitoring system.

Column	Data
1	Time (s)
2	RC RIP
3	ABD RIP
4	Finger Pleth.
5	%SpO ₂
6	Movement
7	Pause
8	Asynchrony

A graphical user interface is provided for storing cardiorespiratory data and its analysis to file (Figure 3-24). This interface permits the user to store descriptors to identify both the recording as well as the patient. Furthermore, the date and time that the recording was performed can be stored.

The screenshot shows a window titled "Apnea Monitor" with a standard Windows-style title bar (minimize, maximize, close buttons). Inside the window, there is a section titled "File Annotation" which contains four text input fields labeled "Recording:", "Patient:", "Start Date:", and "Start Time:". Below these fields are two buttons: "Export to EDF" and "Back".

Figure 3-24: Graphical user interface for exporting cardiorespiratory data records to EDF format, permitting the user to store recording and patient descriptors, as well as the date and time that the recording was performed.

EDF is a simple and flexible digital format for sleep recordings; it is the accepted standard in commercially available equipment and for exchange between different equipment and different laboratories [66]. Because EDF is independent of hardware, as well as operating system and software environment, it can be used to exchange data between different laboratories, expanding the library of available data for validation of the automated algorithms.

Each EDF data file contains one digitized polygraphic recording. A data file consists of a header followed by the data records. The header is variable-length, and contains recording information to identify the patient, the date and time of the recording, as well as the technical characteristics of the recording, such as the transducers used. The data records contain consecutive fixed-duration epochs of the polygraphic recording. Each epoch contains the data obtained from all transducers during that epoch; Table 3-4 outlines the format of an EDF data record in detail.

Table 3-4: EDF format [64].

Header Record

8 ascii	Version of this data format (0)
80 scii	Local patient identification
80 ascii	Local recording identification
8 ascii	Start date of recording (dd mm yy)
8 ascii	Start time of recording (hh mm ss)
8 ascii	Number of bytes in header record
44 ascii	Reserved
8 ascii	Number of data records (-1 if unknown)
8 ascii	Duration of a data record, in seconds
4 ascii	Number of signals (ns) in data record
NS * 16 ascii	NS * label (e.g. EEG, FpzCz, body temp)
NS * 80 ascii	NS * transducer type (e.g. AgAgCl electrode)
NS * 8 ascii	NS * physical dimension (e.g. μ V, $^{\circ}$ C)
NS * 8 ascii	NS * physical minimum (e.g. -500, 34)
NS * 8 ascii	NS * physical maximum (e.g. 500, 40)
NS * 8 ascii	NS * digital minimum (e.g. -2048)
NS * 8 ascii	NS * digital maximum (e.g. 2047)
NS * 80 ascii	NS * prefiltering (e.g. HP 0 1Hz LP 75Hz)
NS * 8 ascii	NS * NR of samples in each data record
NS * 32 ascii	NS * reserved

Data Record

NR of samples[1] * integer	First signal in the data record
NR of sanples[2] * integer	Second signal
:	
NR of samples[ns] * integer	Last signal

4 Analyses of Cardiorespiratory Data Sets

The statistical analyses of two cardiorespiratory data sets, chosen for having a high number of respiratory events, as well as performance evaluations of the analysis of these data sets by the cardiorespiratory monitor, are presented in this section. Representative visual examples are also provided to illustrate how the interface developed permits clinicians to view and analyze cardiorespiratory data records using the event detection algorithms.

The cardiorespiratory data presented in this section was acquired from infants monitored in the post-anesthesia recovery room at the Montreal Children's Hospital. These data sets were previously reported by Dr. Karen A. Brown as part of another study [23]. The data sets were acquired using non-calibrated AC-coupled RespiTrace (NIMSTM, RespiTrace Plus, North Bay Village, Florida). The RIP signals were filtered at 15-Hz using 8-pole Bessel filters (Frequency Devices, Haverhill, MA), sampled at 50 Hz with a 12-bit analog-to-digital converter (Data Translation, Marlborough, MA), and stored on PC desktop computer using LABDATTM data acquisition software (RHT-InfoDat, Montreal).

Dr. Karen A. Brown and colleagues recorded these data from infants recovering from general caudal anesthesia at the Montreal Children's Hospital. The study was approved by the Institutional Ethics Review Board of the MCH and written informed parental consent was obtained prior to data collection for each subject. Data were acquired from 21 infants (12 term, 9 preterm, 18 male, 3 female) whose ages varied from 39 weeks of age to 49 weeks of age ($\mu = 44.2$ weeks, $\sigma = 2.9$ weeks), and whose weights ranged from 2.5kg to 5.9kg ($\mu = 4.17$ kg, $\sigma = 0.99$ kg).

The MCH cardiorespiratory data records were visually analyzed and annotated by Dr. Karen A. Brown and exhibited a range of breathing phenomena including sighs, post-sigh apneas, mixed apneas, central apneas and obstructive apneas, as well as periods of gross body movement.

4.1 Statistical Analyses

The statistical analyses of two data sets acquired and visually annotated by a clinician at the Montreal Children's Hospital (Montreal Children's' Hospital Patient ID's: *MUR* and *MOSS*) was performed.

The data records were segmented using the visual annotation performed by clinicians, into data marked as movement, respiratory pause (central sleep apnea or post-sigh apnea), obstructive sleep apnea, and other. Test statistics were then computed on these segments to generate statistics for each type of respiratory event.

The sample probability density function distributions of these test-statistics were generated and used to set the statistical thresholds that were used to perform the data analyses from which the performance evaluations were generated (Section 4.2), and to generate the representative visual examples presented (Section 4.3). The thresholds (Tables 4-1, and 4-2) were set with a clinician, using their judgment as a standard for optimizing performance. Establishing an optimality criterion for selecting these thresholds is outside the scope of this analysis.

A comprehensive investigation of the statistical properties of all infant cardiorespiratory data obtained at the Montreal Children's Hospital, in order to systematically define these analysis thresholds is the subject of future work (see Chapter 5).

The filter lengths for analysis were established by statistical investigation. The bandpass filter (NBP) was of order 200. The length of the filter for estimating the phase (NA) was chosen to be 2.5 seconds. The length of the energy filters (NRMS) were set to 5s. The lengths of the low pass averaging filter orders were set to 3s for movement (NM) and 2s for respiratory pause (NP).

4.1.1 Methodology for Computing Statistics

To compute the statistics of the cardiorespiratory data records, respiratory events were identified from the visual annotation of the data sets by a clinician. However, this annotation was performed as part of an earlier clinical study, and was not completely adequate for computing statistics. The methodology used to account for these deficiencies in the annotation is described below.

General:

Foremost, the data were annotated coarsely. Ten second segments were annotated for the events they contained, but the start and end points of the respiratory events were not identified. To account for this, the respiratory events were isolated visually by the author. For example, a 2s post-sigh apnea was located in its 10s epoch and the start and end points estimated by visual inspection.

Movement:

When the manual analysis was originally performed, epochs that were corrupted by large amounts of gross body movement were marked as movement in their entirety so as to be disregarded from the original clinical study. As a result, extended periods of data, some as long as ten to fifteen minutes, were annotated as movement. However, these periods contained a spectrum of respiratory events, including periods of normal respiration, asynchrony and other respiratory events. For computing statistics, the entire segment had to be considered movement. As a result, these other respiratory events corrupted the computation of the movement statistics.

Asynchrony:

Periods of thoracoabdominal asynchrony were not annotated by the clinician. Consequently, only periods annotated as obstructive sleep apnea were used for computing statistics.

4.1.2 Methodology for Setting Statistical Thresholds

The distributions presented in Sections 4.1.3 and 4.1.4 are of the estimates of the test-statistics calculated at each sample point of the events. Consequently, longer events contributed a larger number of estimates than shorter events. The respiratory events marked by Dr. Karen Brown exhibited a broad range of lengths, for example, events marked as respiratory pause were as short as a few seconds (mostly post-sigh apneas), and as long as fifteen seconds (mostly central sleep apneas).

However, the apnea monitor performs sample-by-sample detection of respiratory events. As a result, the largest number of sample points correctly detected as being in a certain category does not necessarily result in the highest rate of 'event detection' for that category, which is the ultimate gauge of performance.

For example, if there were five events marked as being in a certain category, four that were 4s in length and one that was 16s in length, half the sample points could be correctly identified as being in that category, but be potentially all from the single longer event, resulting in only one out of the five events being correctly detected. When determining the statistical thresholds that were used to realize the performance evaluations, event detection was used as the standard for optimizing performance.

The clinician Dr. Karen Brown used the off-line capabilities of the cardiorespiratory monitor to analyze the two cardiorespiratory data records and set the thresholds, in order to obtain a performance that she deemed to be optimal with regards to positive detection rate and false detection rate.

This author then assessed the performance of the clinician's thresholds, with regards to sensitivity and specificity. Using the statistical distributions presented in the sections that follow as a guide, the author then attempted to improve the performance, tweaking the thresholds and assessing the resulting event detection performance of the monitor. The detection performance was more sensitive to some thresholds, in which case more

care was spent setting these parameters. In particular, the gross body movement detector was particularly sensitive to the thresholds γ_{M2}^{ab} and γ_{M2}^{rc} .

This methodology for setting the thresholds was used to obtain a reasonable assessment of the performance of the monitor, and was not expected to be optimal. The thresholds that were obtained are provided in Table 4-1, and were used to perform the performance evaluations described in Sections 4.2.

Table 4-1: Statistical thresholds used for the analysis of the (left) *MUR* and (right) *MOSS* data sets by the cardiorespiratory monitor.

Parameter	Value	Parameter	Value
γ_{M1}^{ab}	2.50	γ_{M1}^{ab}	1.00
γ_{M1}^{rc}	2.50	γ_{M1}^{rc}	1.50
γ_{M2}^{ab}	0.43	γ_{M2}^{ab}	0.40
γ_{M2}^{rc}	0.32	γ_{M2}^{rc}	0.65
γ_P^{ab}	0.16	γ_P^{ab}	0.03
γ_P^{rc}	0.16	γ_P^{rc}	0.08
γ_A	0.70	γ_A	0.75
γ_P	0.60	γ_P	0.60
γ_M	0.80	γ_M	0.80

4.1.3 Statistical Analysis: *MUR*

The patient data record *MUR* was obtained from a 45 week old term male infant, weighing 5.5kg. The recordings were performed in the post-operative recovery room at the Montreal Children's Hospital. The data record was annotated by Dr. Karen A. Brown. The statistical thresholds were set with a clinician and are provided in Table 4-1.

Movement Algorithm

The hypotheses used were:

H_0 : Gross body movement absent,

H_1 : Gross body movement present.

Using the annotation performed by the clinician, the entire cardiorespiratory data record was segmented into data marked as movement and data not marked as movement. The test statistics T_3 , T_4 , T_5 and T_6 were then computed on each of these two sets of data. The sample probability density function (PDF) distributions shown in Figures 4-1, 4-2, 4-3 and 4-3 were generated and used to set the statistical thresholds for the *MUR* data with a clinician.

Furthermore, the receiver operating characteristics (ROC's) were computed using these sample PDF distributions. The probability of detection and probability of false alarm values were computed from the areas under the PDF curves. For example, in Figure 4-1, setting a threshold $\gamma_{M1}^{ab}=2.5$, results in a probability of detection of 0.35 and a probability of false alarm of 0.02. Movement is detected if the energy estimated exceeds the threshold γ_{M1}^{ab} on T_3 . Consequently, for this example, energy estimates exceeding 2.5 would be detected as movement. As a result, probability of detection is obtained from the area under the 'gross body movement present' PDF curve above $T_3=2.5$, while the probability of false alarm value is obtained from the area under the 'gross body movement absent' PDF curve above $T_3=2.5$. Each point of the ROC curve is obtained in this manner. The ROC curves for the other test-statistics are computed similarly.

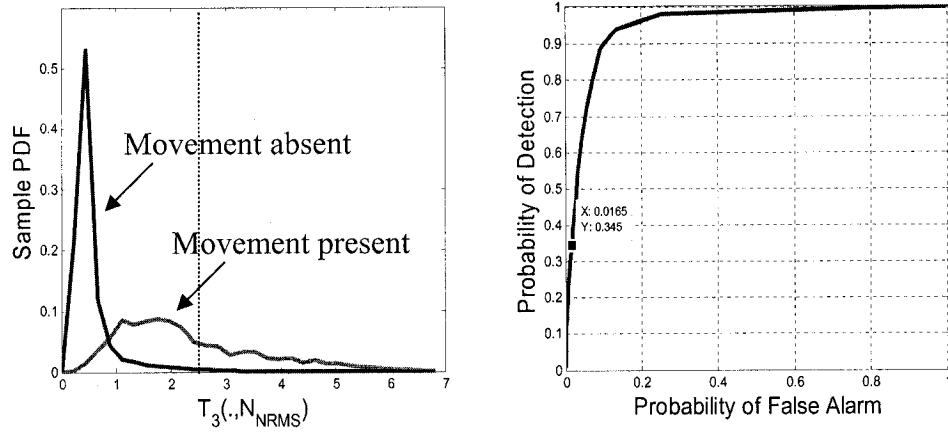


Figure 4-1: (Left) Sample probability density functions of the test statistic $T_3[n;N_{RMS}]$ computed for data marked as ‘gross body movement absent’ and data marked as ‘gross body movement present’ for the abdominal RIP signal of the *MUR* data set. (Right) The receiver operating characteristic or detection performance of $T_3[n;N_{RMS}]$ relative to the visual segmentation made by Dr. Karen A. Brown. The threshold $\gamma_{MI}^{ab}=2.5$ is indicated by a dotted line on the plot of the PDF distributions; the point corresponding to this threshold is indicated with its coordinates on the ROC curve.

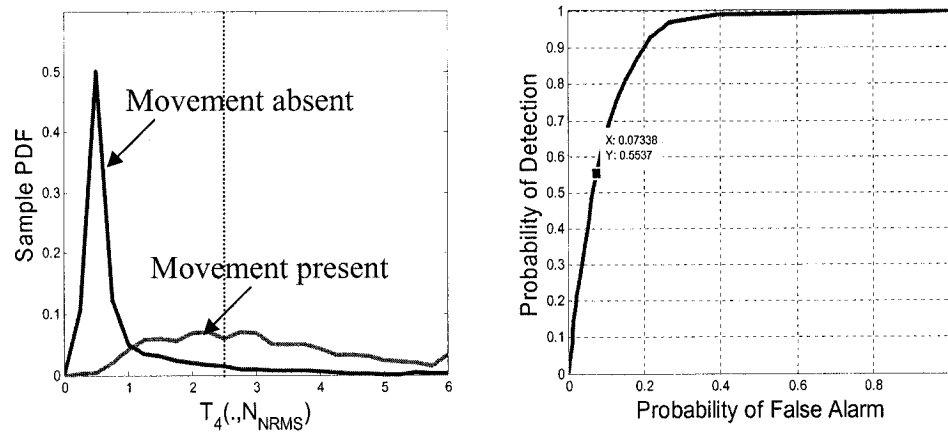


Figure 4-2: (Left) Sample probability density functions of the test statistic $T_4[n;N_{RMS}]$ computed for data marked as ‘gross body movement absent’ and data marked as ‘gross body movement present’ for the ribcage RIP signal of the *MUR* data set. (Right) The receiver operating characteristic or detection performance of $T_4[n;N_{RMS}]$ relative to the visual segmentation made by Dr. Karen A. Brown. The threshold $\gamma_{MI}^c=2.5$ is indicated by a dotted line on the plot of the PDF distributions; the point corresponding to this threshold is indicated with its coordinates on the ROC curve.

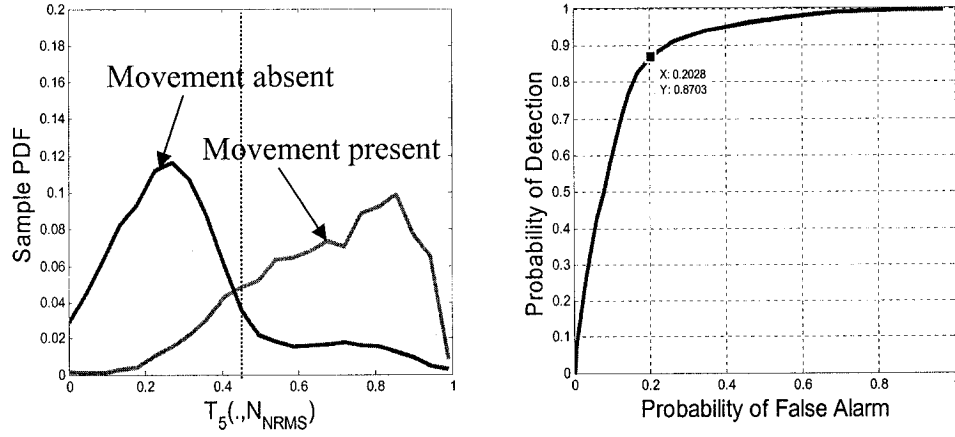


Figure 4-3: (Left) Sample probability density functions of the test statistic $T_5[n;N_{RMS}]$ computed for data marked as ‘gross body movement absent’ and data marked as ‘gross body movement present’ for the abdominal RIP signal of the *MUR* data set. (Right) The receiver operating characteristic or detection performance of $T_5[n;N_{RMS}]$ relative to the visual segmentation made by Dr. Karen A. Brown. The threshold $\gamma_{M2}^{ab}=0.43$ is indicated by a dotted line on the plot of the PDF distributions; the point corresponding to this threshold is indicated with its coordinates on the ROC curve.

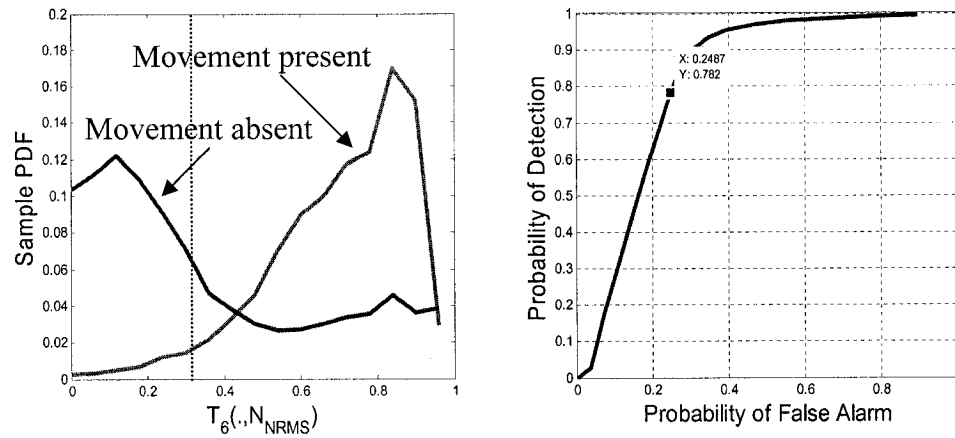


Figure 4-4: (Left) Sample probability density functions of the test statistic $T_6[n;N_{RMS}]$ computed for data marked as ‘gross body movement absent’ and data marked as ‘gross body movement present’ for the ribcage RIP signal of the *MUR* data set. (Right) The receiver operating characteristic or detection performance of $T_6[n;N_{RMS}]$ relative to the visual segmentation made by Dr. Karen A. Brown. The threshold $\gamma_{M2}^c=0.32$ is indicated by a dotted line on the plot of the PDF distributions; the point corresponding to this threshold is indicated with its coordinates on the ROC curve.

Negative values were obtained for estimates of the test statistics T_5 (Figures 4-3 and 4-10) and T_6 (Figures 4-4 and 4-11); these values are not shown—the figures were truncated at zero, to exclude the erroneous values. The negative values occur because the bandpass filter used was non-ideal, exhibiting ripple in the pass-band. This ripple resulted in a gain exceeding unity at some pass-band frequencies (maximum gain: 0.898 dB).

As a result of this gain exceeding unity, when a large fraction of the frequency content of the signal was in the pass-band of the filter (observed bandwidth of regular breathing), some negative values were obtained for test statistics T_5 and T_6 , because they involve subtracting the filtered signal from its unfiltered counterpart. It is expected that these negative values should almost exclusively be produced for non-movement segments of the respiratory signal, while few should be obtained for movement segments, whose frequency content should be mostly outside the bandwidth of breathing.

As expected, it can be observed in Figures 4-3, 4-4, 4-10 and 4-11 that the negative values of the test statistics were obtained almost exclusively for segments marked as non-movement. Only 0.14% of the test statistic estimates obtained for segments marked as movement were negative, which is negligible and potentially attributed to data incorrectly marked by the clinician and have a negligible impact on the performance of the movement detector.

Pause Algorithm

The hypotheses used for generating the test statistics were:

H_0 : Respiratory pause (PSA or CA) absent,

H_1 : Respiratory pause (PSA or CA) present.

Using the annotation performed by the clinician, the entire cardiorespiratory data record was segmented into data marked as being a respiratory pause (post-sigh apnea or central apnea) and data not marked as a respiratory pause. The test statistics T_1 and T_2 were then

computed on each of these two sets of data. The sample distributions shown in Figures 4-5 and 4-6 were generated and used to set the statistical thresholds for the *MUR* data with a clinician.

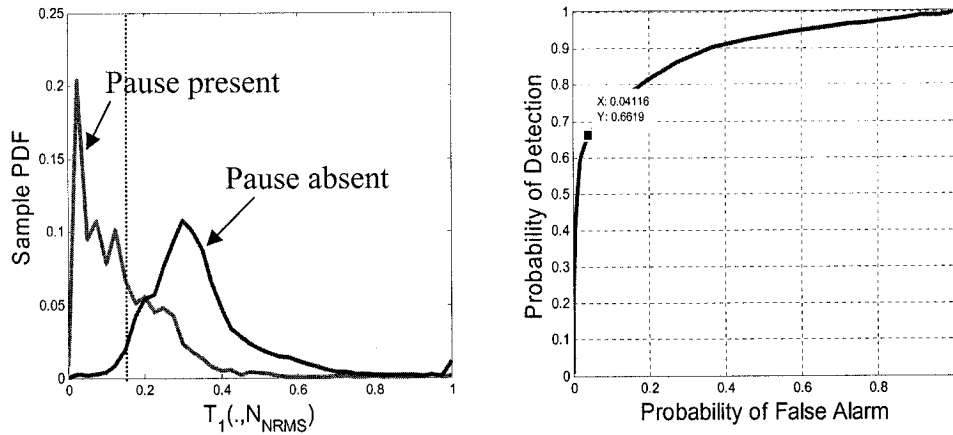


Figure 4-5: (Left) Sample probability density functions of the test statistic $T_I[n;N_{RMS}]$ computed for data marked as ‘respiratory pause absent’ and data marked as ‘respiratory pause present’ for the abdominal RIP signal of the *MUR* data set. **(Right)** The receiver operating characteristic or detection performance of $T_I[n;N_{RMS}]$ relative to the visual segmentation made by Dr. Karen A. Brown. The threshold $\gamma_P^{ab} = 0.16$ is indicated by a dotted line on the plot of the PDF distributions; the point corresponding to this threshold is indicated with its coordinates on the ROC curve.

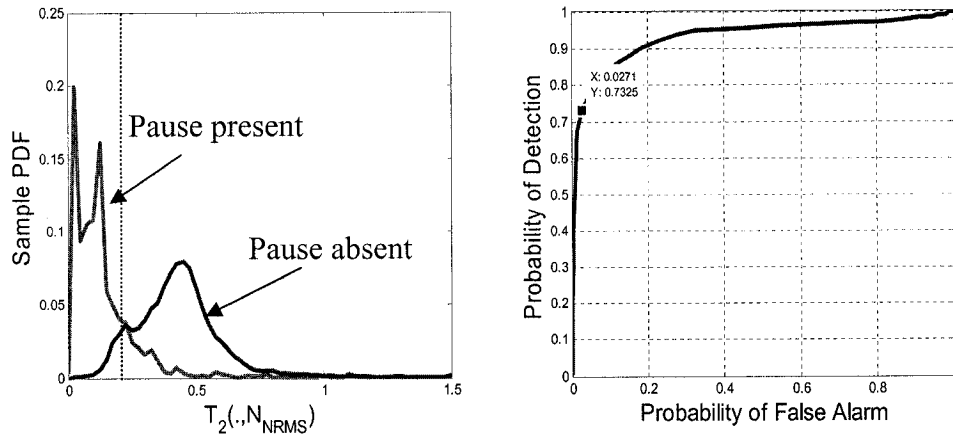


Figure 4-6: (Left) Sample probability density functions of the test statistic $T_2[n;N_{RMS}]$ computed for data marked as 'respiratory pause absent' and data marked as 'respiratory pause present' for the ribcage RIP signal of the *MUR* data set. (Right) The receiver operating characteristic or detection performance of $T_2[n;N_{RMS}]$ relative to the visual segmentation made by Dr. Karen A. Brown. The threshold $\gamma_P^c = 0.16$ is indicated by a dotted line on the plot of the PDF distributions; the point corresponding to this threshold is indicated with its coordinates on the ROC curve.

Asynchrony Algorithm

The hypotheses used for generating the test statistics were:

H_0 : OSA absent,

H_1 : OSA present.

Using the annotation performed by the clinician, the entire cardiorespiratory data record was segmented into data marked as obstructive sleep apnea and data not marked as obstructive sleep apnea. The test statistic T_A was then computed on each of these two sets of data. The sample distribution shown in Figure 4-7 was generated and used to set the statistical threshold for the *MUR* data set with a clinician.

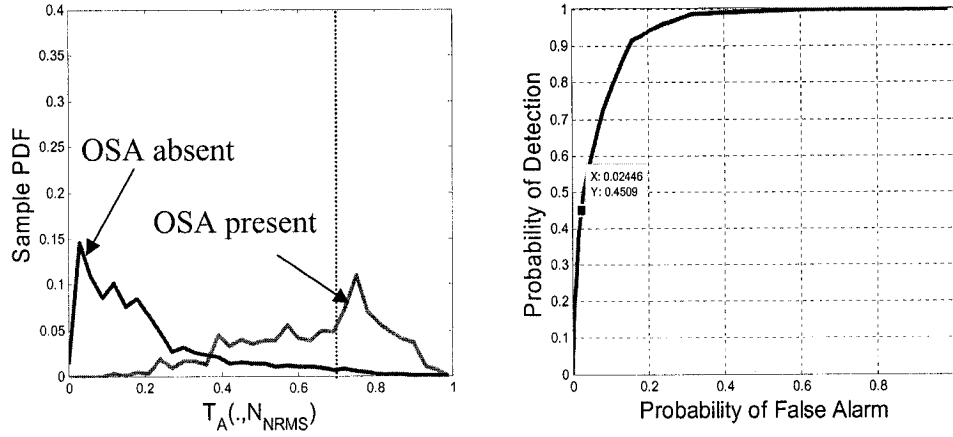


Figure 4-7: (Left) Sample probability density functions of the test statistic $T_A[n;N_A]$ computed for data marked as ‘obstructive sleep apnea absent’ and data marked as ‘obstructive sleep apnea present’ for the *MUR* data set. (Right) The receiver operating characteristic or detection performance of $T_A[n;N_A]$ relative to the visual segmentation made by Dr. Karen A. Brown. The threshold $\gamma_A = 0.70$ is indicated by a dotted line on the plot of the PDF distributions; the point corresponding to this threshold is indicated with its coordinates on the ROC curve.

4.1.4 Statistical Analysis: *MOSS*

The patient data record *MOSS* was obtained from a 45 week old term male infant, weighing 5.4kg. The recordings were performed in the post-operative recovery room at the Montreal Children’s Hospital. The data record was annotated by Dr. Karen A. Brown. The statistical thresholds were set with a clinician and are provided in Table 4-2.

Movement Algorithm

The hypotheses used were:

H_0 : Gross body movement absent,

H_1 : Gross body movement present.

Using the annotation performed by the clinician, the entire cardiorespiratory data record was segmented into data marked as movement and data not marked as movement. The

test statistics T_3 , T_4 , T_5 and T_6 were then computed on each of these two sets of data. The sample distributions shown in Figures 4-8, 4-9, 4-10 and 4-11 were generated and used to set the statistical thresholds for the *MOSS* data set with a clinician.

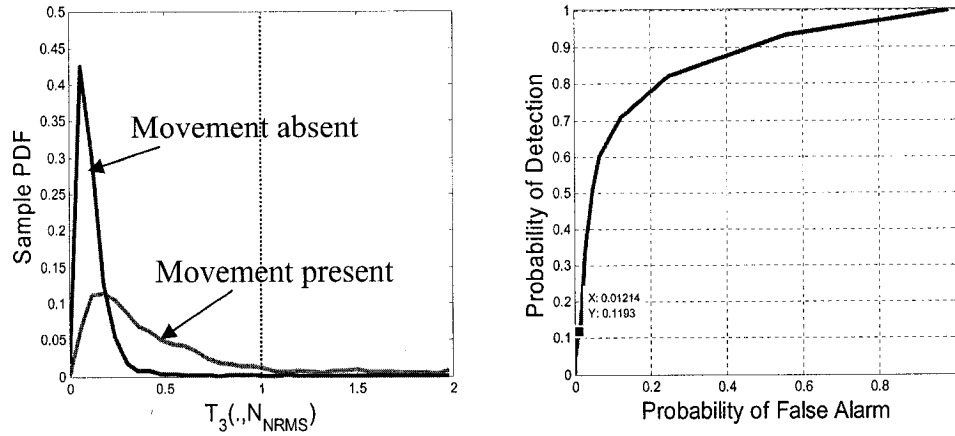


Figure 4-8: (Left) Sample probability density functions of the test statistic $T_3[n;N_{RMS}]$ computed for data marked as ‘gross body movement absent’ and data marked as ‘gross body movement present’ for the abdominal RIP signal of the *MOSS* data set. (Right) The receiver operating characteristic or detection performance of $T_3[n;N_{RMS}]$ relative to the visual segmentation made by Dr. Karen A. Brown. The threshold $\gamma_{MI}^{ab} = 1.00$ is indicated by a dotted line on the plot of the PDF distributions; the point corresponding to this threshold is indicated with its coordinates on the ROC curve.

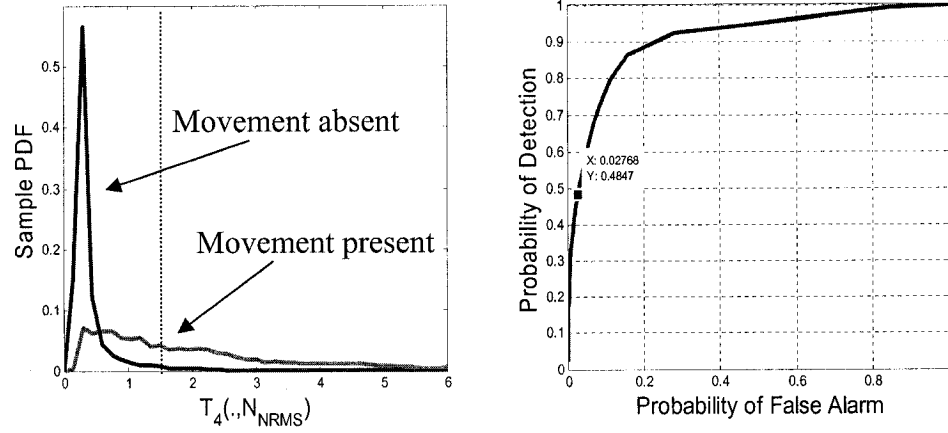


Figure 4-9: (Left) Sample probability density functions of the test statistic $T_4[n;N_{RMS}]$ computed for data marked as 'gross body movement absent' and data marked as 'gross body movement present' for the ribcage RIP signal of the *MOSS* data set. (Right) The receiver operating characteristic or detection performance of $T_4[n;N_{RMS}]$ relative to the visual segmentation made by Dr. Karen A. Brown. The threshold $\gamma_{M1}^c = 1.50$ is indicated by a dotted line on the plot of the PDF distributions; the point corresponding to this threshold is indicated with its coordinates on the ROC curve.

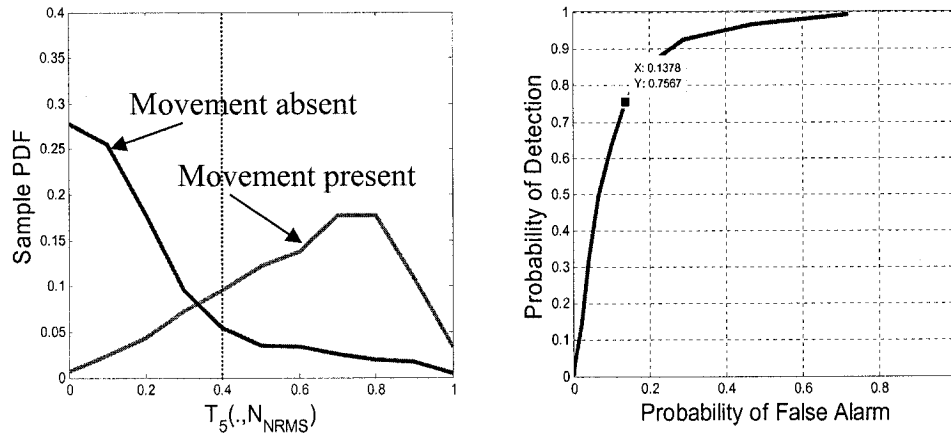


Figure 4-10: (Left) Sample probability density functions of the test statistic $T_5[n;N_{RMS}]$ computed for data marked as 'gross body movement absent' and data marked as 'gross body movement present' for the abdominal RIP signal of the *MOSS* data set. (Right) The receiver operating characteristic or detection performance of $T_5[n;N_{RMS}]$ relative to the visual segmentation made by Dr. Karen A. Brown. The threshold $\gamma_{M2}^{ab} = 0.40$ is indicated by a dotted line on the plot of the PDF distributions; the point corresponding to this threshold is indicated with its coordinates on the ROC curve.

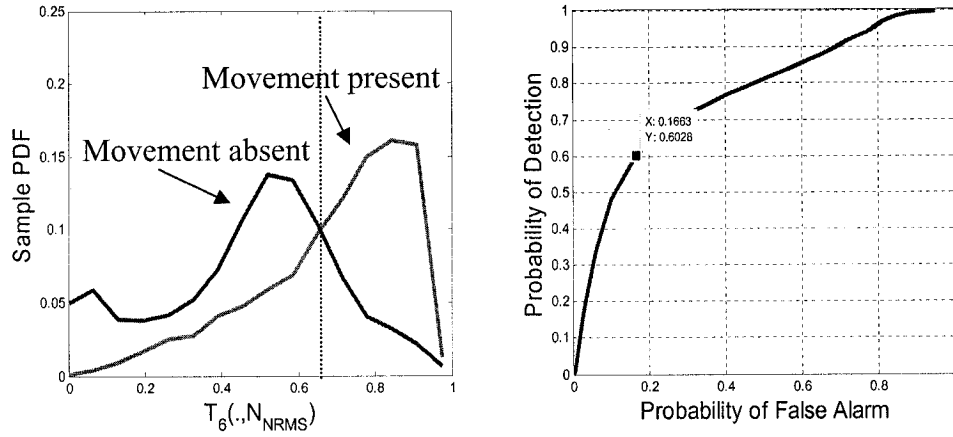


Figure 4-11: (Left) Sample probability density functions of the test statistic $T_6[n; N_{RMS}]$ computed for data marked as ‘gross body movement absent’ and data marked as ‘gross body movement present’ for the ribcage RIP signal of the *MOSS* data set. **(Right)** The receiver operating characteristic or detection performance of $T_6[n; N_{RMS}]$ relative to the visual segmentation made by Dr. Karen A. Brown. The threshold $\gamma_{M2}^c = 0.65$ is indicated by a dotted line on the plot of the PDF distributions; the point corresponding to this threshold is indicated with its coordinates on the ROC curve.

Pause Algorithm

The hypotheses used for generating the test statistics were:

H_0 : Respiratory pause (PSA or CA) absent,

H_1 : Respiratory pause (PSA or CA) present.

Using the annotation performed by the clinician, the entire cardiorespiratory data record was segmented into data marked as being a respiratory pause (post-sigh apnea or central apnea) and data not marked as a respiratory pause. The test statistics T_1 and T_2 were then computed on each of these two sets of data. The sample distributions shown in Figures 4-12 and 4-13 were generated and used to set the statistical thresholds for the *MOSS* data set with a clinician.

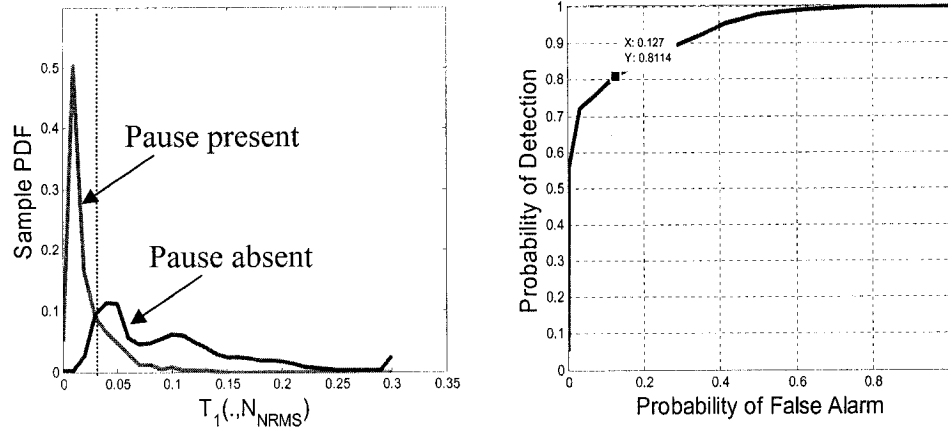


Figure 4-12: (Left) Sample probability density functions of the test statistic $T_1[n;N_{RMS}]$ computed for data marked as ‘respiratory pause absent’ and data marked as ‘respiratory pause present’ for the abdominal RIP signal of the *MOSS* data set. (Right) The receiver operating characteristic or detection performance of $T_1[n;N_{RMS}]$ relative to the visual segmentation made by Dr. Karen A. Brown. The threshold $\gamma_P^{ab}=0.03$ is indicated by a dotted line on the plot of the PDF distributions; the point corresponding to this threshold is indicated with its coordinates on the ROC curve.

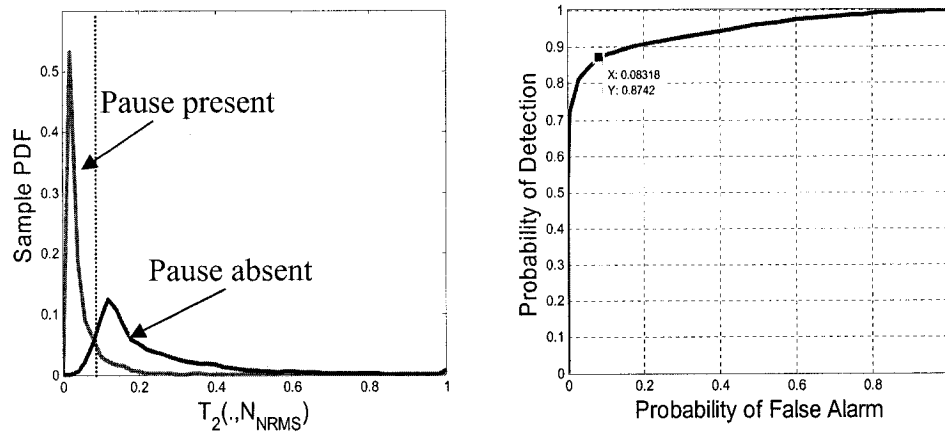


Figure 4-13: (Left) Sample probability density functions of the test statistic $T_2[n;N_{RMS}]$ computed for data marked as ‘respiratory pause absent’ and data marked as ‘respiratory pause present’ for the ribcage RIP signal of the *MOSS* data set. (Right) The receiver operating characteristic or detection performance of $T_2[n;N_{RMS}]$ relative to the visual segmentation made by Dr. Karen A. Brown. The threshold $\gamma_P^{rc}=0.08$ is indicated by a dotted line on the plot of the PDF distributions; the point corresponding to this threshold is indicated with its coordinates on the ROC curve.

Asynchrony Algorithm

The hypotheses used for generating the test statistics were:

H_0 : OSA absent,

H_1 : OSA present.

Using the annotation performed by the clinician, the entire cardiorespiratory data record was segmented into data marked as obstructive sleep apnea and data not marked as obstructive sleep apnea. The test statistic T_A was then computed on each of these two sets of data. The sample distribution shown in Figure 4-14 was generated and used to set the statistical threshold for the *MOSS* data set with a clinician.

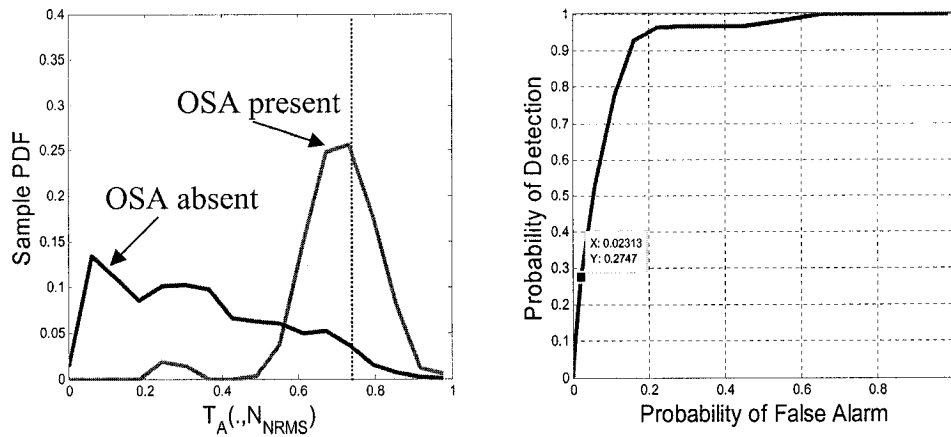


Figure 4-14: (Left) Sample probability density functions of the test statistic $T_A[n;N_A]$ computed for data marked as ‘obstructive sleep apnea absent’ and data marked as ‘obstructive sleep apnea present’ for the *MOSS* data set. (Right) The receiver operating characteristic or detection performance of $T_A[n;N_A]$ relative to the visual segmentation made by Dr. Karen A. Brown. The threshold $\gamma_A = 0.80$ is indicated by a dotted line on the plot of the PDF distributions; the point corresponding to this threshold is indicated with its coordinates on the ROC curve.

4.2 Performance Evaluations

This section provides the performance evaluations of the respiratory event detection algorithms on two complete cardiorespiratory data sets (Montreal Children's Hospital Patient ID's: *MUR* and *MOSS*). The thresholds in Table 4.1 and 4.2 were used for the analysis; these thresholds were set individually for each data record with a clinician, using the statistical distributions provided in Section 4.1, and using the clinician's judgment as the standard for optimizing performance.

We define the following:

N_x : Number of events in category x (as annotated by manual analysis);

n_x : Number of events correctly detected as being in category x ;

n_x^f : Number of events falsely detected as being in category x .

Percentage sensitivity S_x and percentage specificity P_x are defined as:

$$S_x = \frac{n_x}{N_x}(100\%) \quad (4.1)$$

$$P_x = \left(1 - \frac{n_x^f}{N_x}\right)(100\%) \quad (4.2)$$

The assessment of specificity for the cardiorespiratory monitor is not a percent specificity in the conventional sense, because a single cardiorespiratory event can result in multiple false detections, and the percent specificity can potentially be a negative value.

For example, a single normal breathing segment could be on the order of thirty minutes, resulting in multiple false detections from all three detectors. Additionally, though 'normal breathing', could have been classified as an event, they were often on the order

of tens of minutes, representing segments between events, whereas apneas were events on the order of tens of seconds specifically identified by the clinician.

Given the aforementioned points, the specificity definition given above, which computes false detections against the number of events classified in the category of interest, rather than against the total number of events not in the category of interest, was deemed by the author to provide a better sense of the true performance of the monitor.

4.2.1 Methodology for Performance Evaluations

As described in Section 4.1.1, the manual annotation was not completely adequate for computing statistics. The same inadequacies had to be accounted for when realizing the performance evaluations.

General:

The start and end points of the respiratory events were not identified by a clinician, consequently only respiratory event detection was investigated; the fitting of onset and offset of detection with the start-point and end-point of the event was not performed. Periods marked as technically poor, which include disconnections of the patient leads as well as other equipment problems, were disregarded from the performance evaluations.

Movement:

For the performance evaluations, movement segments were considered properly detected if they were marked as movement in their majority. Other respiratory events embedded in these large segments but not marked by the clinician (for the reasons outlined earlier) were disregarded.

Asynchrony:

Because periods of thoracoabdominal asynchrony were not annotated by the clinician, only obstructive sleep apneas could be identified for detection. Consequently, if periods

of thoracoabdominal asynchrony were detected by the monitor, they were identified as false detections.

4.2.2 Performance Evaluation Results

Table 4-2: Performance evaluation results for (top) *MUR* and (bottom) *MOSS* data sets.

<i>MUR</i>	Total	Detected	Undetected	False Detection	Sensitivity S_x	Specificity P_x
Movement	63	55	8	14	87.3%	77.8 %
Pause	52	37	15	7	71.2%	86.5%
Asynchrony	15	8	7	10	53.3%	33.3%
Total	130	100	30	31	76.9%	76.2%

<i>MOSS</i>	Total	Detected	Undetected	False Detection	Sensitivity S_x	Specificity P_x
Movement	73	67	6	17	91.8%	76.7%
Pause	44	37	7	4	84.1%	90.9%
Asynchrony	16	7	9	13	43.8%	18.8%
Total	133	111	22	34	83.5%	72.9%

The results of the performance evaluations for both data sets are provided in Table 4-3. The average sensitivity for the *MUR* data set was 76.9% with a specificity of 76.2%, while the total sensitivity for the *MOSS* data set was 83.5% with a specificity of 72.9%. This gave a total sensitivity for both data sets of 80.2% with a specificity of 75.3%. The results of the analysis of each data set are discussed below. An overall discussion of the total performance of the monitor is provided in Section 4.2.6.

4.2.3 Patient Data Record: *MUR*

Movement:

The monitor detected 55 of the 63 events annotated as movement, resulting in a detection sensitivity of 87.3%. The events that were not detected were brief segments that were annotated by the clinician as movement, but which exhibited amplitudes commensurate with the patient's regular breathing. These segments were generally short, sometimes as brief as 2s, and could potentially have been erroneously marked by the clinician.

The monitor falsely detected 14 events as movement, resulting in a detection specificity of 77.8%. Of the false detections, 7 were due to events marked as sighs, which were generally large amplitude, prolonged sighs followed by a lengthy expiration that slowly fell to baseline, resulting in large energy events. The other 7 false detections were due to large and prolonged baseline shifts in the signal, due to some kind of disturbance, usually a brief period of movement.

Respiratory Pause:

The monitor detected 37 of the 52 events annotated as respiratory pause, resulting in a sensitivity of 71.2%. Of the events that were not detected, 3 were events marked as post-sigh apneas, which exhibited long expiration times, resulting in a signal that was slow to come to baseline. The other 12 events that were not detected were brief periods as short as 3-4s, annotated as pauses, but which either exhibited some minor movement, or were during periods that were erroneously detected as movement due to a shifted baseline on the RIP signals.

The monitor falsely detected 7 events as respiratory pause, resulting in a detection specificity of 86.5%. Of the events that were falsely detected, 4 were events annotated as obstructive apnea, but which exhibited almost imperceptible breathing movements. While 2 of the false detections were due to long expiration times (3-4s) during regular breathing, and 1 was during a low amplitude period, which exhibited non-sinusoidal waveforms on the ribcage and abdominal RIP signals, annotated by the clinician as being the result of braking of expiratory flow at the larynx.

Asynchrony:

The monitor detected 8 of the 15 events annotated as obstructive apnea, resulting in a sensitivity of 53.3%. Of the events that were not detected, 4 were events that were erroneously detected as pause because they exhibited almost imperceptible breathing movement; 2 were events not detected because they did not exhibit enough asynchrony to trigger the detector; and the last event was not detected because it occurred during a period falsely marked as movement due to a shifted baseline on the RIP signals.

The monitor falsely detected 10 events as obstructive apnea, resulting in a detection specificity of 33.3%. Four of the false detections were due to periods annotated as normal breathing, which exhibited enough asynchrony to trigger the detector; and 4 were during periods of breathing that exhibited longer than normal expiratory times—these 8 events could potentially have been thoracoabdominal asynchrony, however TAS was not marked by the clinician. The other 2 false detections were due to a period annotated as movement that went undetected by the monitor and to a non-sinusoidal waveform on the ribcage and abdominal RIP signals, annotated by the clinician as being the result of braking of expiratory flow at the larynx.

4.2.4 Patient Data Record: *MOSS*

Movement:

The monitor detected 67 of the 73 events annotated as movement, resulting in a sensitivity of 91.8%. All the events that were not detected were events that were marked as movement but which exhibited amplitudes that were commensurate with the normal breathing of the patient; these events could potentially have been erroneously marked by the clinician.

The monitor falsely detected 17 events as movement, resulting in a detection specificity of 76.7%. Of these false detections, 16 were due to events annotated as sighs, which were large amplitude, prolonged sighs followed by a lengthy expiration that slowly fell to

baseline. The other false detection was due to period annotated as normal breathing, which exhibited a large and prolonged baseline shift.

Respiratory Pause:

The monitor detected 37 of the 44 events annotated as respiratory pause, resulting in a sensitivity of 84.1%. Of the events that were not detected, 6 were events annotated as post-sigh apneas, which exhibited small movements that were either body movement or small respiratory movement. The other event that was not detected was an event annotated as a central apnea, but which was off baseline because it occurred at the beginning of an expiration.

The monitor falsely detected 4 events as respiratory pause, resulting in a detection specificity of 90.9%. Of the events that were falsely detected, 2 were events that were annotated as normal breathing, but which exhibited very low amplitude respiratory movements; while 1 false detection was due to a non-sinusoidal waveform on the ribcage and abdominal RIP signals, annotated by the clinician as being the result of braking of expiratory flow at the larynx; while 1 false detection was a period annotated as obstructive sleep apnea, but which exhibited almost imperceptible breathing movement.

Asynchrony:

The monitor detected 7 of the 16 events annotated as obstructive apnea, resulting in a sensitivity of 43.8%. Of the events that were not detected, 8 were events annotated as OSA, but which did not exhibit enough asynchrony to trigger the detector; while 1 was falsely detected as a respiratory pause because it exhibited almost imperceptible breathing movements.

The monitor falsely detected 13 events as obstructive apnea, resulting in a detection specificity of 18.8%. Of the events that were falsely detected, 7 were events annotated as normal breathing, but which exhibited enough asynchrony to trigger the detector—these events could potentially have been thoracoabdominal asynchrony, however TAS was not marked by the clinician. Three of the false detections were due a non-sinusoidal

waveform on the ribcage and abdominal RIP signals, annotated by the clinician as being the result of braking of expiratory flow at the larynx; while 2 false detections were events annotated as movement, but which were not detected by the movement algorithm; the remaining false detection was due to an event annotated as a post-sigh apnea but which exhibited low amplitude asynchronous movement.

4.2.5 Discussion of Statistical Analyses

From the statistical distributions obtained for the two patient data records analyzed, it would appear that setting universal thresholds on the detectors is unrealistic. The two records were obtained from infants of similar age (45 weeks) and weight (5.5kg and 5.4kg), yet the distributions for most of the test-statistics were quite dissimilar. As a result, it would seem unlikely that a larger and more disparate set of data records would yield more uniform distributions, allowing static thresholds.

Furthermore, given the dissimilarities of the statistical distributions, despite the similar ages and weights of the patients, it would also seem improbable that the thresholds could be calibrated using patient age and weight *a priori* and obtain effective performance of the monitor in the post-operative recovery room.

Consequently, it is this author's opinion that obtaining a reasonable apnea detection performance from the monitor, using the test-statistics presented, would necessitate adaptive thresholds.

Additionally, from a visual assessment of the statistical distributions, as well as their corresponding receiver operating characteristics, most of the test-statistics would seem to perform adequately. However, the test-statistics calculated from the ribcage signal seem to perform more poorly for both data sets than their counterparts calculated on the abdominal signal. As a result, giving the test-statistics on the abdominal RIP signal more weight when classifying respiratory pause and gross body movement may provide a more

robust classification performance.

However, the analysis of a larger and more disparate set of cardiorespiratory data records from infants with a variety of ages and weights is essential to confidently assess all of the aforementioned statements.

4.2.6 Discussion of Performance Evaluations

The performance evaluations show that the monitor is an effective tool for detecting gross body movement, respiratory pause and obstructive apnea. Even without appropriately annotated data sets the algorithms exhibited a total level of sensitivity of 80.2% and a total specificity of 75.3%. Furthermore, these results were obtained from the analysis of real clinical infant data sets, which were highly variable, and which exhibited significant amounts of gross body movement. A significant amount of the erosion in the performance of the monitor is due to the poor manual annotation against which correct and false detections were measured; the performance of the monitor would undoubtedly be improved if the annotation was performed appropriately and by more than one clinician.

The cardiorespiratory data sets must be visually annotated by a clinician in a systematic fashion appropriate for computing statistics; such data sets would allow the statistical thresholds to be accurately set, and would permit a more appropriate evaluation of the performance of the monitor. The performance of the monitor must be evaluated on these properly annotated data sets

Such an improved annotation must include the characterization of every event of the data record and include the start and end points of that event. Ideally this would be done to permit automation of the statistical analysis and be accurate to the sample point. Specifically, the periods that were previously coarsely marked in their entirety as gross body movement must be parsed into their appropriate components. Thoracoabdominal

asynchrony must also be systematically identified in addition to periods marked as obstructive apnea.

A comprehensive and systematic statistical analysis of these visually re-annotated cardiorespiratory data records must be performed to compute more reliable and accurate statistical descriptions of the data records. The investigation of the entire library of cardiorespiratory data, as well as new data must be performed to determine optimal thresholds, and investigate whether these thresholds will be set universally or adaptively.

Movement:

The events annotated as gross body movement that were not detected by our monitor generally exhibited energy commensurate with or below that of normal breathing; these events did not fit the clinician's own definition of movement (chaotic fluctuations on the ribcage and abdominal RIP signals) and would likely not be annotated as movement on closer examination. As for the false detections, they were mostly respiratory sighs; these false detections would be eliminated if a separate algorithm for sigh detection was implemented.

Respiratory Pause:

The events annotated as respiratory pause that were not detected by the monitor were generally not apneas, but rather brief pauses less than 4s. Because they were under ten seconds in duration, these segments were not apneas by the classical definition. Furthermore, although these periods were annotated as pauses, they exhibited what were either low amplitude movements or small breathing movements; many of these segments would likely be annotated differently on closer examination by a clinician.

Most of the false detections were periods manually annotated as asynchrony, but which were detected by the monitor as pause because they exhibited almost imperceptible breathing movement; these events would need to be investigated further by a clinician to ensure they were properly identified as obstructive apneas.

Asynchrony:

The majority of the obstructive sleep apnea events that were not detected by the monitor were either detected as respiratory pause or did not exhibit enough asynchrony to be detected by the monitor. A more comprehensive annotation of the data would have to be performed to determine whether these events were truly OSA's.

Many of the false detections were potentially due to periods of thoracoabdominal asynchrony. A manual annotation of the data, identifying TAS in addition to OSA, is a necessity; this would further improve the sensitivity of the monitor performance.

4.3 Representative Visual Examples

Three representative visual examples of the analysis of patient data by the cardiorespiratory monitor are provided in this section (Fig.'s 4-15, 4-16 and 4-17). The analyses for the *MUR* data set were performed using the statistical thresholds provided in Table 4-4, while the analyses for the *GAB2* data set were performed using the statistical thresholds provided in Table 4-5. These thresholds were set to fit the annotation to the start and end points of three specific events for illustrative purposes. The thresholds were set with a clinician; for the MUR data set the statistical analyses presented in Section 4.1 were also used.

Table 4-3: Statistical thresholds used for the analysis of the (left) *MUR* and (right) *MOSS* data sets by the cardiorespiratory monitor for the representative visual examples presented.

Parameter	Value	Parameter	Value
γ_{M1}^{ab}	2.50	γ_{M1}^{ab}	0.30
γ_{M1}^c	2.50	γ_{M1}^c	0.30
γ_{M2}^{ab}	0.43	γ_{M2}^{ab}	0.06
γ_{M2}^c	0.32	γ_{M2}^c	0.06
γ_P^{ab}	0.20	γ_P^{ab}	0.07
γ_P^c	0.20	γ_P^c	0.07
γ_A	0.70	γ_A	0.20
γ_P	0.60	γ_P	0.60
γ_M	0.80	γ_M	0.80

The cardiorespiratory monitor displays both the cardiorespiratory data and binary classification signals concurrently, as shown in Figures 4.15, 4.16 and 4.17. The signals are ordered from top to bottom as: RIP ribcage movement, RIP abdomen movement, plethysmographic pulse waveform, blood oxygen saturation (SpO_2), movement classification, pause classification and asynchronous breathing classification.

4.3.1 Gross Body Movement

Most respiratory event detection algorithms exhibit large numbers of false detections during periods of gross body movement, which erodes detection performance. Infants exhibit both a significant amount of movement and a significant number of arousals; as a result it is imperative that gross body movement be identified.

Figure 4-15 shows the automated analysis of a segment of data from a 45 week old term male infant, weighing 5.5kg (Montreal Children's Hospital Patient ID: *MUR*). The data from 3410s to 3430s was visually annotated as containing movement; the rest of the data segment was annotated as normal breathing. The criteria defined by the clinician for annotating a data segment as movement was that either the ribcage abdominal RIP signal,

the abdominal RIP signal, or the pulse plethysmography signal exhibited chaotic fluctuations; the criteria for normal breathing was that the ribcage and abdominal RIP signals exhibited near-synchronous sinusoidal waveforms. The segment from 3417s to 3426s was detected by the monitor as gross body movement, denoted as a logical one on the binary movement classification channel.

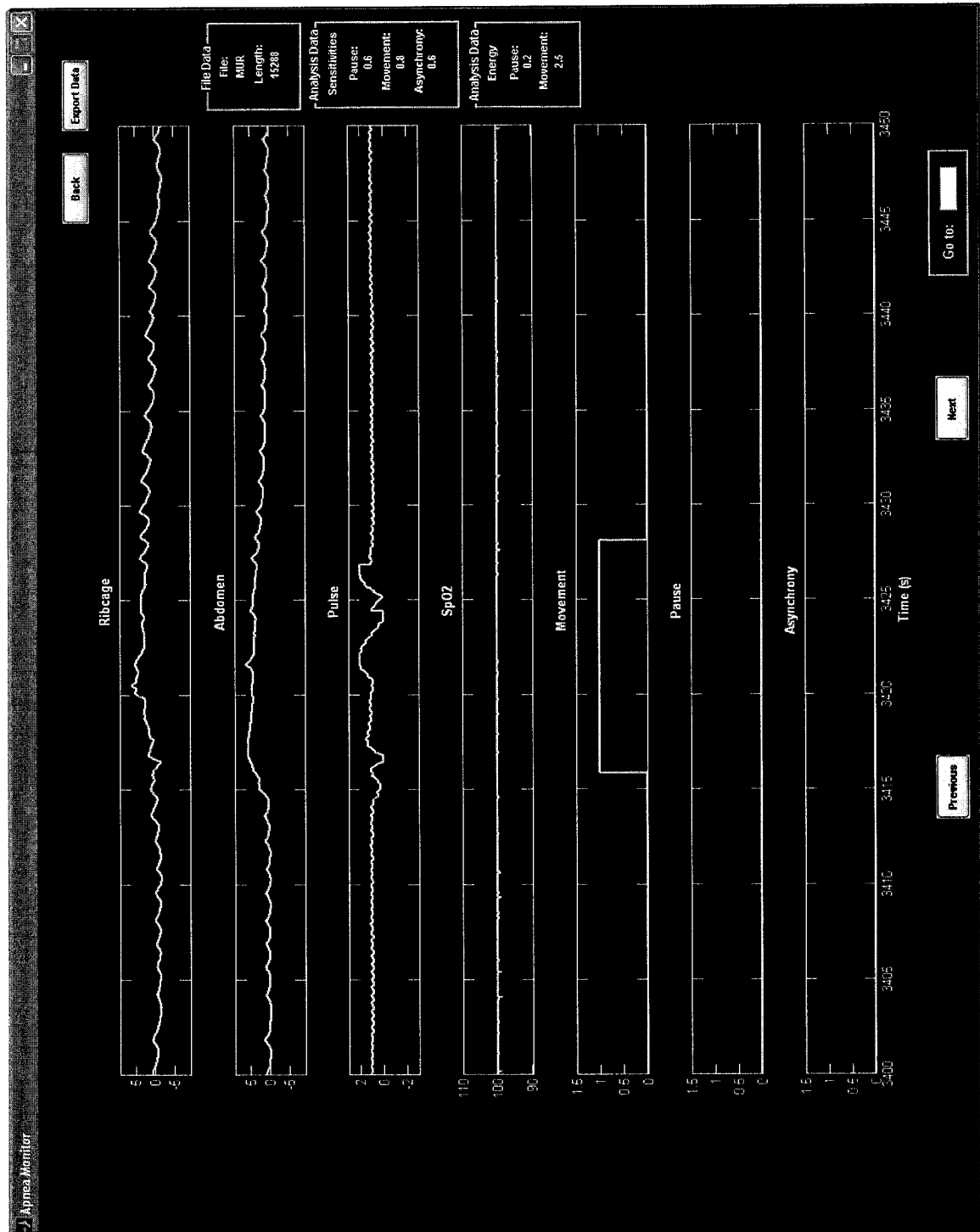


Figure 4-15: Graphical user interface of cardiorespiratory workstation, showing automated analysis of patient cardiorespiratory data record containing a segment marked as movement by Dr. Karen A. Brown and annotated as such by the monitor (denoted as a logical one on the binary movement classification channel) (Montreal Children's Hospital Study ID: *MUR*).

4.3.2 Respiratory Pause

Respiratory pauses are defined as either central sleep apnea or post-sigh apnea. Figure 4-16 shows the automated analysis of a segment of data from a 45 week old term male infant, weighing 5.5kg (Montreal Children's Hospital Patient ID: *MUR*).

The data from 600s to 620s were annotated as containing a 17.3s central apnea, the data from 620s to 630s were annotated as containing a respiratory sigh, while the remainder of the data segment were annotated as normal breathing. The criteria defined by the clinician for annotating a data segment as a respiratory pause was that there was a period with no detectable movement on either the ribcage or abdominal RIP signals. The definition of a sigh was a breath where the inspiratory time was greater than or equal to twice the preceding tidal inspiratory time. The segment from 608s to 6021s was detected as a respiratory pause by the monitor, denoted as a logical one on the binary pause classification channel.

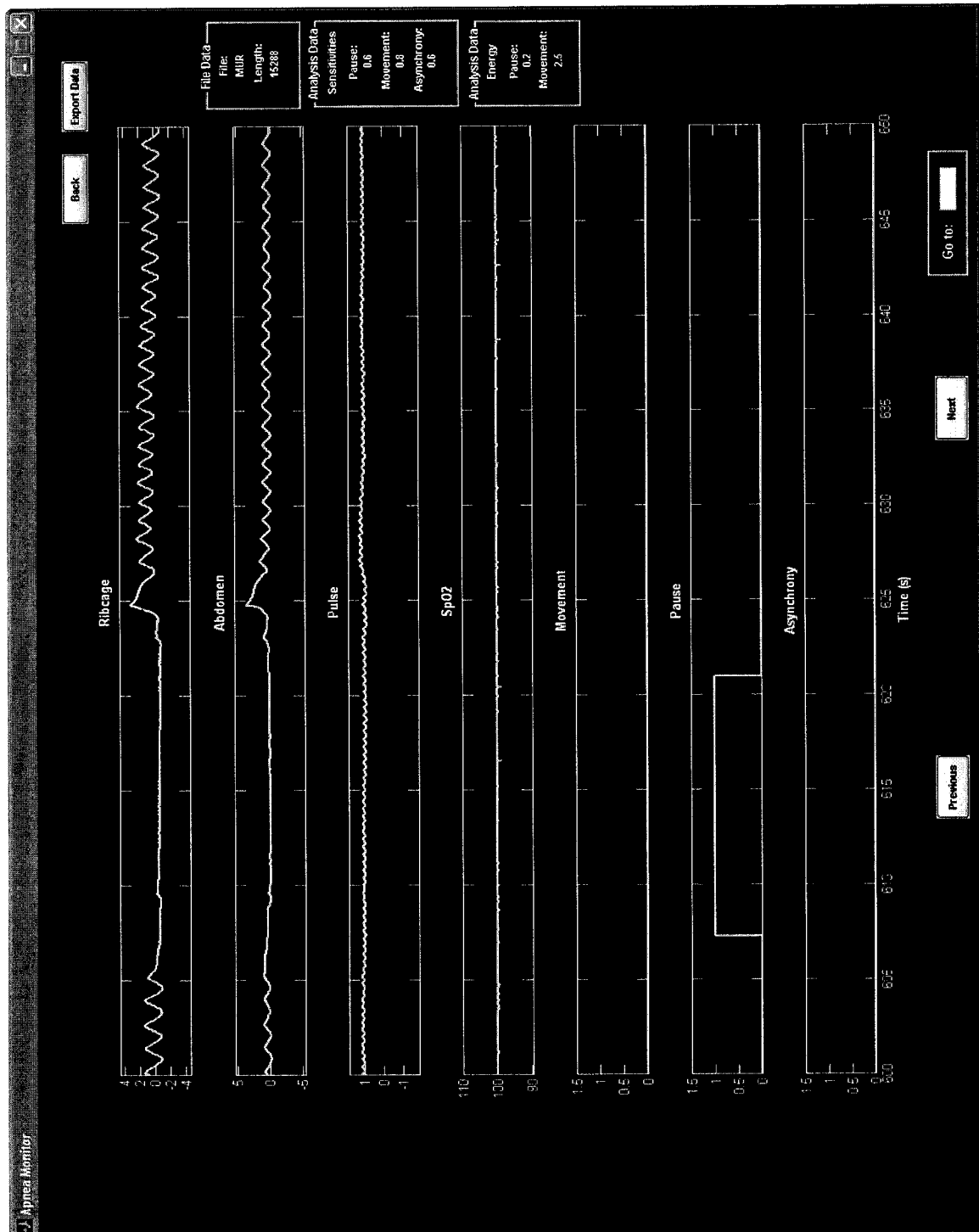


Figure 4-16: Graphical user interface of cardiorespiratory workstation showing automated analysis of patient cardiorespiratory data record containing a segment marked as central apnea by Dr. Karen A. Brown and annotated as such by the monitor (denoted as a logical one on the respiratory pause classification channel) (Montreal Children's Hospital Study ID: *MUR*).

4.3.3 Asynchrony

Figure 4-17 shows the automated analysis of a segment of data from a 41 week old pre-term male infant, weighing 3.0kg (Montreal Children's Hospital Patient ID: *GAB2*). The data from 33230s to 33240s were visually annotated as containing an obstructive apnea, while the segment from 33250s to 33260s was annotated as containing movement. The criteria defined by the clinician for annotating a data segment as obstructive apnea was that the ribcage abdominal RIP signal and the abdominal RIP signal were out of phase concomitant with the evidence of a pause. The segment from 33230s to 33248s was detected as asynchronous breathing by the monitor, denoted as a logical one on the binary asynchrony classification channel. The segment from 33248s to the end of the segment was detected as movement by the monitor, denoted as a logical one on the binary movement classification channel.

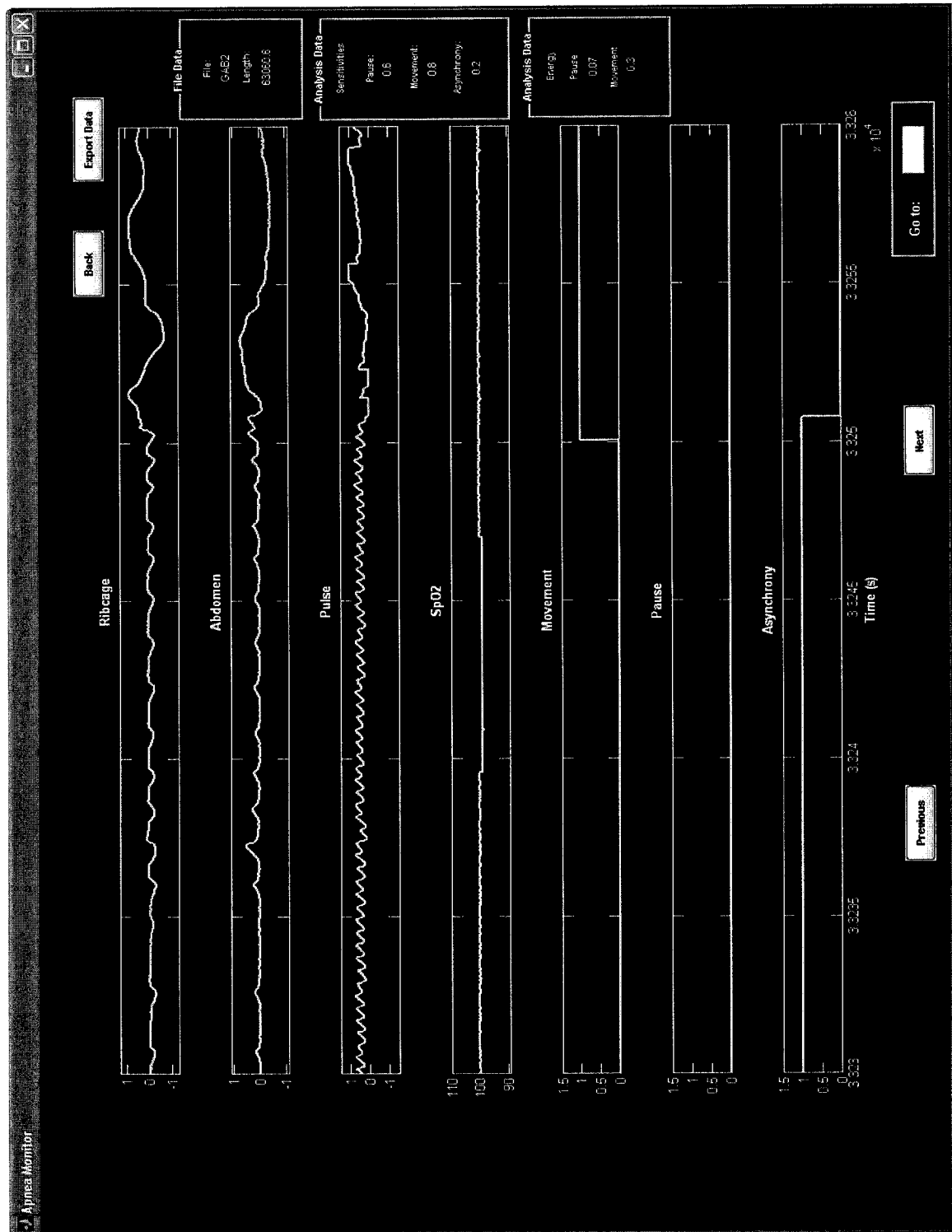


Figure 4-17: Graphical user interface of cardiorespiratory workstation showing automated analysis of patient cardiorespiratory data record containing a segment marked as obstructive apnea by Dr. Karen A. Brown and annotated as such by the monitor (denoted as a logical one on the asynchronous breathing classification channel) (Montreal Children's Hospital Study ID: GAB2).

5 Summary and Future Work

The aim of this thesis was to develop a monitor to perform the off-line analysis of previously acquired cardiorespiratory data sets, as well as to perform on-line analysis and acquisition of additional data sets in the post-operative recovery room at the Montreal Children's Hospital.

Hardware and software was acquired and configured into a monitor capable of non-invasively measuring and logging patient cardiorespiratory data, and providing a digital signal processing architecture to physically realize the respiratory event detection methods previously developed. The automated detection methods were modified for real-time use, and the monitor can apply them to analyze data on-line, as it is acquired.

The monitor was constructed to be robust, portable and battery-operated to make it suitable for use in the post-operative recovery room at the Montreal Children's hospital as a point-of-care diagnostic tool. A software toolbox was developed to provide an interactive graphical user interface for cardiorespiratory data analysis, on-line patient monitoring and for performing file archiving and management.

The monitor provides a tool for clinicians to apply the respiratory event detection algorithms to analyze previously acquired cardiorespiratory data sets, as well as a tool for acquiring and analyzing new data sets and detecting apneas directly in the post-operative recovery room. Even without appropriately annotated data sets the performance results obtained from the analysis of real clinical infant data sets exhibited a total level of sensitivity of 80.2% and a total specificity of 75.3%.

The performance evaluations showed that the monitor was effective at detecting gross body movement, respiratory pauses and breathing asynchrony. The performance of the monitor would be further improved with appropriately annotated data sets, because the statistics used to determine the thresholds would not be corrupted by the incorrect

classification of some respiratory events, nor would the detection performance of the monitor be assessed against incorrectly classified respiratory events.

The monitor has been approved for clinical use by the Biomedical Engineering Department at the Montreal Children's Hospital, and has also been approved by the Institutional Ethics Review Board of the MCH to be used in the post-operative recovery room for a clinical study of post-operative apnea.

5.1 Future Work

5.1.1 Statistical Thresholds and Test-Statistics

The monitor must be applied in the post-operative recovery room to acquire additional patient cardiorespiratory data. The visual annotation of this additional data, as well as previously acquired data sets must be used to systematically determine the statistical thresholds of the event detection algorithms.

Statistical distributions for the test-statistics obtained from the analysis of only two cardiorespiratory data sets still exhibited significant disparities. As a result, it is this author's opinion that obtaining a reasonable detection performance using the test-statistics presented is unlikely with universally set thresholds.

Additionally, the two data sets analyzed were obtained from infants with similar ages and weights, consequently it would also seem unlikely that static thresholds, calibrated using these parameters, could be used; it would appear to be more realistic that adaptive threshold would have to be realized to obtain adequate performance from the monitor.

Furthermore, from a preliminary assessment of the statistical distributions, as well as their corresponding receiver operating characteristics, it would appear that test-statistics calculated from the abdomen RIP signal seem to provide a more robust performance than their counterparts calculated on the abdominal signal. As a result, investigating the

possibility of giving the test-statistics on the abdominal RIP signal more weight when classifying respiratory pause and gross body movement should be explored.

However, the analysis of a larger and more disparate set of cardiorespiratory data records from infants with a variety of ages and weights is essential to confidently assess all of the aforementioned statements.

Finally, the two other cardiorespiratory data channels (%SpO₂, finger plethysmographic heart rate) must be included in the analysis performed by the respiratory event detection algorithms; a 4% drop in blood oxygen saturation from baseline forms part of the definition of an apneic event, and must to be included.

Furthermore, although the pulse oximeter sensors are optimized to prevent movement corruption, the reality is that these channels were observed to exhibit a large degree of sensitivity to movement; consequently, instead of being detrimental, this sensitivity to movement could be used as an advantage to provide important supportive data for the detection of gross body movement.

5.1.2 Evaluating the Performance of the Monitor

The respiratory event detection algorithms must be validated by comparison to manual analysis by trained experts. Less than 10% disagreement with manually analyzed records could be considered acceptable, since human expert agreement in apnea detection is typically no better than 90% [67]. One performance goal of the system could be to achieve the accuracy of human experts in detecting apneas.

Ideally the monitor would be assessed against records marked by multiple clinicians, where an apneic event is only defined as such if there is agreement among the group. This would reflect the fact that there exists few precise definitions of an apneic event, and most often medical decision on apneas is a matter of general consensus among experts.

However, another valuable assessment of the utility of the monitor would be to investigate what rate of apnea detection is necessary in the pediatric ICU to avoid infant mortality, as this is the ultimate goal. The monitor could fall far short of having the same apnea detection rate as an expert, but given that the clinician cannot be continuously monitoring the patient, whereas the monitor can, the monitor could still significantly improve outcomes in the post-operative recovery room.

As a result, the cardiorespiratory monitor must be applied at the MCH to investigate the feasibility of detecting apnea events in real-time immediately as they occur in the post-operative recovery room. This would permit the monitor to be applied to predict which children may be at a health risk because of post-operative apnea immediately following surgery. This could potentially permit clinicians to reduce the length of time infants are monitored, as well as the number of infants monitored overnight following surgery.

Automating cardiorespiratory data analysis will eventually permit a systematic investigation of apnea. Factors such as post-conceptional age, anemia, hypothermia and opioid administration, sigh and pause frequency, and respiratory rate, will be investigated in conjunction with apnea. This will allow the investigation of the etiology and pathophysiology of apnea.

6 Appendices

6.1 *User Operating Manuals*

Presented here is an operating manual for the cardiorespiratory monitor. This includes a guide for the hardware of the clinical monitoring system, as well as a guide for the software toolbox of the cardiorespiratory workstation.

The Cardiorespiratory Monitor

Operating Manual

Department of Biomedical Engineering

McGill University, Montreal

December, 2005

Table of Contents

Table of Contents	
Introduction	
A Hardware Guide.....	
A.1 Front Panel.....	
A.2 Back Panel	
A3 System cables.....	
A3.1 Portable Respiratory Inductance Plethysmograph and Pulse Oximeter	
A3.2 Battery and Clinical Monitoring System Output.....	
B Software Guide.....	
B.1 On-Line Interface.....	
B.2 Off-Line Interface	
B.2.1 Chime File Analysis Interface.....	
B.2.2 Labdat File Analysis Interface	
B.2.3 Library File Analysis Interface	
B.2.4 Modifyin Underlying Classification Algorithms	

Introduction

This guide describes the full operation of the cardiorespiratory monitor. It is presented in two parts: a guide to explain the functionality and use of the software toolbox of the cardiorespiratory workstation, as well as a guide for the operation of the hardware of the clinical monitoring system.

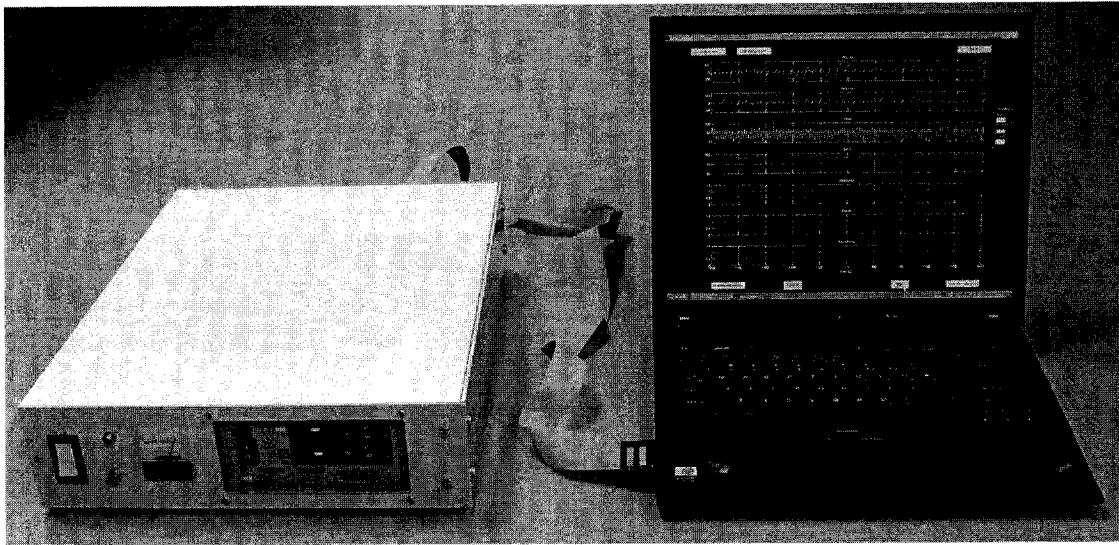


Figure 1: The cardiorespiratory monitor: (left) clinical monitoring system, (right) cardiorespiratory workstation.

A Hardware Guide

The hardware of the clinical monitoring system is all contained in a single enclosure with both front and back panels. The front panel has the system power switch, the voltage level display, the pulse oximeter display, as well as the cable connections for the respiratory inductance plethysmograph. The back panel has the connection for the PCMCIA cable, the fuse, and the system power jack pin connector. Both panels are discussed separately below. For more detail than is presented in this guide about the maintenance, operation and functionality of the hardware components, their individual manuals should be referenced.

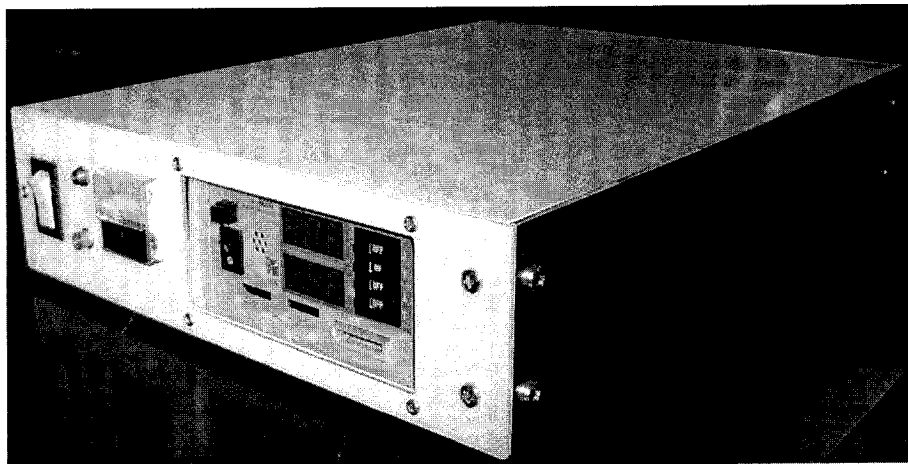


Figure A-1: Clinical monitoring system.

A.1 Front Panel

The front-panel permits the user to monitor system power level using the voltmeter display, as well as the operation of the pulse oximeter, using the pulse oximeter display. Additionally, system power is turned on and off using a switch on the far left of the panel. The power and data cables that interface the respiratory inductance plethysmograph to the clinical monitoring system are also provided on this front panel. Furthermore, the patient cables connect to the front panel of the clinical monitoring system. The components of the front panel are described in detail in Figure A-2.

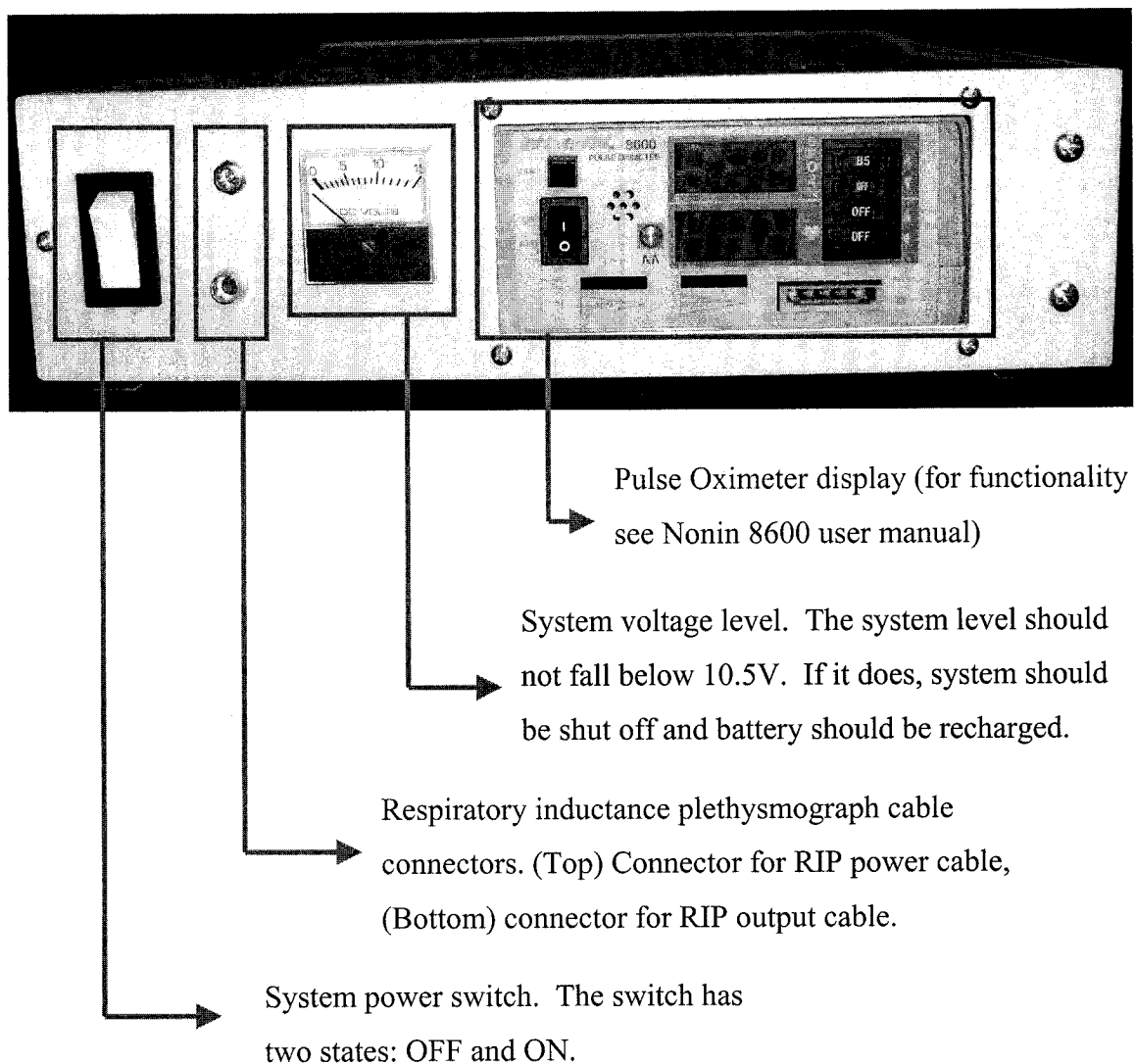


Figure A-2: Front panel of clinical monitoring system.

A.2 Back Panel

The back-panel provides the PCMCIA connector for interfacing the analog outputs of the clinical monitoring system (RIP RC, RIP AB, %SpO₂, finger plethysmography, system ground) to an external device. A power pin receptacle is provided for connecting the system battery. A fuse cap provides access to the system fuse.

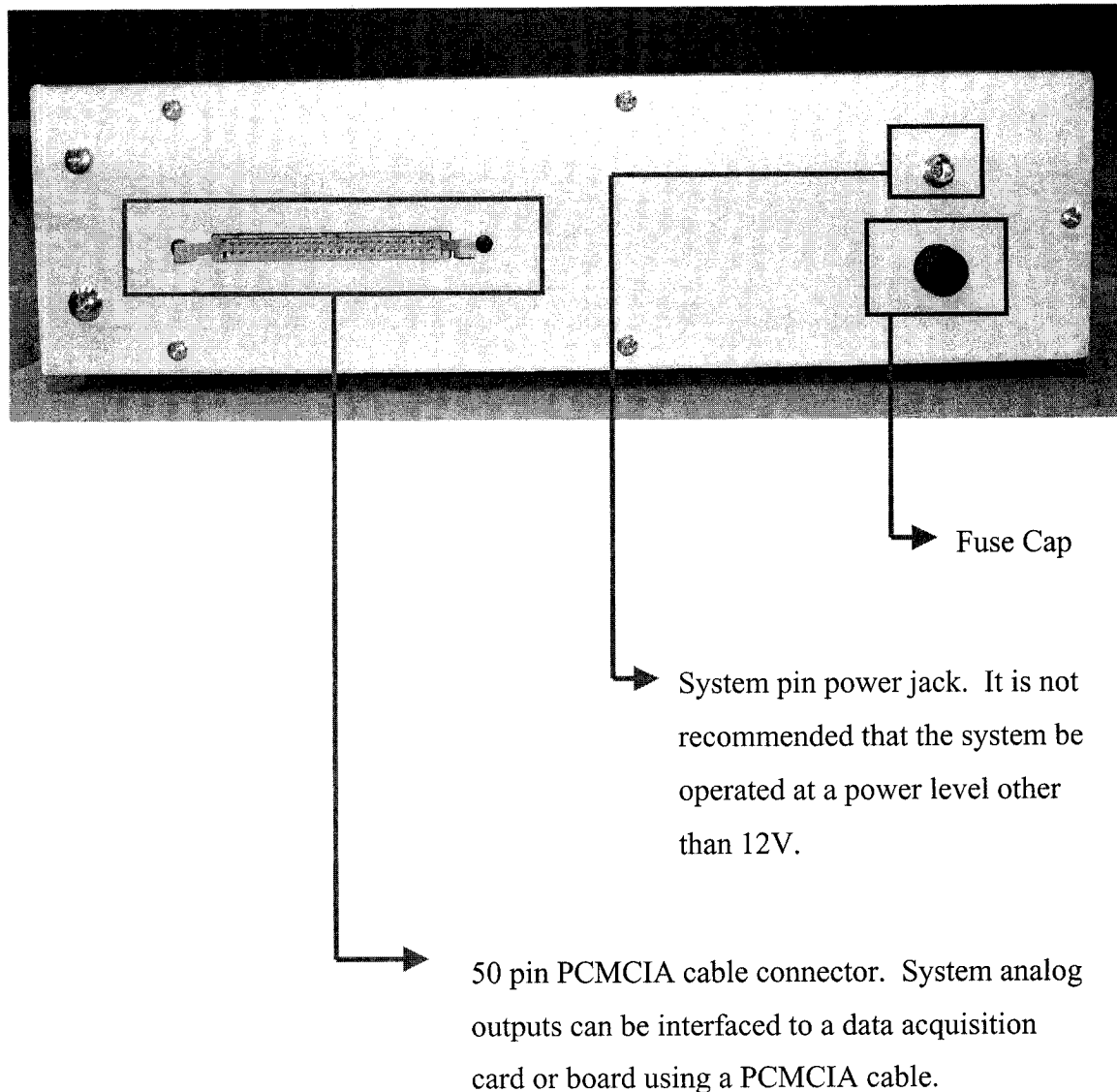


Figure A-3: Back panel of clinical monitoring system.

B.3 System Cables

A.3.1 Portable Respiratory Inductance Plethysmograph and Pulse Oximeter

The respiratory inductance plethysmograph has two cables (Fig. A-4) that interface with the clinical monitoring system—a data cable and a power cable—and one patient cable. The output data cable, which connects to the front of the clinical monitoring system, provides the RIP ribcage and abdomen signals to the monitoring system; the power cable delivers power from the clinical monitoring system battery to the plethysmograph unit.

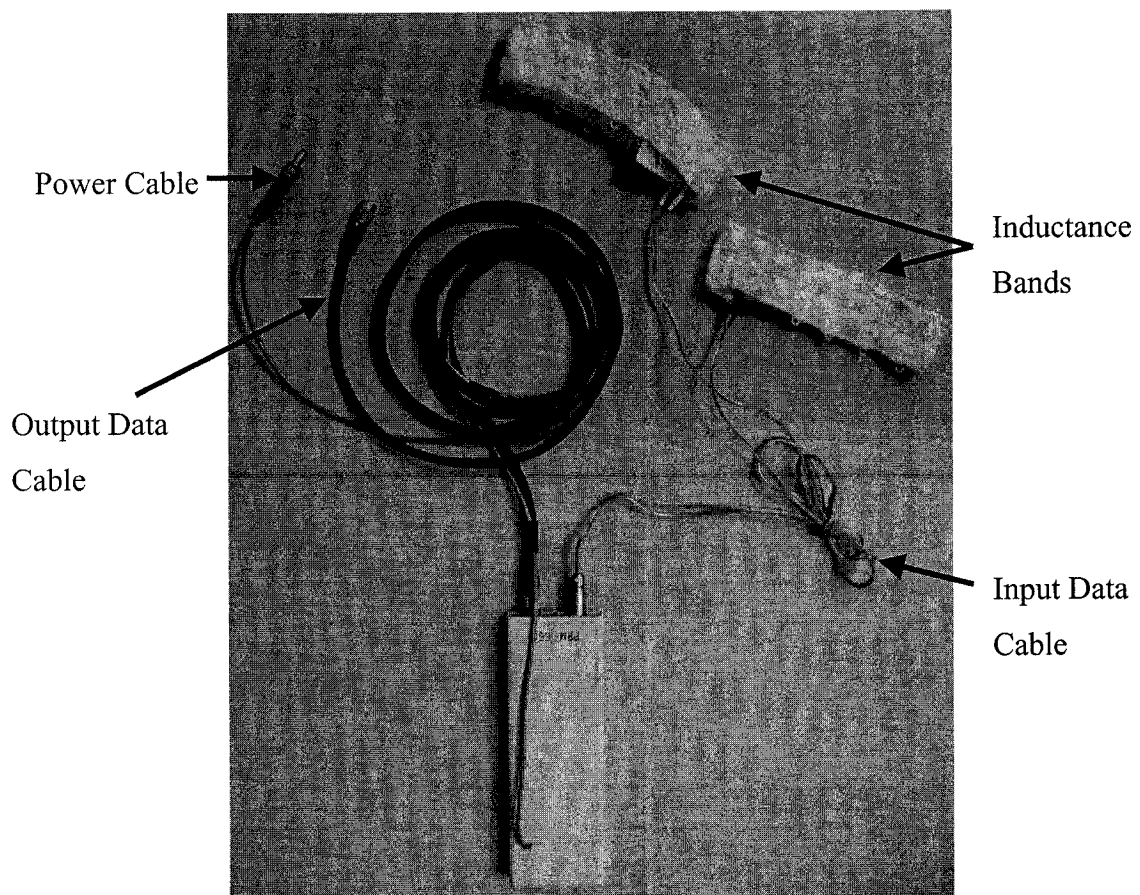


Figure A-4: Cables for portable respiratory inductance plethysmograph.

The cables for the portable RIP, as well as the patient cable for the pulse oximeter, connect to the front panel of the clinical monitoring system (Fig. A-5). The power cable is screw-locking, to avoid the risk of disconnection and interruption of operation.

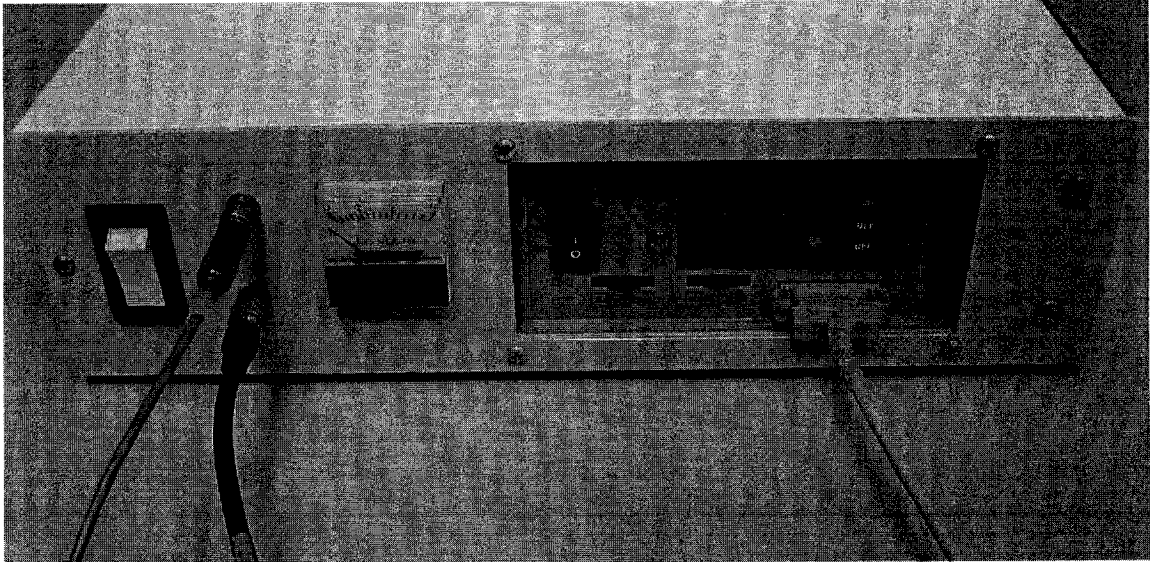


Figure A-5: Connecting cables to the front panel of the clinical monitoring system.

A.3.2 Battery and Clinical Monitoring System Output

The external battery for the clinical monitoring system connects to the monitor using a cable with a screw locking power pin connector; the output data is available from a PCMCIA cable, that mates with a PCMCIA cable (Fig. A-6).

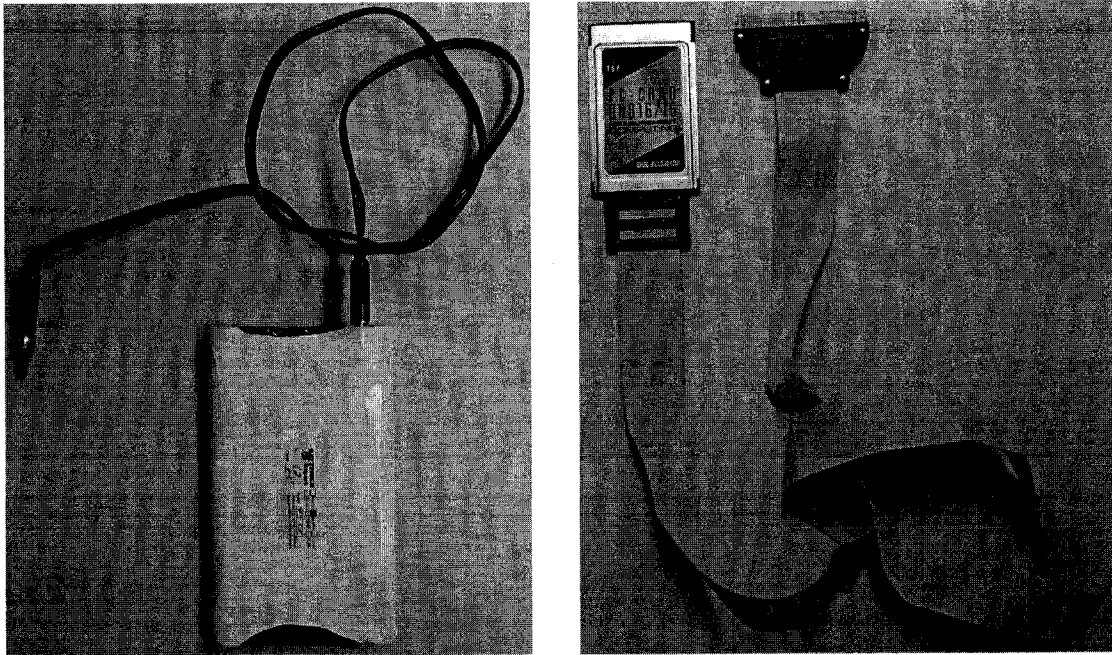


Figure A-6: (Left) System battery with power cable. (Right) Clinical monitoring system data output cable.

The system battery cable as well as the data output cable connect to the rear panel of the clinical monitoring system (Fig. A-7).

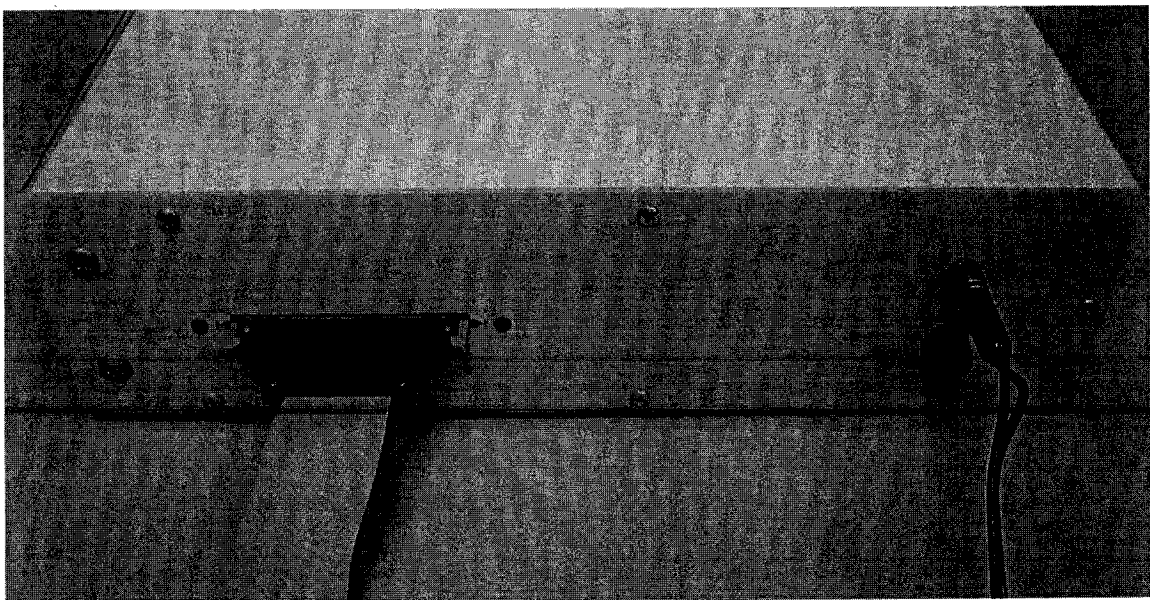


Figure A-7: Connecting cables to the rear panel of the clinical monitoring system.

B Software Guide

The software toolbox is contained in a single folder titled *Apnea*. This folder contains four subfolders as shown in Figure B.2. To install the software toolbox, the *apnea* folder can be placed anywhere on the notepad or desktop PC that will run the software.

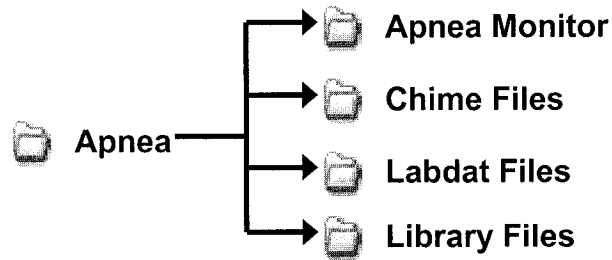


Figure B-2: Software hierarchy.

The *Apnea Monitor* subfolder contains the Matlab toolbox for the cardiorespiratory workstation; while the *Chime Files* folder contains the data files from the Chime group and the *Labdat Files* folder contains the data files previously acquired at the Montreal Children's Hospital. The *Library Files* folder contains all files, both those analyzed and acquired on-line as well as those analyzed off-line and stored by the monitor.

Once the *Apnea* folder has been saved on the PC, the interactive graphical user interface can be executed by following the steps below:

- 1) Open Matlab
- 2) If the working directory is not already set to the *Apnea\Apnea Monitor* folder (this can be checked by typing *cd* in the Matlab workspace), then it should be set as such by typing *cd* then the path of the folder; for example if the folder is stored on the C Drive, the user should type:

cd C:\Apnea\Apnea Monitor

- 3) To execute the software, in the Matlab workspace type

Apnea

4) Then press Return

The next screen that will appear will be the introductory screen:

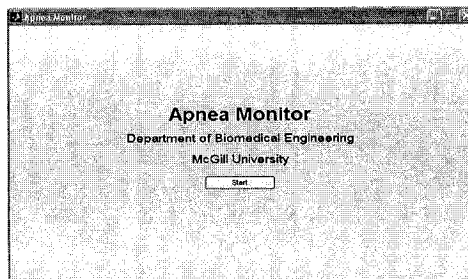


Figure B-3: Introductory screen.

Then the user will be prompted to select whether they wish to perform on-line or off-line analysis:

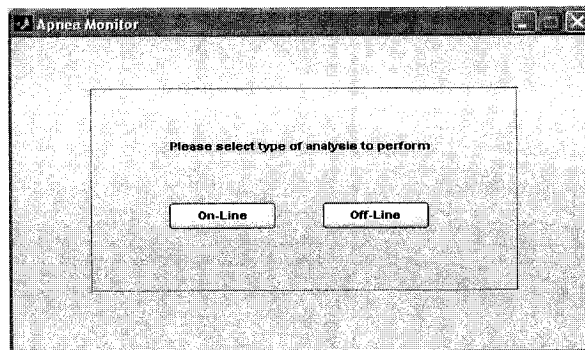


Figure B-4: Selection of analysis type.

The *on-line* analysis button accesses the interface that permits the user to acquire and analyze data from the clinical monitoring system. Conversely, the *off-line* analysis button accesses the interface that allows the user to analyze Chime and Labdat files, and to view and analyze all files stored to the library of the monitor. Both the on-line and off-line analysis interfaces are presented individually in the sections that follow.

B.1 On-Line Interface

The on-line analysis interface allows the user to execute and manipulate acquisition and analysis of cardiorespiratory data from the transducers of the clinical monitoring system.

Begin acquisition of cardiorespiratory data from the clinical monitoring system.

Manipulate the sensitivity of the respiratory event detection algorithms.

(0 maximally sensitive, 1 minimally sensitive)

Stop acquisition of cardiorespiratory data.

Store data to library folder once execution is stopped.

Return to *Analysis Selection* interface.

Close interface.

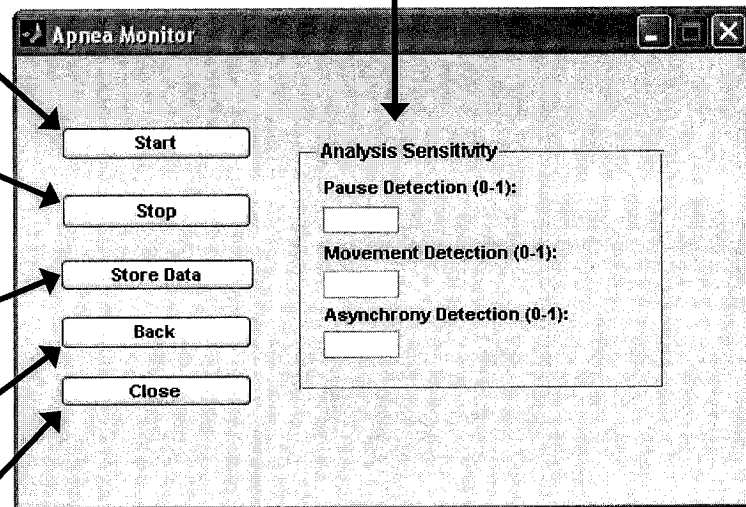


Figure B-5: On-line analysis interface.

Using the on-line analysis interface, the analysis and acquisition of cardiorespiratory data can be executed and halted, and the cardiorespiratory data and its annotation can be stored to the library folder. Furthermore, the sensitivity parameters on the right of the display allow the user to manipulate the sensitivity of the respiratory event detection algorithms. These sensitivities can be between zero and one, where a zero makes the algorithm maximally sensitive, while one makes the algorithm minimally sensitive.

These sensitivities can be manipulated on-line during acquisition. The display showing the data and its annotation as it is acquired is shown in Fig. B-6.

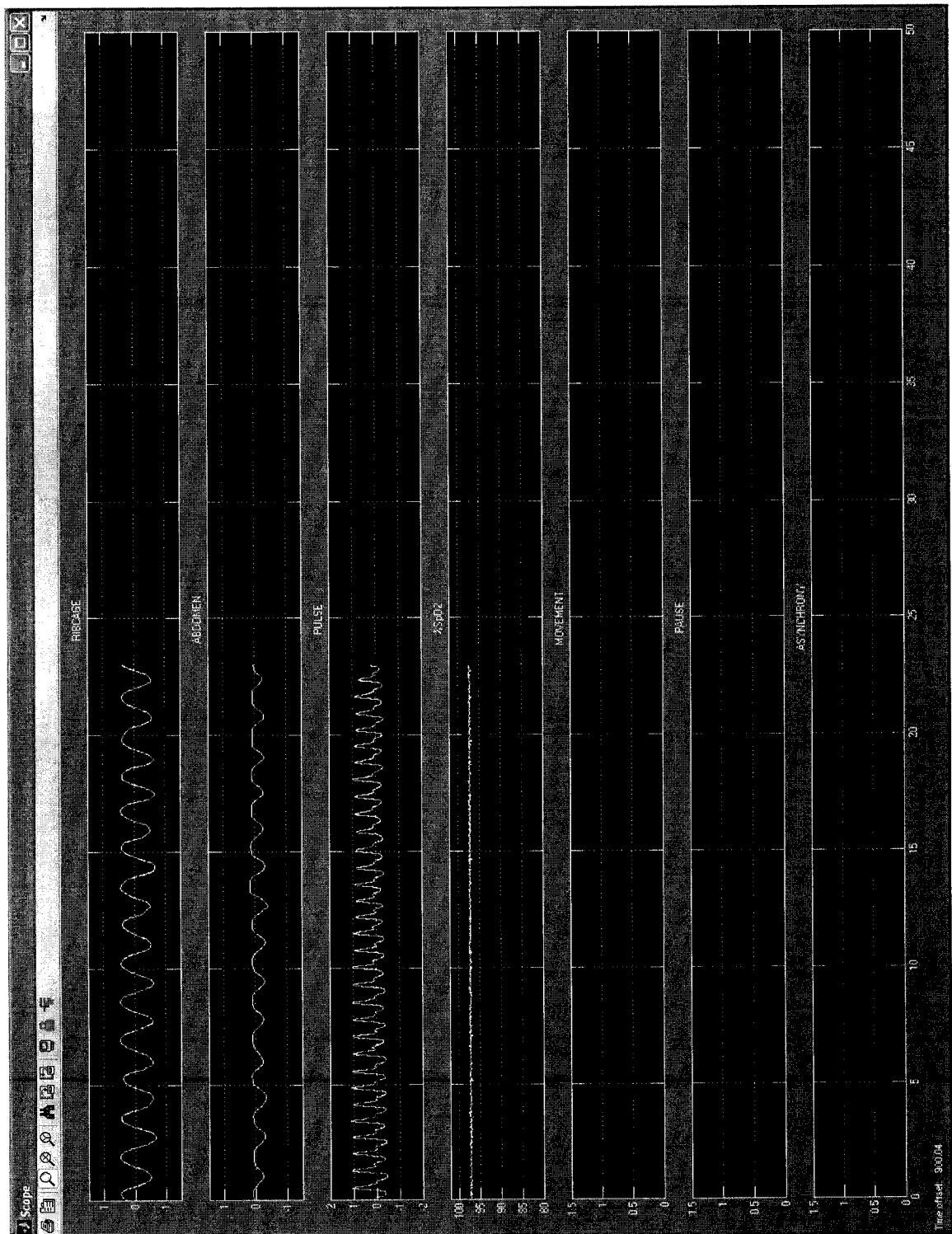


Figure B-6: On-line data analysis.

When data acquisition and analysis has been stopped, the user can select the store data button; they are then prompted by a screen that allows them to choose a filename and save the data and its analysis (Fig. B-7).

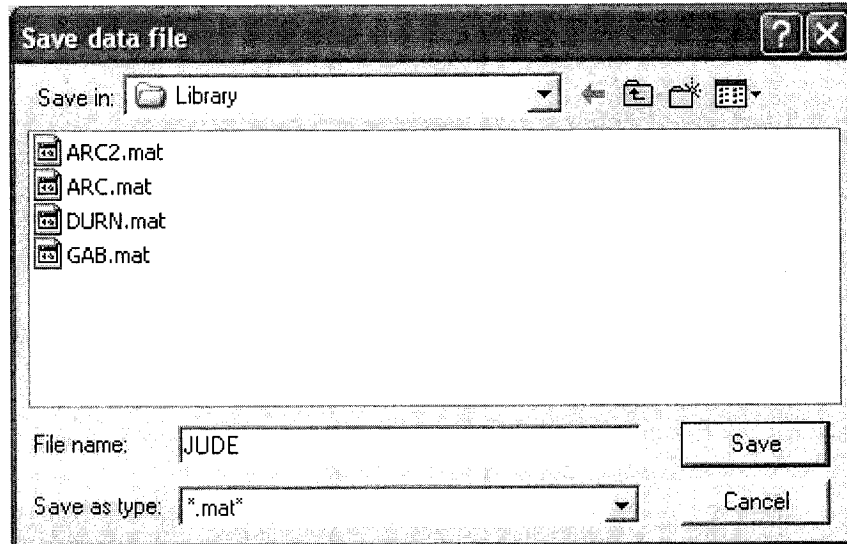


Figure B-7: Storing data files acquired on-line.

After they enter the filename and click *save*, the file is stored in the folder *Apnea\Library* as a Matlab type data file. The Matlab file can be viewed using the off-line analysis interface. The data were also stored as a Microsoft Excel file. The Excel file stores the numerical data in a column format (Table B-1); the data were also stored in the *Apnea\Library* folder. This file can be opened and viewed using Microsoft Excel.

Table B-1: Excel output file data format.

Column	Data
1	Time in seconds
2	Ribcage RIP
3	Abdomen RIP
4	Finger plethysmography
5	%SpO ²
6	Movement Detection
7	Pause Detection
8	Asynchrony Detection
9	Phase Estimate in degrees

B.2 Off-Line Interface

The off-line interface permits the user to view and analyze cardiorespiratory data sets from file. The user is prompted for the type of data file they wish to investigate (Figure B-8). This includes data files from the Chime group, stored in EDF format; data files acquired previously at the Montreal Children's Hospital, stored in the Labdat format; and files stored to the library.

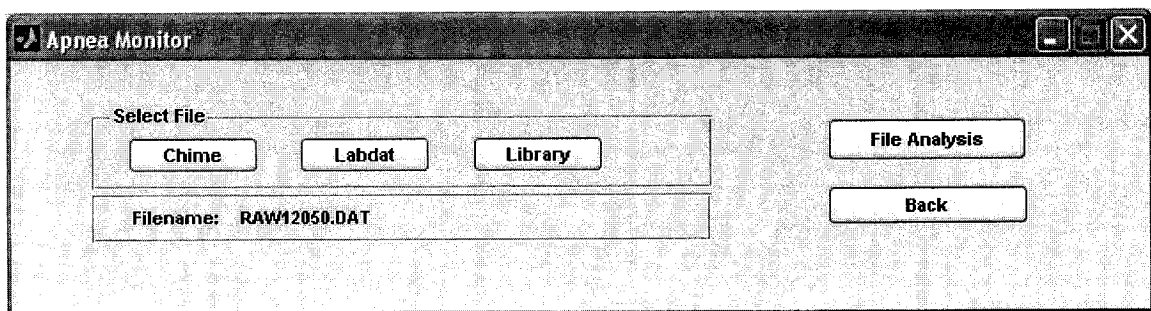


Figure B-8: Selection of Off-line analysis file.

Clicking on each button (Chime, Labdat or Monitor) displays the data files stored in each of the respective folders. As a representative example, the display shown when the Labdat button is clicked is given in Figure B-9. The user then selects the file they wish to analyze, and clicks on the *file analysis* button, which opens the file analysis interface. Each interface is described individually in the sections below.

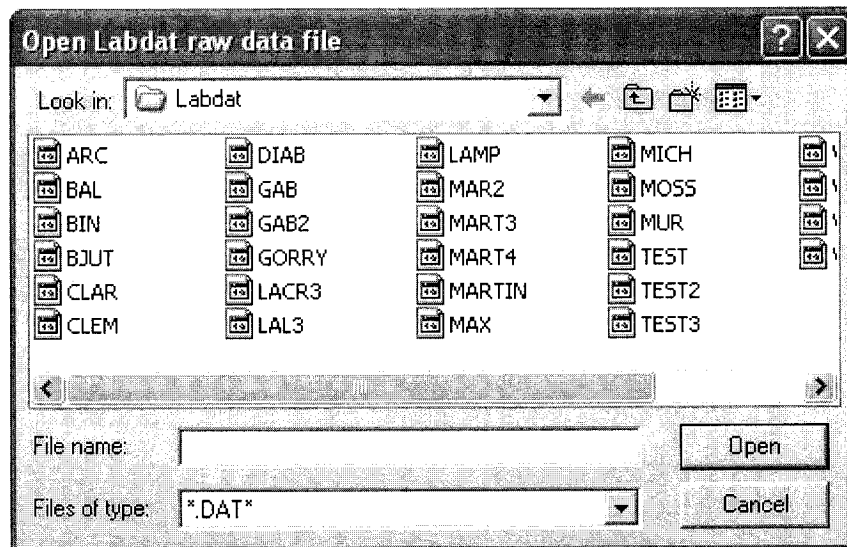


Figure B-9: Opening a Labdat file.

B.2.1 Chime file analysis interface

Cardiorespiratory data records, along with annotation performed by the Chime group can be viewed (Fig. B-10). Chime cardiorespiratory data records can also be viewed and analyzed using McGill's respiratory event detection algorithms (Fig. B-11).

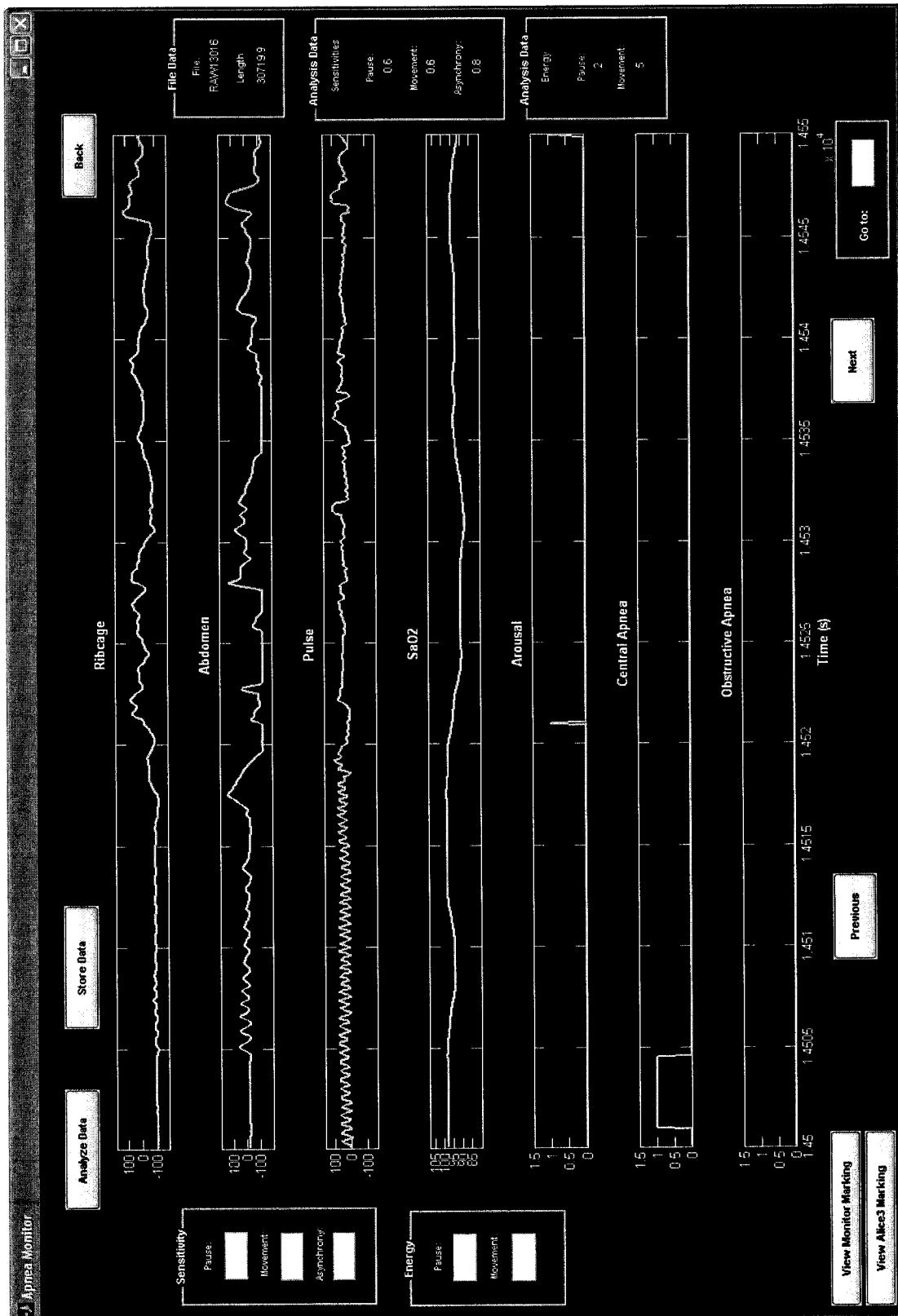


Figure B-10: Interface for viewing Chime cardiorespiratory data with Chime annotation.

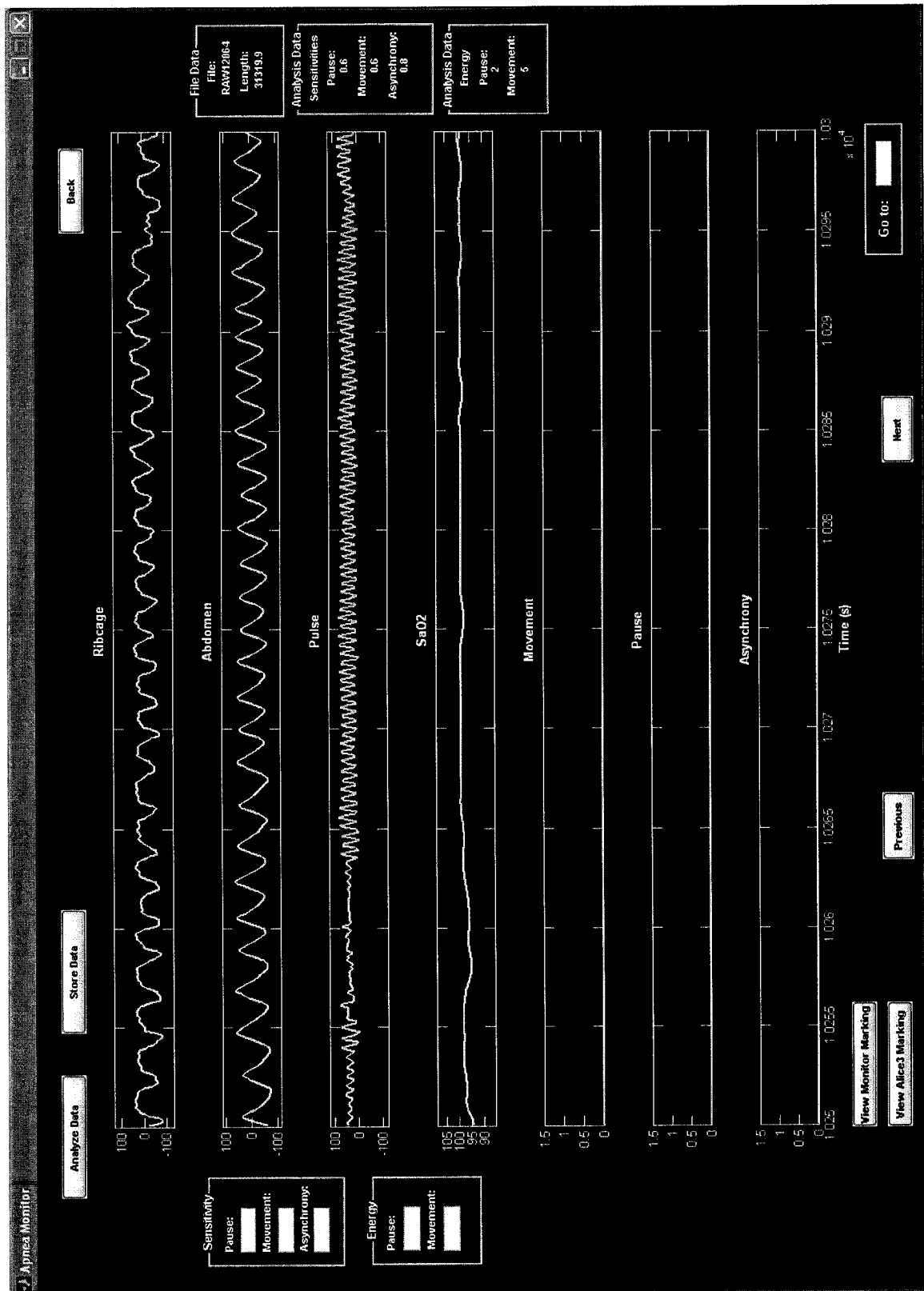


Figure B-11: Interface for viewing and analyzing Chime data using McGill's respiratory event detection algorithms.

The functionality of the interface for viewing and analyzing Chime cardiorespiratory data records using the respiratory event detection algorithms is described below.

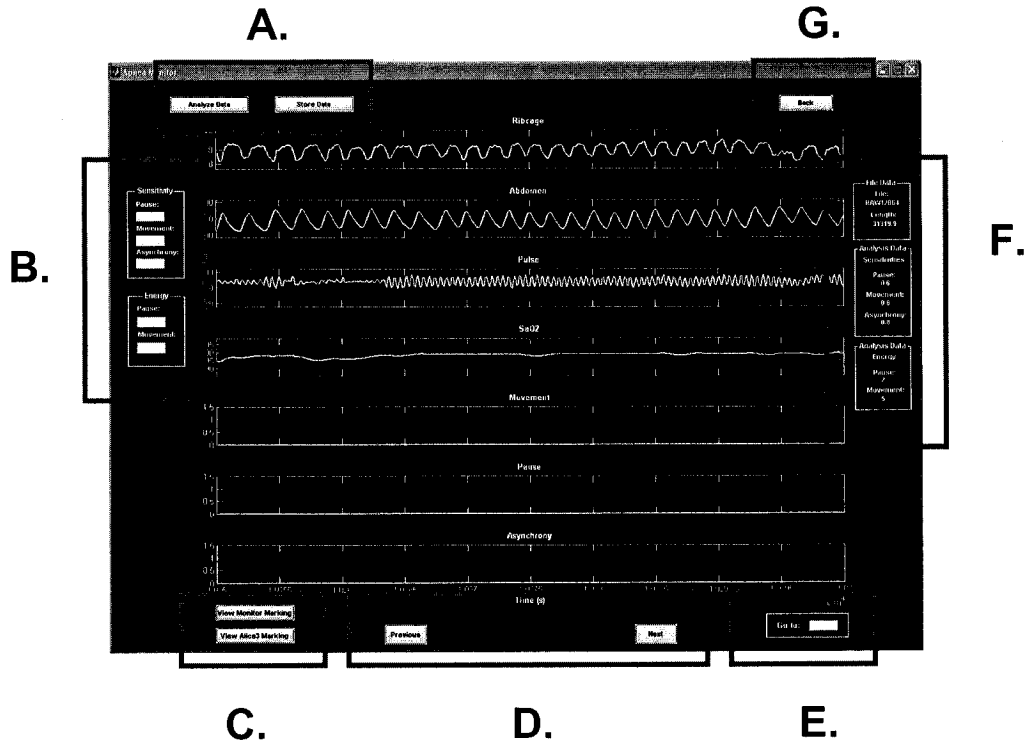


Figure B-12: Layout of Chime data analysis interface.

A.: The *analyze data* button executes analysis of the Chime data file using the McGill analysis algorithms. If analysis parameters have been entered by the user (B.) they are used, otherwise defaults are used. The *store data* button prompts the user for a file name, and then stores the data and its annotation in the *Apnea\Library* folder.

B.: These fields permit the user to set the analysis parameters of the algorithms. The sensitivities can be between zero and one, where a zero makes the algorithm maximally sensitive, while a one makes the algorithm minimally sensitive. The user can also set the RMS level, below which the RIP signal is deemed pause; as well as the RMS level above which the RIP signal is deemed movement. (these are discussed in greater length below)

C.: The user can toggle between the interface for analyzing the data with the McGill algorithms and the interface for viewing the annotation performed by the Chime group.

D.: Return to the previous 50s of data or advance to the next 50s of data.

E.: Select a specific point in the data record (value specified in seconds).

F.: The current parameters used to analyze the data record are displayed. These are the sensitivities and RMS thresholds that are set by the user in the analysis fields (see B.). These parameters are discussed at greater length below.

G.: Return to the *offline analysis type selection* interface.

User Defined Analysis Parameters:

The analysis parameters set by the user using the data entry fields (see B.) and displayed to the user during analysis (see F.) are, ordered from top to bottom: the pause detector sensitivity, movement detector sensitivity, asynchrony detector sensitivity, pause RMS threshold and movement RMS threshold.

The sensitivities can be between zero and one, where a zero makes the algorithm maximally sensitive, while a one makes the algorithm minimally sensitive. The pause RMS threshold (lower limit zero) is the energy level of the RIP signal below which signals are deemed pause; the movement RMS threshold (lower limit zero) is the RMS energy level of the RIP signal above which RIP signals are deemed movement.

B.2.2 Labdat file analysis interface

The labdat interface permits data obtained at the Montreal Children's Hospital, acquired using LABDATTM data acquisition software (RHT-InfoDat, Montreal), to be viewed and analyzed using the McGill respiratory event detection algorithms (Figure B-13).

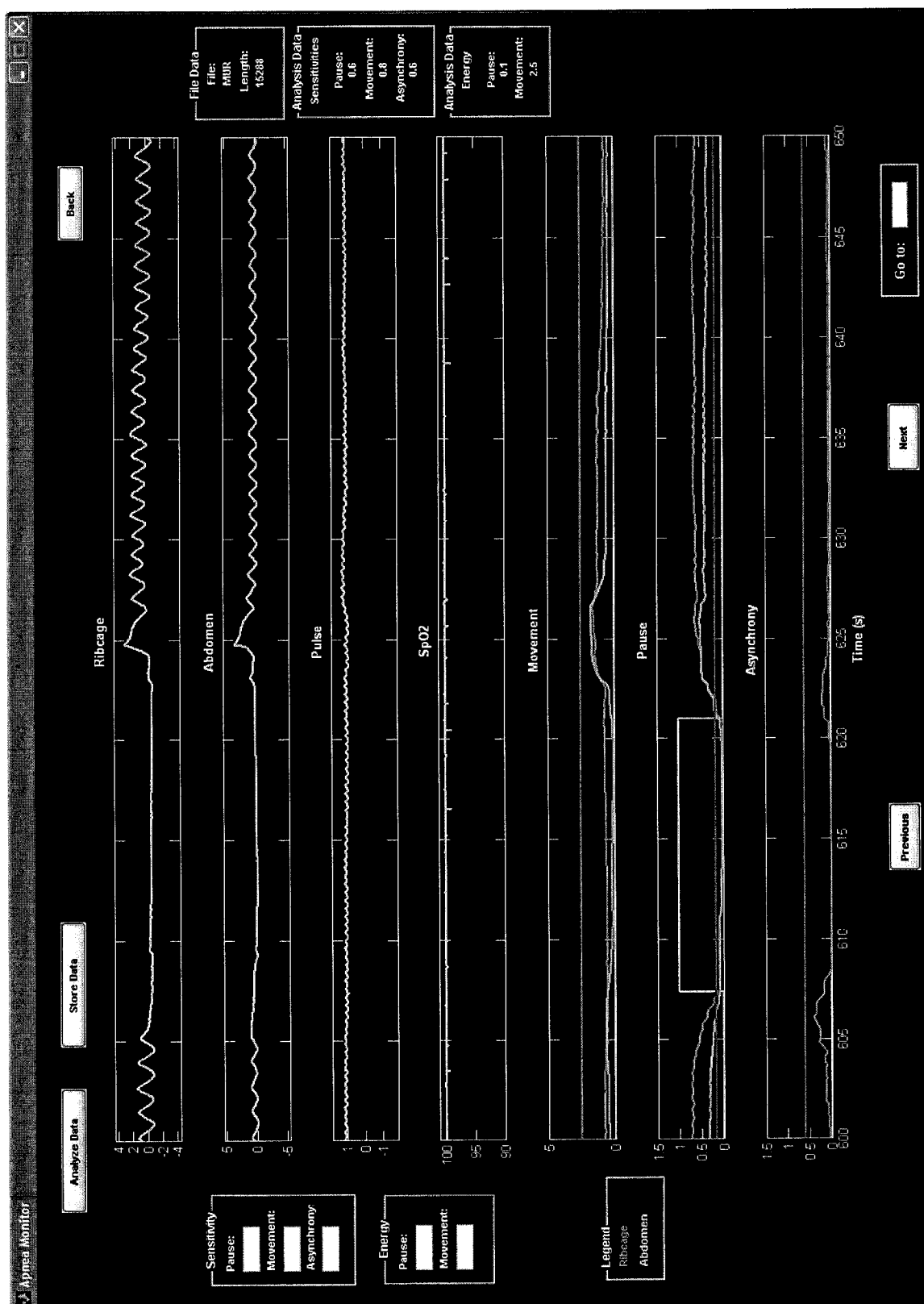
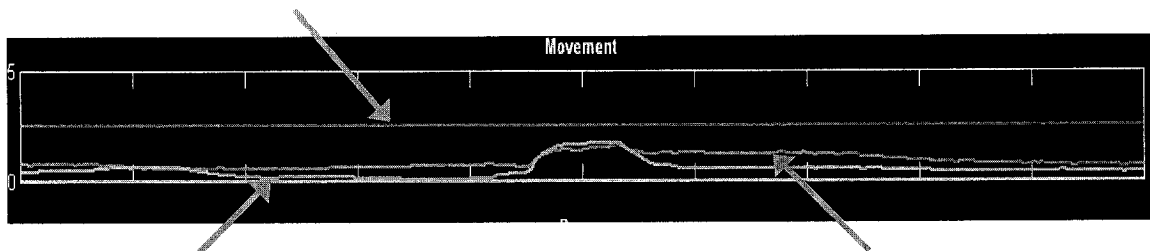


Figure B-13: Interface for viewing and analyzing Labdat cardiorespiratory data files.

In the Labdat display, the cardiorespiratory data signals (first four channels) are provided in yellow. The respiratory event decision signals are yellow. However, additional signals are provide as an aid to clinicians for analyzing data and tuning the analysis parameters; these additional signals, and their color coding is provided below:

Movement:

RED: Movement RMS Threshold (RIP signals with energy in excess of this threshold are considered movement).

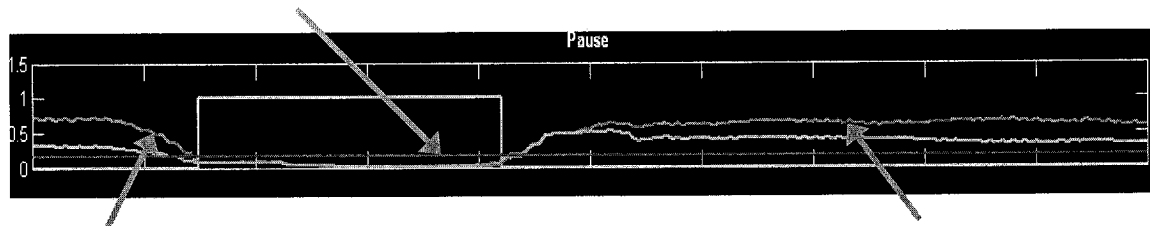


Turquoise: Estimated RMS of abdomen RIP signal

Pink: Estimated RMS of ribcage RIP signal

Pause:

RED: Pause RMS Threshold (RIP signals with energy below this threshold are considered respiratory pause).

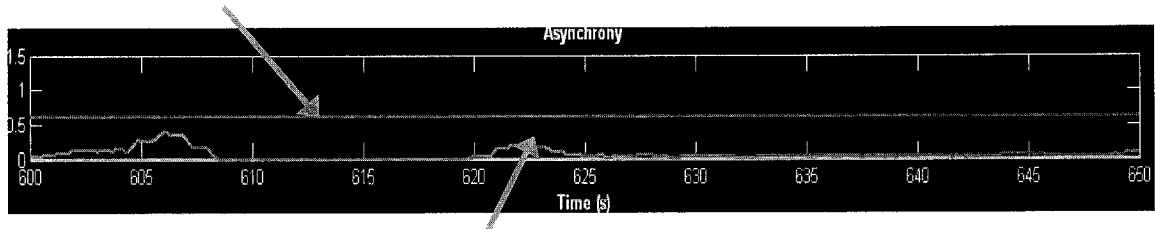


Turquoise: Estimated RMS of filtered abdomen RIP signal

Pink: Estimated RMS of filtered ribcage RIP signal

Asynchrony:

RED: Asynchrony Threshold (set by adjusting the asynchrony sensitivity: 0=0%, 1=180%).



Pink: Asynchrony estimate (0=0%, 1=180%).

The fields for entering the analysis parameters are described below.

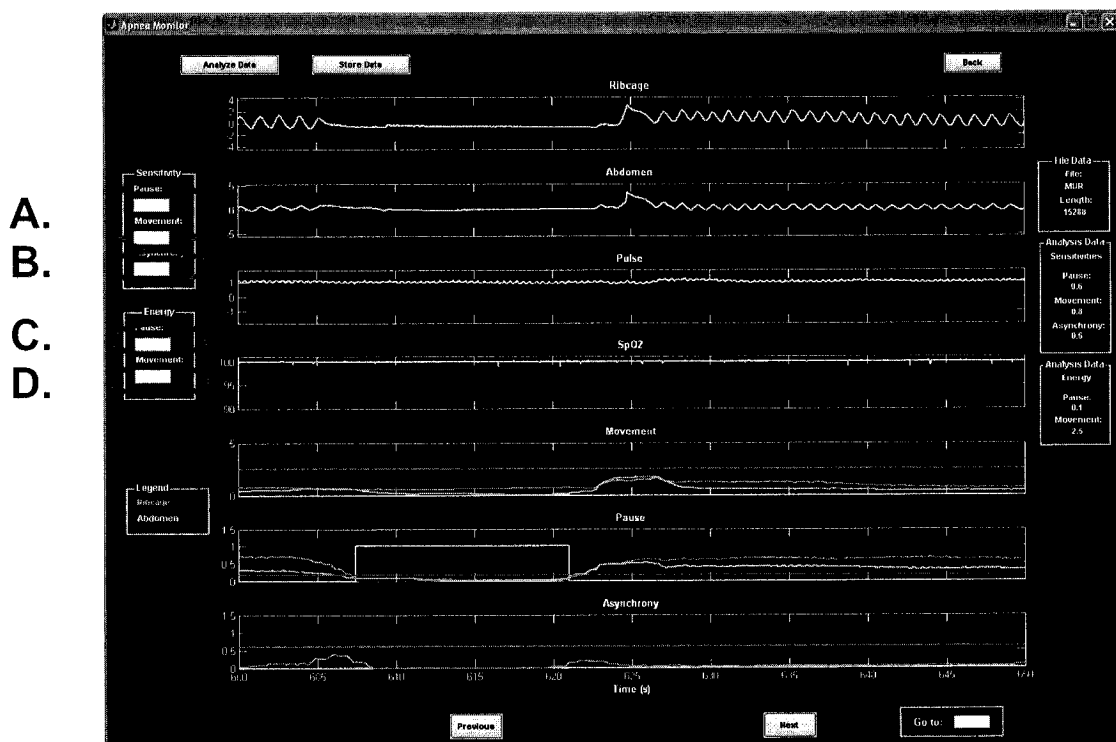


Figure B-14: Layout of Labdat cardiorespiratory data analysis interface.

A.: These fields permit the user to set the sensitivities of the movement and respiratory pause algorithms: sensitivities can be between zero and one, where a zero makes the algorithm maximally sensitive, while a one makes the algorithm minimally sensitive.

B.: The field for entering the asynchrony threshold: 0=0%, 1=180%.

C.: The field for entering the respiratory pause RMS Threshold (lower limit zero). RIP signals with energy below this threshold are considered respiratory pause.

D.: The field for entering the movement RMS Threshold (lower limit zero). RIP signals with energy in excess of this threshold are considered movement.

B.2.3 Library file analysis interface

The library file analysis interface (Fig. B-15) allows files stored to the library folder (both from on-line and off-line data), to be viewed. The analysis parameters with which the data was analyzed are given on the right-hand side of the display. Furthermore, the data can be exported to the EDF format.

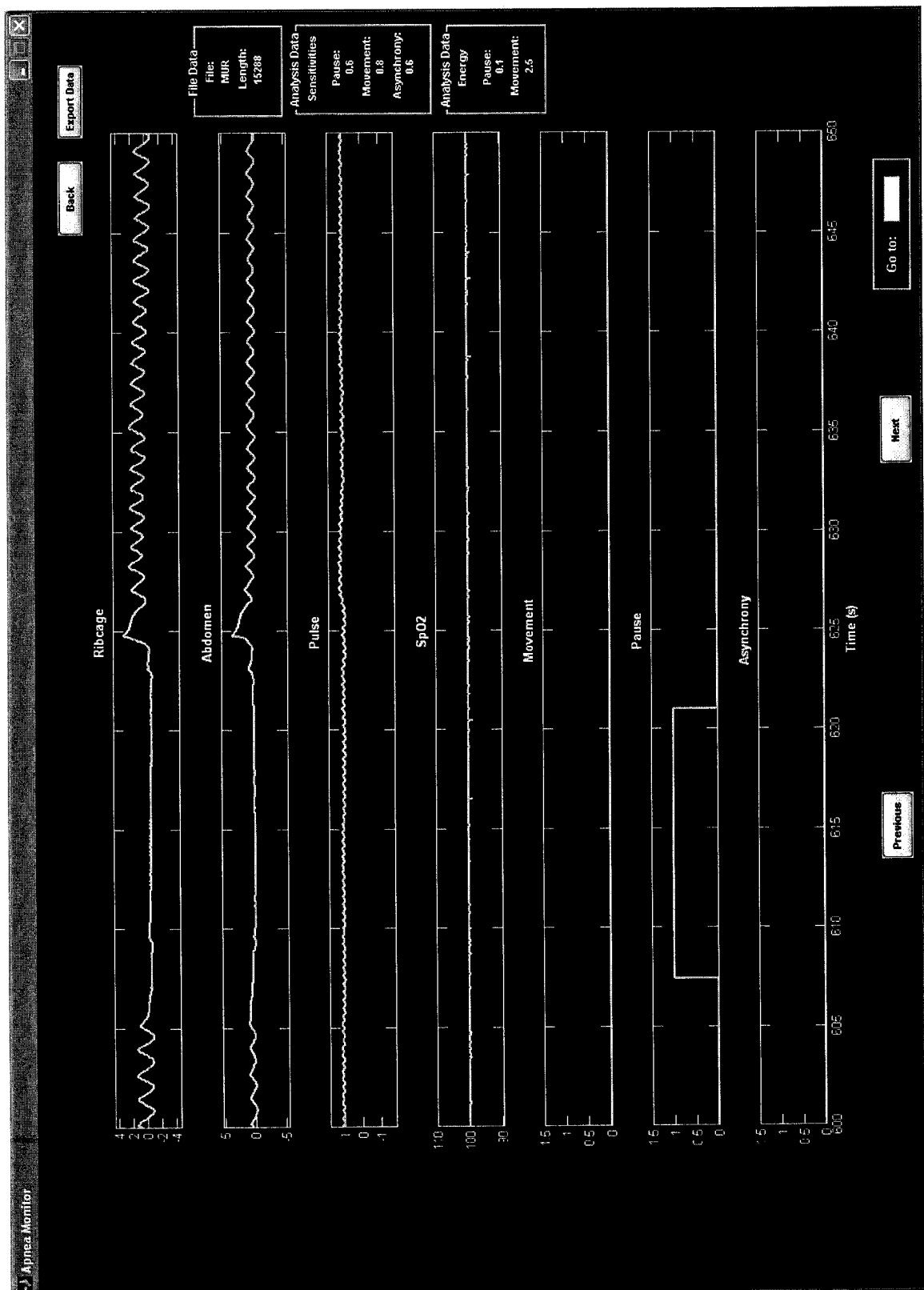
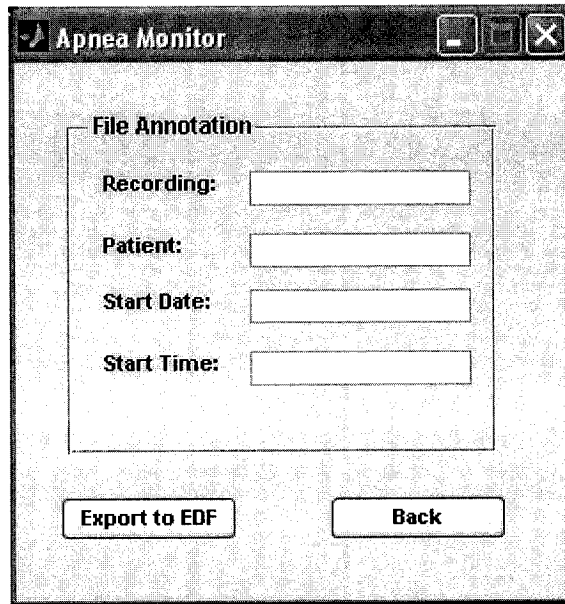


Figure B-15: Interface for viewing library cardiorespiratory data files.

When the EDF pushbutton is clicked an EDF export interface opens (Fig B-16).



The screenshot shows a window titled "Apnea Monitor" with a standard Windows-style title bar. Inside the window, there is a section titled "File Annotation" which contains four text input fields labeled "Recording:", "Patient:", "Start Date:", and "Start Time:". Below these fields, there are two buttons: "Export to EDF" and "Back".

Figure B-16: EDF export interface.

The interface prompts the user for a recording identifier and a patient identifier, as well as the time and date that the recording began. When the *export to EDF* button is clicked, the user is prompted for a filename. The EDF file is then stored in the library folder.

B.2.4 Modifying Underlying Classification Algorithms

Should a user want to change the classification algorithms for both on-line and off-line analysis this can be done by modifying two *Simulink* block diagrams. Off-line analysis is performed by the *Matlab Simulink* file *Apnea_Offline*, while on-line analysis is performed by the *Matlab Simulink* file *Apnea_Online*. These block diagrams can be modified using the *Matlab Simulink* user-interface, adding or removing components as the user sees fit (this simply requires a familiarity with *Matlab's Simulink*).

For, off-line analysis altering the block diagram is all that is required. For on-line analysis, once the block diagram has been altered, the user must select the *Simulink build*

icon (see *Simulink* documentation). Consequently, the *Simulink* block diagram containing the classification algorithms is compiled into executable c-code, which is then stored in a folder in the working directory by *Matlab*. When analysis is executed the file *Apnea_online.m* will automatically access the code in this folder to analyze data on-line as it is acquired.

7 References

- [1] H. Gastaut, C. A. Tassarini, and B. Duron, "Polygraphic study of the episodic diurnal and nocturnal (hypnic and respiratory) manifestations of the Pickwick syndrome," *Brain Res*, vol. 1, no.2, pp. 167-186, 1966.
- [2] U.S. National Library of Medicine - On-Line Encyclopedia [Online]. Available: <http://www.nlm.nih.gov/medlineplus/>. Accessed: January 1, 2006.
- [3] G. .M. Nixon, and R. T. Brouillette, "Diagnostic techniques for obstructive sleep apnoea: Is polysomnography necessary?" *Pediatric Respiratory Reviews*, vol. 3, pp. 18-24, 2002.
- [4] D. Gordon, D. P. Southall, D. H. Kelly, A. Wilson, S. Akselrod, J. Richards, B. Kenet, R. Kenet, R. J. Cohen, and D. C. Shannon, "Analysis of heart rate and respiratory patterns in sudden infant death syndrome victims and control infants," *Pediatr Res*, vol. 20, pp. 680-684, 1986.
- [5] A. Kahn, D. Blum, E. Rebuffat, M. Sottiaux, J. Levitt, A. Bochner, M. Alexander, J. Grosswasser, and M. F. Muller, "Polysomnographic studies of infants who subsequently died of sudden infant death syndrome," *Pediatrics*, vol. 82, pp. 721-727, 1988.
- [6] S. Lord, et al., "Interrater reliability of computer-assisted scoring of breathing during sleep," *Sleep*, vol. 12, pp. 550-558, 1989.
- [7] A. L. Motto, H. L. Galiana, K. A. Brown, and R. E. Kearney, "Automated estimation of the phase between thoracic and abdominal respiratory movement signals," *IEEE Trans Biomed Eng*, vol. 52, no. 4, pp. 614-621, 2005.
- [8] A. L. Motto, H. L. Galiana, K. A. Brown, and R. E. Kearney, "Detection of Movement Artifacts in Respiratory Inductance Plethysmography: Performance Analysis of a Neyman-Pearson Energy-based Detector," *Proceedings of the 26th Annual International Conference of the IEEE Engineering in Medicine and Biology Society*, pp. 2183-2187, 2004.
- [9] A. L. Motto, H. L. Galiana, K. A. Brown, and R. E. Kearney, "On stochastic representation of residual time series from observed respiratory movements,"

- Proceedings of the Canadian Conference on Electrical and Computer Engineering*, pp. 356-359, 2005.
- [10] American Sleep Apnea Association [Online]. Available: <http://www.sleepapnea.org>. Accessed: January 1, 2006.
- [11] T. Young, et al., "The occurrence of sleep-disordered breathing among middle-aged adults," *N Engl J Med*, vol. 328, pp. 1230-1235, 1993.
- [12] T. D. Bradley, J. S. Floras, "Sleep Apnea and Heart Failure: Part I: Obstructive Sleep Apnea," *Circulation*, vol. 107, pp. 1671-1678, 2003.
- [13] T. D. Bradley, J. S. Floras, "Sleep Apnea and Heart Failure: Part II: Central Sleep Apnea," *Circulation*, vol 107, pp. 1822-1826, 2003.
- [14] T. Young, J. Skatrud, P. E. Peppard, "Risk Factors for Obstructive Sleep Apnea in Adults," *JAMA*, vol. 291, no. 16, pp. 2013-2016, 2004.
- [15] K. A. Brown, "Pattern of ventilation during halothane anaesthesia in infants less than two months of age," *Can. J. Anaesth*, vol. 43, pp. 121-128, 1996.
- [16] D. M. Fisher, "When is the ex-premature infant no longer a risk for apnea?" *Anesthesiology*, vol. 82, pp. 807-808, 1995.
- [17] I. Kato, J. Groswasser, P. Franco, et al., "Developmental characteristics of apnoea in infants who succumb to sudden infant death syndrome," *Am J Respir Crit Care Med*, vol. 164, pp. 1464-1469, 2001.
- [18] Family practice notebook [Online]. Available: <http://www.fpnotebook.com>. Accessed: January 1, 2006.
- [19] J. F. Nunn, *Applied Respiratory Physiology*, 2nd ed., London-Boston: Butterworths, 1977.
- [20] Institute for Natural Language Processing [Online]. Available: <http://www.ims.uni-stuttgart.de>. Accessed: January 1, 2006.
- [21] S. Sovik, "Quantifying infant respiratory variability: how to capture complexity," *Acta Paediatr*, vol. 89, pp. 1401-1407, 2000.
- [22] C. L. Marcus, K. J. Omlin, D. J. Basinski, S.L. Bailey, A. B. Rachal, W. S. VonPechmann, et al., "Normal polysomnographic values for children and adolescents," *Am Rev Respir Dis*, vol. 1146, pp. 1235- 1279, 1992.

- [23] K. A. Brown, R. Platt, and J. H. Bates, "Automated analysis of paradoxical ribcage motion during sleep in infants." *Pediatr Pulmonol*, vol. 33, pp. 38-46, 2000.
- [24] J. C. T. Pepperell, R. J. O. Davies, and J. R. Stradling, "Sleep studies for sleep apnoea," *Physiol. Meas*, vol. 23, pp. 39-74, 2002.
- [25] WebMD [Online]. Available: <http://www.webmd.com>. Accessed: January 1, 2006.
- [26] L. Wiegand, C. W. Zwillich, and D. White, "Collapsibility of the human upper airway during normal sleep," *J. Appl. Physiol*, vol. 66, pp. 1800-1808, 1989.
- [27] P. Várady, S. Bongár, and Z. Benyó, "Detection of airway obstruction and sleep apnea by analyzing the phase relation of respiration movement signals," *IEEE Transaction on Instrumentation and Measurement*, Vol. 52, No. 1, pp. 2-7, February 2003.
- [28] A. D. Groote, et al., "Detection of obstructive apnea events in sleeping infants from thoracoabdominal movements," *J Sleep Res*, vol. 11, pp. 161-168, 2002.
- [29] The CHIME website. [Online]. Available: http://dccwww.bumc.bu.edu/chimenisp/Main_Chime.asp. Accessed: January 1, 2006.
- [30] S. Onizuka, T. Kasaba, T. Hamakawa, M. Takasaki, "Lidocaine excites both pre- and postsynaptic neurons of reconstructed respiratory pattern generator in *Lymnaea stagnalis*," *Anesth Analg*, vol. 100, pp. 175-182, 2005.
- [31] J. G. Jones, D. J. Sapsford, and R. G. Wheatley, "Postoperative hypoxemia: mechanisms and time course," *Anaesthesia*, vol. 45, pp. 566-573, 1990.
- [32] N. P. Gill, B. Wright, C. S. Reilly, "Relationship between hypoxaemic and cardiac ischaemic events in the perioperative period," *Br J Anaesth*, vol. 68, pp. 471-473, 1992.
- [33] K. Brown, et al., "The Hering-Breuer reflex in anesthetized infants: end-inspiratory vs. endexpiratory occlusion technique," *J Appl Physiol*, vol. 84, pp. 1437-1446, 1998.
- [34] P. S. Rabbette, J. Stocks, "Influence of volume dependency and timing of airway occlusions on the Hering-Breuer reflex in infants," *J Appl Physiol*, vol. 85, pp. 2033-2039, 1998.

- [35] American Sleep Disorders Association Task Force. The Chicago criteria for measurements, definitions, and severity of sleep related breathing disorders in adults. Presented at the Association of Professional Sleep Societies Conference; June 20, 1998; New Orleans, LA.
- [36] B. A. Phillips, M. I. Anstead, and D. J. Gottlieb, "Monitoring sleep and breathing: methodology. Part I: monitoring breathing," *Clinics Chest Med*, vol. 19, no. 1, pp. 203–212, 1998.
- [37] P. Flemming, "Changes in respiratory pattern resulting from the use of a facemask to record respiration in newborn infants," *Pediat Res*, vol. 18, pp. 58-62, 1962.
- [38] Respiflow [Online]. Available: <http://www.respiflow.com>. Accessed : January 1, 2006.
- [39] D. K. Cheng, *Field and Wave Electromagnetics*, 2nd ed., Addison-Wesley, 1989.
- [40] H. L. Watson, D. A. Poole, and M. A. Sackner, "Accuracy of respiratory inductive plethysmographic cross-sectional areas," *J Appl Physiol*, vol. 65, no. 1, pp. 306–308, 1988.
- [41] Philips Medical Systems [Online]. Available: [http:// www.medical.philips.com](http://www.medical.philips.com). Accessed : January 1, 2006.
- [42] M. W. Wukitisch, M. T. Peterson, D. R. Tobler, and J. A. Pologe, "Pulse oximetry: analysis of theory, technology, and practice," *J Clin Monit*, vol. 4, pp. 290–301, 1988.
- [43] Y. Mendelsonn, "Pulse Oximetry: Theory and Applications for Noninvasive Monitoring," *Clin Chem*, vol. 38, no. 9, pp. 1601-1607, 1992.
- [44] A. Jubran, "Pulse oximetry," *Intensive Care Med*, vol. 30, pp. 2017-2020, 2004.
- [45] A. Van de Louw, C. Cracco, C. Cerf, A. Harf, P. Duvaldestin, F. Lemaire, and L. Brochard, "Accuracy of pulse oximetry in the intensive care unit," *Intensive Care Med*, vol. 27, pp. 1606–1613, 2001.
- [46] C. Guilleminault, M. Partinen, *Obstructive Sleep Apnea Syndrome, Clinical Diagnosis & Treatment*, New York: Raven Press, 1990.
- [47] S. Gyulay, L. G. Olson, M. J. Hensley, M. T. King, K. M. Allen, N. A. Saunders, "A comparison of clinical assessment and home oximetry in the diagnosis of obstructive sleep apnea," *Am Rev Respir Dis*, vol. 147, pp. 50-53, 1993.

- [48] B. H. Taha, et al., "Automated detection and classification of sleep-disordered breathing from conventional polysomnography data," *Sleep*, vol. 20, pp. 991-1001, 1997.
- [49] G. K. Prisk, J. Hammer, C. L. Newth, "Techniques for measurement of thoracoabdominal asynchrony," *Pediatric Pulmonology*, vol. 34, pp. 462-472, 2002.
- [50] R. K. Millard, "Inductive plethysmography components analysis and improved non-invasive postoperative apnoea monitoring," *Physiol Meas*, vol. 20, pp. 175-86, 1999.
- [51] P. M. Macey, J. S. J. Li, and R. P. K. Ford, "Expert system for the detection of apnoea," *Engineering Applications of Artificial Intelligence*, vol. 11, pp. 425-438, 1998.
- [52] F. Steimann, K.P. Adlassnig, "Clinical monitoring with fuzzy automata," *Fuzzy Sets and Systems*, vol. 61, no. 1, pp. 37-42, 1994.
- [53] K. Brown, C. Aun, E. Jackson, A. Mackersie, D. Hatch, J. Stocks, "Validation of respiratory inductance plethysmography using the Qualitative Diagnostic Calibration method in anaesthetized infants," *Eur Respir J*, vol. 12, pp. 935-943, 1998.
- [54] A. V. Oppenheim, A S. Willsky, *Signals and Systems, 2nd ed.*, Boston: Prentice Hall, 1997.
- [55] H. V. Poor, *An Introduction to Signal Detection and Estimation, 2nd Edition*, New York: Springer-Verlag, 1994.
- [56] Switchcraft [Online]. Available: <http://www.switchcraft.com>. Accessed : January 1, 2006.
- [57] Ambulatory Monitoring Inc., *Inductotrace Portable Respiration Monitor (User Instructions)*, 2001.
- [58] D. H. Crowell, *An atlas of infant polysomnography (The encyclopedia of visual medicine series)*, The Parthenon Publishing Group, 2003.
- [59] J. L. Allen, M. R. Wolfson, K. McDowell, and T. H. Shaffer, "Thoracoabdominal asynchrony in infants with airway obstruction," *Am Rev Respir Dis*, vol. 141, pp. 337-342, 1990.
- [60] B. A. Staats, H. W. Bonekat, C. D. Harris, and K. P. Offord, "Chest wall motion in sleep apnea," *Am Rev Resp Dis*, vol. 130, pp. 59- 63, 1984.

- [61] A. R. Stark, and B. T. Thach, "Mechanisms of airway obstruction in newborn infants," *J Pediatr*, vol. 89, pp. 982, 1976.
- [62] Matlab Official Website [Online]. Available: <http://www.themathworks>. Accessed : January 1, 2006.
- [63] Measurement Computing, *PC-Card-DAS16/16 & PC-Card-DAS16/16-AO User's Manual*, 2001.
- [64] B. Kemp, A. Varri, A. C. Rosa, K. D. Nielsen, J. Gade, "A simple format for exchange of digitized polygraphic recordings," *Electroencephalography and clinical Neurophysiology*, vol. 82, pp. 391-393, 1992.
- [65] The Mathworks Inc., *Real-Time Windows Target User's Guide*, 2004
- [66] B. Kemp, "European data format (EDF): current availability and additional applications," *J Sleep Res*, 2002.
- [67] P. M. Macey, et al., "Apnoea detection: human performance and reliability of a computer algorithm," *Acta Paediatr*, vol. 84, pp. 1103-1107, 1995.